EFFECTS OF CHRONIC NICOTINE EXPOSURE AND LACK OF HIGH AFFINITY NICOTINIC RECEPTORS ON CORTICO-HIPPOCAMPAL AREAS IN THE AGING MOUSE BRAIN

A Dissertation

by

PEI-SAN HUANG

Submitted to the Office of Graduate Studies of
Texas A&M University
in partial fulfillment of the requirements for the degree of

DOCTOR OF PHILOSOPHY

May 2012

Major Subject: Biomedical Sciences

Effects of Chronic Nicotine Exposure and Lack of High Affinity Nicotinic Receptors on Cortico-Hippocampal Areas in the Aging Mouse Brain

EFFECTS OF CHRONIC NICOTINE EXPOSURE AND LACK OF HIGH AFFINITY NICOTINIC RECEPTORS ON CORTICO-HIPPOCAMPAL AREAS IN THE AGING MOUSE BRAIN

A Dissertation

by

PEI-SAN HUANG

Submitted to the Office of Graduate Studies of
Texas A&M University
in partial fulfillment of the requirements for the degree of

DOCTOR OF PHILOSOPHY

Approved by:

Co-Chairs of Committee,	Louise C. Abbott
	Ursula H. Winzer-Serhan
Committee Members,	C. Jane Welsh
	William H. Griffith
Head of Department,	Evelyn Tiffany-Castiglioni

May 2012

Major Subject: Biomedical Sciences

ABSTRACT

Effects of Chronic Nicotine Exposure and Lack of High Affinity Nicotinic Receptors on Cortico-Hippocampal Areas in the Aging Mouse Brain. (May 2012)

Pei-San Huang, B.V.M., National Taiwan University, Taiwan

Co-Chairs of Advisory Committee: Dr. Louise C. Abbott
Dr. Ursula H. Winzer-Serhan

Nicotine, the major psychoactive ingredient of tobacco smoke, underlies numerous effects by activating neuronal nicotinic acetylcholine receptors. Both *in vitro* and *in vivo* studies suggest that nicotine is neuroprotective and improves cognitive performance. Epidemiology studies show that smoking is negatively correlated with the incidence of Parkinson's disease and Alzheimer's disease. Postmortem research and neuroimaging studies show that loss of nicotinic binding sites in the brain is the major feature of neurodegenerative diseases related to dementia and cognitive impairment. Caloric restriction, a regimen that extends the lifespan in all mammalian species studied so far including rodents and primates, is a highly regulated response to food deprivation. It is believed that the longevity effect of caloric restriction is mediated by SIRT1, a NAD-dependent deacetylase, and its related genes. Nicotine's effect on body weight could also lead to weight loss by decreasing caloric absorption consumption. The goal of this study was to find the possible correlation between nicotine's effects and the activation of SIRT1 and its related genes. Using β2-/- mice that lack high affinity β2 nicotinic acetylcholine receptors (nAChRs), we first demonstrated that β2* nAChRs do

not directly regulate expression of survival genes. However, we found that loss of β2* nAChRs could result in augmented cellular stress, which indirectly increased expression of SIRT1, Nampt, and Ku70, possibly as an adaptive response to provide protection against neurodegeneration. We also found that loss of endogenous activation of β2* nAChRs had less effect on synaptic connections but strongly impaired survival of hippocampal GABAergic neurons. To activate β2* nAChRs in normal mice, we administered nicotine through drinking water. In a short-term exposure study, we determined the dose of nicotine to be used in young adult mice, and found that chronic nicotine treatment was anxiolytic, decreased caloric consumption, increased nAChR binding sites, and most importantly, increased expression of SIRT1 and its related genes. Finally, we compared long-term nicotine treatment with caloric restriction in middle-aged mice to examine their effects to brain aging, and our results indicated that in mice long term caloric restriction and nicotine treatment both tend to improve memory in aging mice, but appear to act through different mechanisms.

To my parents

ACKNOWLEDGEMENTS

Words cannot express how many thanks I have for Dr. Abbott and Dr. Winzer-Serhan for nurturing me to become a neuroscientist. I am also deeply grateful for all the guidance from my committees, Dr. Griffith and Dr. Welsh. Special thanks to Dr. Pine and Dr. Ko for their advice on my graduate study and to those who had helped but I failed to mention their names here. Thank you.

NOMENCLATURE

Aβ	β-amyloid
AD	Alzheimer's disease
ADHD	Attention-deficit hyperactivity disorder
ANOVA	Analysis of variance
APP	Amyloid precursor protein
β2-/-	β2 knock-out
BDNF	Brain-derived neurotrophin factor
CNE	Chronic nicotine exposure
CNS	Central nervous system
CR	Caloric restriction
DAPI	4'-6-diamidino-2-phenylindole
DG	Dentate gyrus
EC	Entorhinal cortex
EPM	Elevated plus maze
ER	Endoplasmic reticulum
FoxO	Forkhead box O
GABA	Gamma-aminobutyric acid
GAD	Glutamic acid decarboxylase
GAPDH	Glyceraldehyde-3-phosphate dehydrogenase
mEPM	Modified elevated plus maze

MHb	Medial habenular nucleus
MPTP	1-methyl-4-phenyl-1,2,3,6-tetrahydropyridine
MRI	Magnetic resonance imaging
MWM	Morris water maze
nAChR	Nicotinic acetylcholine receptor
NAD	Nicotinamide adenine dinucleotide
NAMPT	Nicotinamide phosphoribosyltransferase
NMJ	Neuromuscular junction
NRT	Nicotine replacement therapy
NT-3	Neurotrophin-3
PD	Parkinson's disease
PNS	Peripheral nervous system
PSD95	Postsynaptic density protein 95
PV	Parvalbumin
ROD	Raw optical density
RT	Room temperature
SEM	Standard error of the mean
SSC	Saline sodium citrate
SST	Somatostatin
UCP	Mitochondria uncoupling protein
VGCC	Voltage-gated Ca^{2+} channel
WT	Wild type

TABLE OF CONTENTS

CHAPTER Page

LIST OF FIGURES

FIGURE Page

FIGURE Page

LIST OF TABLES

CHAPTER I

INTRODUCTION

NICOTINE AND NEURONAL NICOTINIC ACETYLCHOLINE RECEPTORS

Nicotine is the major bioactive ingredient in tobacco leaves where it acts as a botanical insecticide (Soloway, 1976; Tomizawa and Casida, 2003). Nicotine is not the direct cause of most tobacco related negative health consequences, but it is highly addictive (Benowitz, 1999; Balfour, 2002). The addictiveness of nicotine is the reason for continued use of tobacco products. On average, about 1.0 to 1.5 mg of nicotine is absorbed systemically during smoking one cigarette, and high levels of nicotine reach the brain in 10 to 20 seconds, producing rapid behavioral reinforcement through the activation of the dopaminergic reward system (Benowitz and Jacob, 1984). There are various formulations of nicotine replacement therapy (NRT), such as nicotine gum, transdermal patch, nasal spray, inhaler, and sublingual lozenges. Absorption of nicotine from these NRTs is slower and the increase in nicotine blood levels more gradual than from smoking (Hukkanen et al., 2005). For example, oral nicotine administration is a common exposure method in animal experiments, and peak concentrations of nicotine are achieved in about 1 hour (Benowitz et al., 1991; Zins et al., 1997). The oral bioavailability of nicotine is about 20 to 45% (Benowitz et al., 1991; Compton et al., 1997; Zins et al., 1997).

This dissertation follows the style of Neuroscience.

Oral bioavailability of nicotine is incomplete because of hepatic first-pass metabolism. The slow delivery of nicotine in NRT also results in a lower brain nicotine levels than experienced with smoking, and the gradual rise in levels of nicotine in the central nervous system (CNS) allows for development of considerable tolerance to pharmacologic effects (Henningfield and Keenan, 1993). After absorption, nicotine enters the bloodstream. Based on human autopsy samples taken from smokers, the highest affinity for nicotine is in the liver, kidney, spleen, and lung and the lowest affinity is found in adipose tissue (Urakawa et al., 1994). Nicotine also binds to brain tissues with high affinity, and the receptor binding capacity is increased in smokers compared to nonsmokers (Benwell et al., 1988; Breese et al., 1997; Perry et al., 1999).

The major metabolite of nicotine in mammalian species is cotinine. In humans, about 70 to 80% of nicotine is converted to cotinine (Benowitz and Jacob, 1994). However, the elimination half-life of cotinine (700-1130 min in human) is much longer than nicotine (100-150 min in humans) (Hukkanen et al., 2005). This fact makes blood cotinine concentrations fluctuate less throughout the day compared to blood nicotine levels, so cotinine is commonly used as a biomarker for nicotine intake (Benowitz, 1996). The clearance of nicotine is also affected by age. In humans, clearance of nicotine is decreased in the elderly (age > 65) compared to young adults (Molander et al., 2001). The total nicotine clearance is lower by 23% and renal clearance lower by 49% in the elderly compared with young adults. Neonates have diminished nicotine metabolism such that the nicotine half-life in newborns is 3 to 4 times longer than observed in adults (Dempsey et al., 2000).

In the brain, nicotine binds to nicotinic acetylcholine receptors (nAChRs) with high affinity. Nicotinic AChRs are ligand-gated pentameric cation channels. They are composed of 5 subunits organized around a central pore and are further divided into two categories or types: 1) muscle type nAChRs, which are found in vertebrate skeletal muscle, where they mediate neuromuscular transmission at the neuromuscular junction (NMJ), and 2) neuronal type nAChRs, found mainly throughout the peripheral nervous system (PNS) and CNS, but neuronal nAChRs are also found in some non-neuronal tissues such as lymphocytes, monocytes, macrophages, dendritic cell, adipocytes, keratinocytes, endothelial cells, and epithelial cells of the intestine and lung (Kalamida et al., 2007). The embryonic form of muscle type nAChRs are formed by α1, β1, δ, and γ subunits, in a ratio of 2:1:1:1, respectively. In adults, muscle type nAChRs are formed by the combination of α1, β1, δ, and ε, in a ratio of 2:1:1:1, respectively. Neuronal nAChRs have nine identified possible α subunits (α2-α10) and three possible β subunits (β2-β4), each encoded by a difference gene (Picciotto et al., 2001) (Fig. I-1). The α2, α3, α4 and α6 subunits form heteromeric receptors with β2, 3 or 4 (Couturier et al., 1990). The α7, α8, α9, and α10 subunits form homomeric receptors (Le Novere and Changeux, 1995) (Fig. I-2). These multiple combinations of nAChRs subunits possess distinct pharmacological and physiological properties and show different affinities for ligands, as well as variability in the permeability for cations and rate of desensitization (Changeux et al., 1998). The binding site for acetylcholine is located where α subunits form junctions with neighboring subunits. Thus more than one molecule of acetylcholine could bind simultaneously to one nAChR.

Muscular type nAChRs are an important autoantigen involved in myasthenia gravis, which is caused by failure of neuromuscular transmission as a result of the binding of autoantibodies to muscular nAChRs and leading to defective signaling at the NMJ. Myasthenia gravis is therefore characterized by clinical fatigable weakness that muscles become weaker during periods of activity, and the muscles that control eye and eyelid movement, facial expressions, chewing, talking, and swallowing are especially susceptible (Lindstrom, 2000).

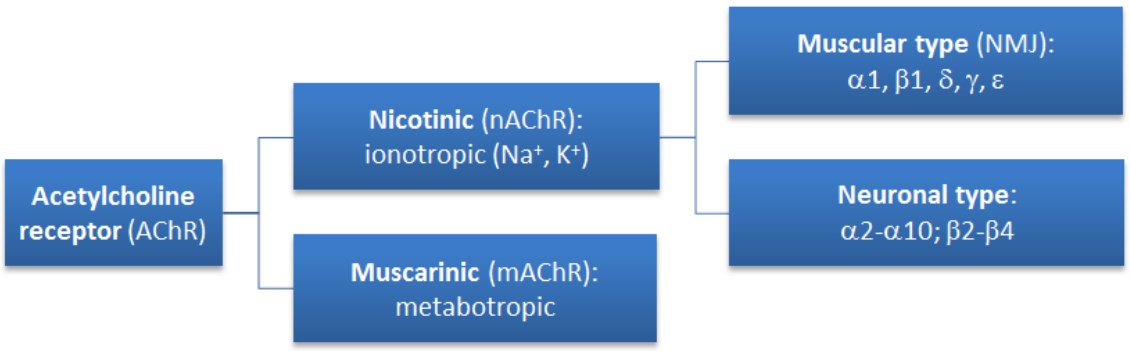

Figure I-1. Acetylcholine receptors can be divided into muscarinic type and nicotinic type, which can be further categorized as muscular type and neuronal type.

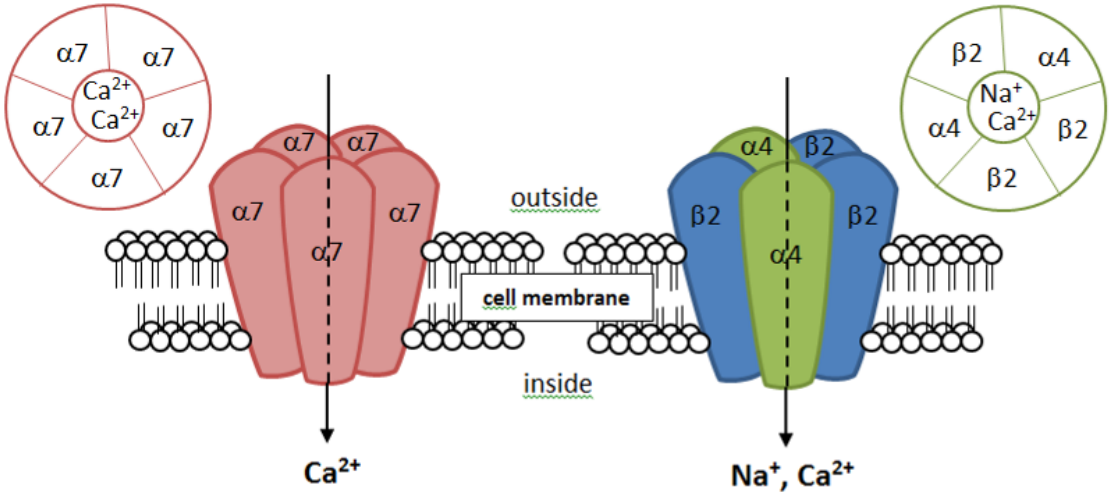

Figure I-2. Homomeric and heteromeric nAChRs subunit composition.

Neuronal nAChRs are located in both the CNS and PNS. In the CNS, α4β2 heteromeric and α7 homomeric receptors are the most widely distributed. The α4 and β2 subunits are present in the entire nervous system, and expression of the α7 mRNA is robustly expressed in certain layers of the cerebral cortex, hippocampus, hypothalamus, and some brain stem nuclei (Wada et al., 1989; Seguela et al., 1993). The α2 subunit is expressed at very low levels and only in restricted brain regions such as hippocampus (Wada et al., 1989). The α5 subunit is expressed at high levels in the subiculum, pre- and parasubiculum, substantia nigra, ventral tegmental area, and weakly expressed in the cerebral cortex (Wada et al., 1990). The α3 and β4 subunits are highly expressed in the medial habenula and are the main nAChR responsible for acetylcholine transmission in autonomic ganglia (Le Novere and Changeux, 1995). The α6 and β3 subunits are selectively enriched in catecholaminergic nuclei such as the dopaminergic neurons of the

substantia nigra, and the norepinephric neurons of the locus coeruleus (Le Novere and Changeux, 1995). The α8 subunit has been found only in the chick nervous system as homopentamers or in combination with the α7 subunit, while the α9 subunit is mainly expressed in the cochlea and sensory ganglia of the nervous system (Elgoyhen et al., 1994). Lastly, the α10 subunit appears in the cochlear mechanosensory hair cells (Elgoyhen et al., 2001; Plazas et al., 2005). In the PNS, autonomic ganglia express α3 and β4 at high levels, but they also contain transcript for the α4, α5, α7, and β2 subunits. These autonomic nAChRs control the activities of the cardiac system, enteric movement, urinary tract activities and more (De Biasi, 2002).

Once the subunits are synthesized, they must assemble into pentameric channels and be transported from the endoplasmic reticulum (ER) through the Golgi apparatus and then transported to the cell surface. nAChRs that have not been properly assembled are targeted to go to the proteasome for degradation (Kalamida et al., 2007). NAChRs are found in pre-, peri- and postsynaptic areas (Lena et al., 1993; Wonnacott, 1997) (Fig. I-3). Peri- and presynaptic nAChRs act as autoreceptors regulating the release of acetylcholine (Tani et al., 1998), serotonin, dopamine, norepinephrine (Summers and Giacobini, 1995), glutamate (Gray et al., 1996), and gamma-aminobutyric acid (GABA) (Ji and Dani, 2000). Presynaptic nAChRs modulate neurotransmitter release by promoting exocytosis either through activation of voltage-gated Ca^{2+} channels (VGCCs) or by direct alteration of the intracellular Ca^{2+} concentration (Kalamida et al., 2007). In addition to Ca^{2+} dependent exocytosis, nAChRs modulate neurotransmitter release

through second messenger pathways as well, which allow nAChRs to exert more subtle regulatory actions (Kalamida et al., 2007).

Postsynaptic nAChRs mediate fast excitatory transmission in the CNS. The α4β2 nAChR binds nicotine with a high affinity, while the α7 nAChR binds nicotine with a low affinity, but has higher Ca^{2+} permeability than α4β2 nAChR (Lena and Changeux, 1998). When ligands bind to nAChRs, the receptor undergoes a conformational change, which allows the central channel pore the open. Functionally, the nAChR complex exist three conformational states: closed, open, and desensitized. Activation of nAChRs occurs when acetylcholine or nicotine binds at the interface between an α and a neighboring α or β subunit, causing a conformational change and opening of the channel pore. A fundamental property of nAChRs is their susceptibility to desensitization and inactivation that follows. In the desensitization state, the channel does not respond to further stimulation, being functionally inactivated (Romanelli et al., 2007; Picciotto et al., 2008).

Neuronal nAChRs also regulate intracellular Ca^{2+} concentration primarily from direct permeation of the nAChR pore. Ca^{2+} influx causes membrane depolarization and subsequent activation of VGCCs or triggers Ca^{2+} release from intracellular stores, generating prolonged Ca^{2+} signals (Rathouz and Berg, 1994; Brain et al., 2001; Shoop et al., 2001; Dajas-Bailador et al., 2002; Beker et al., 2003). The most Ca^{2+} permeable homomeric α7 nAChRs mainly induce Ca^{2+} currents, which subsequently trigger the

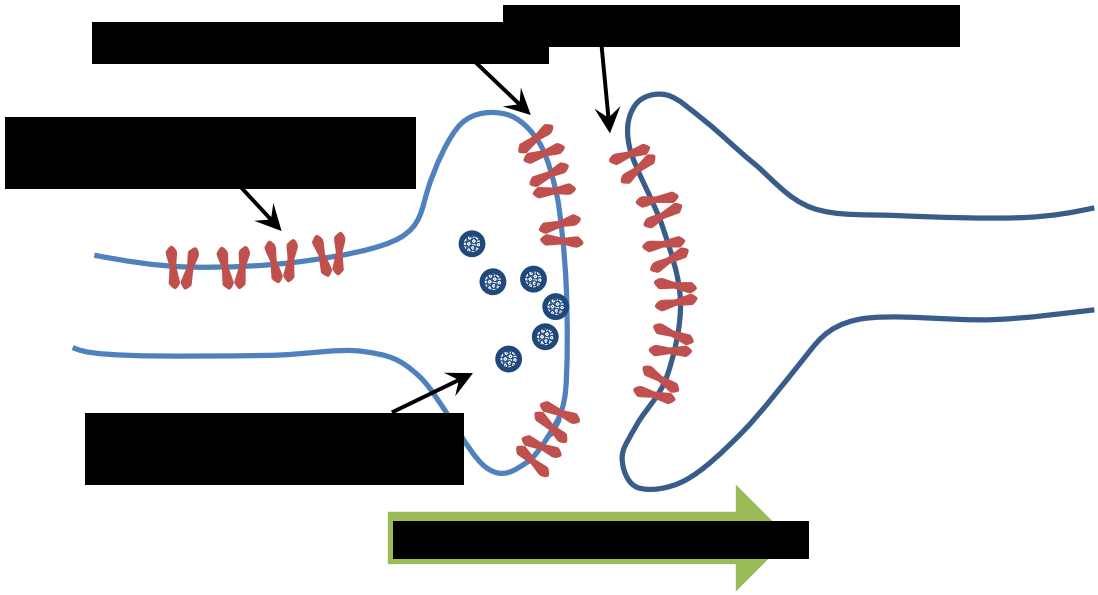

Figure I-3. Neuronal nAChRs can be found at perisynaptic, presynaptic and postsynaptic areas.

release of Ca^{2+} intracellular store (Tsuneki et al., 2000; Sharma and Vijayaraghavan, 2001; Dajas-Bailador et al., 2002). The α4β2 nAChRs operate primarily through Ca^{2+} signals coupled with the opening of VGCCs (Tsuneki et al., 2000; Shoop et al., 2001; Dajas-Bailador et al., 2002).

Chronic nicotine exposure (CNE) has been shown to lead to robust nAChR upregulation in both human and animal models. In humans, increased high affinity nAChR binding has been observed in several CNS regions including the cortex, hippocampus and striatum in post-mortem studies as well as in a single-photon emission computed tomography imaging study (Benwell et al., 1988; Perry et al., 1999; Staley et al., 2006). Animal studies, which also show nAChRs upregulation after CNE, indicate

that both α7- and β2-containing nAChRs are up regulated, although β2 containing nAChRs appear to be more consistently up regulated, and β2 subunit knockout mice do not show upregulation of nicotinic binding sites (Marks et al., 1983; Schwartz and Kellar, 1985; McCallum et al., 2006). A maturational enhancer model has been proposed to explain the possible mechanism of high affinity nAChRs upregulation after CNE proposing that intracellular nAChR precursors are the pharmacological target of nicotine. Nicotine binds to the standard nicotinic binding site at the α/β interface, and in addition to that, nicotine also binds to intracellular nAChRs precursors to trigger a key step in receptor maturational process in the ER (Corringer et al., 2006).

NEUROPROTECTION PROVIDED BY ACTIVATION OF NACHRS

It is believed that nicotine exerts its neuroprotective effects mostly through neuronal nAChRs, although some effects of nicotine may be independent from binding to nAChRs (Picciotto and Zoli, 2008b). Clinically, neuronal nAChRs are associated with a wide range of neurological diseases such as Alzheimer's diseases (AD), schizophrenia, attention-deficit hyperactivity disorder (ADHD), Parkinson's disease (PD), epilepsy, and autism. In AD, the cholinergic hypothesis is based on the observation that AD patients have pronounced loss of cholinergic function (Terry and Buccafusco, 2003). Studies have reported reduced numbers of central nAChRs in aged and AD patients. It has been hypothesized that this reduction might be caused by loss of nAChRs located on degenerating presynaptic projection neurons (Whitehouse et al., 1986). Activation of nAChRs and treatment with nicotinic agonists has been proven to protect neurons from

loss in AD and also ameliorate memory and attention deficits in AD patients (Kihara et al., 2001; Newhouse et al., 2001). Nicotine has been shown to inhibit the development of cellular toxicity induced by β-amyloid (Aβ) (Wang et al., 2000). Both 42-amino acid Aβ peptide, the predominant form of Aβ in amyloid plaques, and α7 nAChRs are present in neuritic plaques, and they colocalize in cortical neurons as detected by coimmunoprecipitation (Wang et al., 2000). In addition, there is evidence that smokers have a reduced risk of developing AD (Lee, 1994). This observation correlates with the fact that, acetylcholinesterase inhibitors have been widely used in AD patients to slow their loss of cognition (Kalamida et al., 2007).

Epidemiological studies show a negative correlation between the incidence of PD and smoking (Tanner et al., 2002), and an animal study using monkeys, has demonstrated beneficial effects of an α4β2 nAChRs agonist in this animal model of PD (Schneider et al., 1998). Also, acute i.v. administration of nicotine has been shown to improve reaction time, speed of processing and reduce tracking errors in PD patients (Fratiglioni and Wang, 2000). The incident of smoking in schizophrenic patients (80-90%) is higher than the general population (25-30%) (de Leon et al., 1995).

Studies have shown that tobacco use can at least transiently restore cognitive deficits of schizophrenic patients, and smoking cessation can exacerbate the disease symptoms (Adler et al., 1993). Post-mortem binding study shows decreased numbers of hippocampal nAChRs and a higher prevalence of promoter mutations in α7 nAChRs in brains of people diagnosed with schizophrenia (Freedman et al., 1995; Leonard et al., 2002). It has been noted that the incidence of smoking in ADHA patients (40%) also is

higher than for the general population (25-30%) (Pomerleau et al., 1995). α4β2 nAChRs activation has been shown to improve attention and reduce memory deficits in rat model of ADHD (Ueno et al., 2002). NAChRs agonists improve clinical symptoms and reduce hyperactivity and attention deficits in ADHD patients (Wilens et al., 1999; Levin and Rezvani, 2000). Significantly reduced numbers of α3 and α4β2 nAChRs have been found in autistic patients, and an increase in α7 subunits has also been observed (Lee et al., 2002; Martin-Ruiz et al., 2004). Finally, some forms epilepsy has been associated with mutations in the α4 nAChR gene (Steinlein et al., 1995).

If one examines the literature that goes beyond that which discusses neurodegenerative diseases and other neurological disorders, it is noted that many additional studies have analyzed the effect of nAChR agonists on cognitive performance in a variety of behavioral tests in rats, non-human primates and humans. Nicotine has specifically been shown to improve learning and memory in normal humans (Warburton et al., 1986). A great amount of information has been published on the specific involvement of NAChRs in cognition, including attention, learning, sensory perception, memory consolidation and arousal (Levin and Simon, 1998). Administration of nAChR agonists improves cognition in non-human primates and in rodents, and by contrast, nAChR antagonists impairs memory function (Levin and Rezvani, 2000; Gould and Higgins, 2003; Buccafusco et al., 2005). Working memory and attention tasks are also improved by nicotine administration (Gioanni et al., 1999; Levin et al., 2002). Epibatidine has been found to induce long-term potentiation, improve memory and learning in human and animal models and to also be neuroprotective (Jonnala et al.,

2002). The nicotinic agonist SIB-1508Y, which is selective for α4β2 nAChRs, and SIB-1553A, which is selective for β4 nAChRs, are able to improve cognition and learning in a variety of experimental models (Vernier et al., 1999). Nicotinic agonists protect against neocortical neuronal loss induced by nucleus magnocellularis lesions in rats and delayed hippocampal CA1 subregion neuronal death by ischemia and against septal cholinergic neuronal death following fimbrial transaction (Nanri et al., 1998; Martin et al., 2004). CNE protects against neurodegeneration of dopaminergic neurons in the 1-methyl-4-phenyl-1,2,3,6-tetrahydropyridine (MPTP) and the methamphetamine mouse model of PD (Janson et al., 1988; Maggio et al., 1998).

There also are model systems in which nicotine has shown protective effects *in vitro*, including exposure to cytotoxic insults of glutamate or 6-OHDA (Ryan et al., 2001). Nicotine rescues PC12 cells from death induced by NGF deprivation (Jonnala et al., 2002). Nicotine has been observed to prevent Aβ toxicity in hippocampal neurons as well as cortical neurons (Shimohama and Kihara, 2001; Zamani and Allen, 2001) and it appears to specifically inhibit Aβ aggregation by preventing conversion of Aβ from the α-helix conformation to the β-sheet conformation (Salomon et al., 1996). Nicotine induces protection of cultured cortical and striatal neurons against cytotoxicity mediated by NMDA and AMPA receptor activation and it also protects cultured hippocampal and cerebellar neurons against kainic acid induced neurotoxicity (Semba et al., 1996; Kaneko et al., 1997).

Potential mechanisms underlying nicotine mediated neuroprotection are still not well defined. Thus far, several directions have been suggested for the possible

mechanisms of neuroprotection provided by nAChR activation, and they can be either direct or indirect (Picciotto and Zoli, 2008b). With respect to the direct mechanism(s), nAChR activation regulates Ca^{2+} entry either by direct entry of Ca^{2+} or depolarization leading to opening of VGCCs as mentioned previously. These actions decrease the ability of glutamate or other excitotoxic agents to increase Ca^{2+} levels through VGCCs or from intracellular stores in the ER. Nicotine can also modulate apoptosis signaling pathways by decreasing the levels of pro-apoptotic factors such as caspases, JNK kinase or cytochrome c, and increasing the levels of anti-apoptotic factors such as Bcl-2 (Garrido et al., 2000; Toborek et al., 2000; Garrido et al., 2001; Kihara et al., 2001; Onoda et al., 2001; Liu and Zhao, 2004). Nicotine increases the synthesis and release of growth factors such as NGF and FGF-2 and increases the levels of their receptors like TrkA and TrkB (Maggio et al., 1998; French et al., 1999; Jonnala et al., 2002). Indirectly, nicotine regulates neurotransmitter release that in turn, decreases neuronal excitability. One such example is nicotine regulation of GABA.

β2 KNOCK-OUT MICE

β2 knock-out (β2-/-) mice were first generated in 1995 (Picciotto et al., 1995). These mutant mice survive, eat and mate normally, and the brains of these animals exhibit normal organization and morphology (Lena and Changeux, 1999). The binding of nicotine, cytisine and epibatidine is dramatically decreased in most brain regions of β2-/- mice, while binding of α-bungarotoxin, which corresponds to α7-containing nAChRs, is not changed in these mutant mice (Orr-Urtreger et al., 1997; Lena and

Changeux, 1999). No high-affinity nicotine binding has been observed in any brain region. The epibatidine binding activity persists in a few brain regions including the habenulo-interpeduncular system, dorsal medulla oblongata, and dorsal cortex of the inferior colliculus. This pattern largely overlaps with the pattern of expression of the β4 subunit and it is thought to correspond to the binding activity of β4-containing nAChRs (Zoli et al., 1995; Lena and Changeux, 1999). β2-/- mice have been tested for memory retention using a passive avoidance task, which is widely used to measure cognitive effects, and β2-/- mice showed marked differences compared to non-mutant siblings; wild type mice consistently increased the delay time to enter the dark chamber after nicotine administration while β2-/- mice were completely unresponsive to nicotine treatment (Picciotto et al., 1995). These data suggest that β2-containing nAChRs are the major target of nicotine's actions in passive avoidance learning. The effects of nicotine in the dopaminergic system have also been tested in β2-/- mice. Nicotine significantly increased the discharge frequency in the mesencephalic dopaminergic neurons in normal mice while this effect disappeared in β2-/- mice, when examined in electrophysiology experiments (Picciotto et al., 1998). Microdialysis of the striatum showed that nicotine produces a dose-dependent increase in the extracellular dopamine concentration in wild type mice but not in β2-/- mice (Picciotto et al., 1998). Increased neurodegeneration during aging also has been reported for β2-/- mice. These mutant mice exhibit neural tissue atrophy and neuronal loss with accompanying gliosis in the somatosensory cortex during aging, and deficits in spatial learning when tested using the Morris water maze

(Zoli et al., 1999). Aged β2-/- mice are impaired in both contextual and tone-conditioned fear in fear conditioning and latent inhibition tasks, while young β2-/- mice do not differ in either tests compared to age-matched wild type mice (Caldarone et al., 2000).

The olfactory bulb granule cell layer in β2-/- mice displays nearly 50% more newborn neurons and significantly fewer apoptotic cells than do wild type mice. Conversely, *in vivo* chronic nicotine exposure significantly decreases the number of newborn granule cells in wild type but not β2-/- adult mice in the olfactory bulb, confirming that the survival of newborn neurons can be controlled by the activation of β2-containing nAChRs. However, when investigating the behavioral consequence of an increased number of granule cells in β2-/- mice, it has been noted that these animals have a less robust short-term olfactory memory than their wild-type counterparts (Mechawar et al., 2004). β2-/- mice also display increased vulnerability to excitotoxic lesions and decreased positive effects that can be observed from experiencing an enriched environment (Zanardi et al., 2007).

HIPPOCAMPUS AND NEOCORTEX ANATOMY

The hippocampus plays an important role in memory formation. Human imaging studies show involvement of the hippocampal region when healthy subjects perform memory tasks (Eldridge et al., 2000; Burgess et al., 2002). Patients with confirmed hippocampal damage have long been known to suffer from memory deficits (Vargha-Khadem et al., 1997; Tulving and Markowitsch, 1998; Corkin, 2002; Langston et al., 2010). The hippocampus is part of the limbic system and is composed of a curved and

recurved sheet of cortex that is folded into the medial surface of the temporal lobe. Transverse sections reveal that the hippocampus has three distinct zones: 1) the dentate gyrus (DG); 2) the hippocampal proper (also called the Ammon's horn or cornu ammonis (CA)); and 3) the subiculum. In each section, the DG and the hippocampal proper have the form of two interlocking "C"s. The hippocampal proper is made up of three regions: CA1, CA2 and CA3. The subiculum is a transitional zone continuous with the hippocampal proper at one of its edges and the cortex of the parahippocampal gyrus at the other edge. The hippocampal proper and the DG consist of three layers of neurons, that include a superficial molecular layer and a deep polymorphic layer. The middle layer consists of the granular cell layer in the DG and the pyramidal cell layer in the hippocampal proper. The subiculum, as a transition zone, changes gradually from the three layers of neurons seen in the hippocampus proper to the six layers of neurons that are characteristic of the neocortex.

The entire hippocampus receives inputs from the entorhinal cortex (EC) and outputs via the subiculum and fimbria/fornix. The EC receives projections from the cingulate gyrus, orbital cortex, amygdala, olfactory cortex, and other areas of the temporal lobe, such that almost all types of sensory information have access to the hippocampus (Nolte, 2002). The fornix is a prominent output pathway of the hippocampus, through which fibers reach an assortment of anteriorly situated forebrain structures. In addition, many fibers pass directly from the subiculum to the EC and amygdala, or backward along the cingulate gyrus (Nolte, 2002). Within the hippocampus, there are at least two routes of information flow (Langston et al., 2010).

The first is the indirect pathway (trisynaptic circuit) in which information primarily from layer II of the EC is projected to the DG, then to CA3 via the mossy fiber pathway, and finally reaching CA1 via the Schaffer collateral connections. The second pathway is the direct pathway – a monosynaptic connection between EC layer III and CA1 (Witter et al., 1989; Langston et al., 2010).

The cerebral cortex that is visible on the surface of the brain is called the neocortex, and pyramidal cells are the most numerous neocortical neurons. These neurons have a conical cell body from which a series of spine-studded dendrites emerge including a long apical dendrite that leaves the top of each cell and ascends vertically toward the cortical surface. Neocortical pyramidal neurons also exhibit a series of basal dendrites that emerge closer to the base of the cell and spread out horizontally. Neocortical pyramidal cells range in size from 10 μm in diameter up to 70 to 100 μm. Most neocortical pyramidal cells have long axons that leave the cortex to reach either other cortical areas or various subcortical sites, where they make excitatory synapses. The dendritic spines of pyramidal cells are sites of synaptic contact. Cells of neocortex are arranged is a series of six layers. Most superficial is a cell-poor molecular layer (layer I), and the deepest is the polymorphic layer (layer VI). In between these two are the external granular layer (layer II), external pyramidal layer (layer III), internal granular layer (layer IV), and internal pyramidal layer (layer V) from outside to inside, and they are all variously populated by small (granular) cells or large pyramidal cells. The six neocortical cell layers are not equally prominent throughout the neocortex (Nolte, 2002).

NORMAL AGING BRAIN

As the normal brain ages it changes structurally and functionally. Functionally, deficits in memory that are un-related to any specific neuropathology are associated with age (Lister and Barnes, 2009). Aged rats and mice demonstrate impairments in spatial memory testing by the Morris water maze and the Barnes circular platform task despite the continued presence of normal visual perception and motivation (Barnes, 1979; Rapp et al., 1987; Bach et al., 1999). Consistent with rodent studies, spatial memory deficits are also seen in aged humans when they experience an analog of the Morris water maze (Lister and Barnes, 2009). Structurally, the aging brain declines in volume with the frontal cortex more severely affected compared to the temporal, parietal and occipital cortices (Haug, 1983; Haug and Eggers, 1991). Longitudinal studies using structural magnetic resonance imaging (MRI) in humans from age 3 to 70 years show an increase in cortical gray matter volume until age 5 followed by a gradual decline in volume until age 70 (Pfefferbaum et al., 1994). Several other studies also have indicated significant gray matter tissue volume loss with age (Blatter et al., 1995; Thompson et al., 2003; Sullivan et al., 2004), while still other studies have shown greater white matter loss in aging (Guttmann et al., 1998; Jernigan et al., 2001). Studies using diffusion tensor imaging have shown that age-related changes in white matter are greatest in the anterior regions, and it has been suggested that the myelinated fibers in this region are more susceptible to breakdown (Bartzokis, 2004; Head et al., 2004). Volume-based imaging studies also show that age-related decline in gray matter is also greatest in frontal regions (Raz et al., 1997).

The hippocampus, which is involved in memory processes as previously mentioned, also shows structural changes in normal aging. Studies have reported that hippocampal atrophy and volume loss is associated with memory loss in the normal aging brain, although the degree and importance of specific neuronal loss in the hippocampus has been debated (Morrison and Hof, 1997; Raz et al., 1998; Raz et al., 2005; Persson et al., 2006; Head et al., 2008). In the DG of hippocampus, quantification of synapse number using stereological methods has revealed reductions of about 24% of axospinous synapses in the dentate gyrus molecular layer of aged rats compared with young rats (Geinisman et al., 1992). Compared to the hippocampus, the surrounding entorhinal cortex, which is consistently targeted by early AD pathology, remains relatively unaffected during the normal aging process (Raz, 2005).

In general, brain volume changes are not linear across the life span; brain volumes decline minimally in younger adults and the loss of volume accelerates with age (Raz et al., 2005). Another measure of brain atrophy is ventricular expansion, which occurs at an annual rate of 0.43% in young adults, but increases to an annual rate of 4.25% after the age of 70 (Raz, 2005). Normal aging brains also exhibit decreases in resting blood flow, the metabolic rate of oxygen consumption, and vascular reactivity of cerebral vessels to various chemical modulators (Gazzaley and D'Esposito, 2005). A study using MRI in rhesus monkeys reveals a significant inverse correlation between cerebral blood volume and age, and a significant correlation between cerebral blood volume and performance on the delayed non-matching to sample task, which is a hippocampal dependent task of memory function (Small et al., 2004). In this study DG

showed the most changes compared to the CA1 of the hippocampus, the subiculum, and the entorhinal cortex (Small et al., 2004). Another cellular compartment analysis of temporal activity using fluorescent *in situ* hybridization (catFISH) study also showed a significant age-related reduction in the percentage of Arc-positive cells, that was restricted to the DG but not CA1 or CA3 of the hippocampus (Small et al., 2004). Arc is an immediate early gene whose expression is induced following behavioral relevant neural activity (Small et al., 2004).

Several hypotheses have been proposed for the mechanism of normal brain aging (Drag and Bieliauskas, 2010). The dopamine hypothesis of aging posits that age-related dysregulation in the dopamine system mediates the cognitive deficits associated with normal aging (Backman et al., 2006). In support of this hypothesis, several studies have demonstrated that dopamine markers can be used as predictors of cognitive performance in normal aging (Volkow et al., 1998; Backman et al., 2000; Erixon-Lindroth et al., 2005; Cropley et al., 2006). There also is evidence suggesting that normal aging is accompanied by dopamine dysregulation in multiple areas including the striatum and frontal cortex (Suhara et al., 1991; Mozley et al., 2001; Reeves et al., 2002; van Dyck et al., 2002; Stark and Pakkenberg, 2004) and fluctuations in dopamine levels can significantly affect cognition (Luciana et al., 1998). Anatomically, the frontal lobes are especially sensitive to the aging process and the declines in frontal lobe functional efficiency can account for many of the cognitive deficits associated with cognitive aging, such as executive function, language, and memory (West, 1996; Raz et al., 1997). Another possible explanation for normal brain aging comes from the speed of processing

hypothesis, which suggests that age-related cognitive decline can be accounted for through a decrease in the speed to process information (Salthouse, 1996). Finally, the inhibitory control hypothesis proposes that decreases in the ability to inhibit or suppress task-irrelevant stimuli, which is also is especially relevant to frontal lobe function, can explain age-related changes in cognitive function (Hasher and Zachs, 1988).

CALORIC RESTRICTION AND SIRT1

Epidemiology studies have reported an inverse relationship between caloric intake and risk of AD and PD (Luchsinger et al., 2002; Mattson et al., 2002; Mattson, 2003). These findings fit well within the context of the beneficial effects of the caloric restriction (CR) paradigm, one of the most robust in gerontology (Weindruch and Sohal, 1997; Masoro, 2005; Piper and Bartke, 2008). As demonstrated using numerous animal models, CR has proven to be the most effective means to significantly delay or slow brain aging. Reducing intake of a caloric consumption by 20-50% can increase lifespan, reduce incidence and slow onset of chronic disease, enhance stress protection, and maintain youthful behavioral function (Weindruch and Sohal, 1997; Masoro, 2005; Piper and Bartke, 2008). Recent studies in mouse models of AD confirm that restricting caloric intake by 30 to 40% from normal levels can markedly slow pathogenesis of the disease (Qin et al., 2006b; Halagappa et al., 2007). Short-term CR substantially decreases the accumulation of Aβ plaques and gliosis marked by astrocytic activation in two AD mouse models (Patel et al., 2005). A CR dietary regimen prevents Aβ peptide generation and neuritic plaque deposition in the brain of Tg2576 mice, which are a

mouse model of AD (Wang et al., 2005). Aβ deposition in monkeys on a CR regimen is also reduced (Qin et al., 2006a). Similarly, long-term studies of monkeys conducted at the National Institute on Aging and the University of Wisconsin have produced data indicating that 30% CR animals are healthier than fully fed counterparts based on reduced incidence of various diseases, exhibition of better indices of predisposition to disease, and slower rates of aging based on analysis of several biomarkers (Ramsey et al., 2000; Roth et al., 2004; Mattison et al., 2007; Raman et al., 2007). CR monkeys in these studies exhibited relative preservation of volume in the mid-cingulate cortex, lateral temporal cortex bilaterally, and the right dorsolateral frontal cortex as well as various subcortical regions, when grey matter volume measured in vivo by MRI. In contrast, grey matter volume generally declined in the frontal and temporal cortex during the third decade of the life of non CR monkeys (Colman et al., 2009). Diffusion tensor imaging shows preservation of white matter in CR monkeys in the fronto-occipital fasciculus, superior longitudinal fasciculus, external capsule, and brainstem (Bendlin et al., 2011). In addition, while both CR and control monkeys showed iron deposition in the globus pallidus and substantia nigra, the CR animals had significantly less iron in these regions and they also exhibited less iron deposition in the red nucleus and parietal, temporal, and perirhinal cortices (Kastman et al., 2010). A recent report also indicates a significant increase in survival in CR monkeys as well as attenuation of age-related declines in brain volume in selected regions (Colman et al., 2009). Formal clinical studies of CR lasting only 6 months in duration have also documented positive impact

on many indices of health and risk factors for chronic disease in human (Civitarese et al., 2007).

However, it is evident that such a stringent regimen would be problematic in the human population due to difficulties with compliance, as well as other quality of life issues impacted by CR in humans (McCaffree, 2004; Dirks and Leeuwenburgh, 2006). This has increased the attention of the development of CR mimetic substances, which are compounds that can mimic CR by targeting metabolic and stress response pathways affected by CR, but without restricting caloric intake. One such compound is resveratrol, a SIRT1 activator (Howitz et al., 2003; Hursting et al., 2003; Ingram et al., 2004; Chen and Guarente, 2007).

SIRT1 has actions similar to that of CR. SIRT1 is the mammalian homolog of the yeast silent information regulator2 (Sir2) gene (Tang and Chua, 2008). This class of genes called sirtuins is nicotinamide adenine dinucleotide (NAD)-dependent histone deacetylase that regulate a variety of stress responses, including CR (Guarente, 2007; Michan and Sinclair, 2007; Lavu et al., 2008). Observations of a link between the Sir complex and the length of the yeast replicative lifespan (i.e., the number of generations the yeast can bud) was made more than ten years ago (Tang and Chua, 2008). Over-expression of Sir2 increases the replicative lifespan of yeast, as well as increases longevity in invertebrate animal models, including the nematode, *C. elegans* (Tissenbaum and Guarente, 2001), and in the fruit fly, *Drosophila melanogaster* (Rogina and Helfand, 2004). Studies have demonstrated that increased longevity induced by CR in yeast requires activation of Sir2, by NAD, and that disabling or knocking out Sir2

eliminated the lifespan extension induced by CR (Guarente, 2007; Michan and Sinclair, 2007; Lavu et al., 2008). Results from a variety of recent rodent studies show that resveratrol, the SIRT1 activator, can also produce a remarkable range of beneficial effects including protection against adverse effects of high fat diets, neurodegeneration and age-related pathologies, such as decreased cardiac function and the incidence of cataracts (Baur and Sinclair, 2006; Fukuda et al., 2006; Kim et al., 2007b; Lu et al., 2008; Pearson et al., 2008). In the mouse embryo, SIRT1 is expressed at high levels in the heart, brain, spinal cord, and dorsal root ganglia (Sakamoto et al., 2004). High SIRT1 levels in the embryonic brain suggest that it might have a role in neuronal and brain development. In SIRT1 knock-out mice, postnatal survival is infrequent and developmental defects such as exencephaly and retinal anomalies have been observed (Cheng et al., 2003; McBurney et al., 2003). If SIRT1 promotes survival and stress tolerance in mammalian cells in general, it is likely to do so for CNS neurons as well. It has been noted that SIRT1 activation protects mouse neurons against the cytotoxicity of the mutant polyglutamine protein huntingtin (Parker et al., 2005). Over-expression of SIRT1 and resveratrol treatment also markedly reduced Aβ deposition and had other more general neuroprotective effects (Chen et al., 2005a).

Mammalian SIRT1 interacts with and regulates not only histone proteins but also interacts with various other substrates. Acetylation of lysine residues in the C-terminal regulatory domain of p53, the tumor suppressor, enhances the sequence-specific binding of p53, and SIRT1 deacetylation of p53 represses its transcriptional activity (Luo et al., 2001; Vaziri et al., 2001). SIRT1 repressed p53-dependent apoptosis in response to DNA

damage and oxidative stress and promotes cell survival under cellular stress induced by etoposide treatment or irradiation (Luo et al., 2001; Vaziri et al., 2001).

Mammalian forkhead (FOXO) transcription factors consist of FOXO1, 3, 4, and 6. FOXOs have been implicated in regulating metabolism, cell-cycle progression, stress tolerance, repair of DNA damage and apoptosis (Accili and Arden, 2004). In mammals, SIRT1 deacetylates FOXO3, and shows a dual effect on FOXO3's function of inducing cell death (Brunet et al., 2004). Ku70 another substrate of SIRT1, has also been shown to attenuate apoptosis (Sawada et al., 2003; Cohen et al., 2004a). In most cells, Ku, which is an heterodimer of two tightly associated subunits called Ku70 and Ku80, is an abundant protein located in the nucleus, where it plays a key role in the non-homologous end joining process, which is responsible for repairing a major fraction of DNA double strand breakages (Jackson, 2002). SIRT1 promotes DNA repair activity and deacetylate Ku70, causing it to sequester the proapoptotic factor Bax away from mitochondria, thereby inhibiting stress-induced apoptotic cell death (Cohen et al., 2004b; Jeong et al., 2007). While SIRT1 functions as a key mediator to multiple cellular stresses, nicotinamide phosphoribo-syltransferase (Nampt) - mediated NAD biosynthesis functions as a pace maker that regulates circadian oscillatory NAD production and fine-tunes SIRT1 activity at the systemic level (Garten et al., 2009; Imai, 2009; Haigis and Sinclair, 2010; Imai, 2010; Imai and Guarente, 2010), because sirtuins require NAD for their enzymatic activities. Recent studies have demonstrated the tight functional connection between Nampt-mediated NAD biosynthesis and SIRT1 in a number of different cell types (Garten et al., 2009; Imai, 2010).

OBJECTIVE OF THIS DISSERTATION

Nicotine and nAChR agonists share many similar effects with CR and SIRT1 activation. First, they both regulate metabolism by decreasing caloric consumption and body weight. Nicotine decreases appetite and increases energy expenditure, which results in the fact that cigarette smokers tend to have lower body weights compared to non-smokers. Second, they both show well-demonstrated neuroprotective effects *in vitro* and *in vivo*. Nicotine is proposed to exert its neuroprotective functions by anti-apoptosis, calcium regulation, and growth factor mediation. However, there could still be unknown pathways through which nicotine could act that are correlated with CR or SIRT1 activation. Third, both nicotine and CR prevent β-amyloid plaque accumulation by regulating the amyloid precursor protein (APP) processing. **The goal of this study** was to find a possible correlation between nicotine's effects and activation of SIRT1 and other SIRT1-related genes (SIRT1's substrates such as p53, Ku70, FoxO, and its upstream regulator, Nampt). Because nicotine can be neurotoxic under certain circumstances (depending on the dose, duration and time of exposure), it is important to elucidate the mechanisms underlying nicotine's neuroprotective effects for better potential therapies against neurodegenerative diseases. On the other hand, although SIRT1 mediated neuroprotection and anti-degeneration effects can be achieved by the natural activator, resveratrol, and the non-invasive regimen of CR, there are still limitations to the use of resveratrol and CR. For example, the bioavailability of resveratrol is very low, and resveratrol cannot pass through the blood-brain-barrier to exert its actions directly in the brain. CR is a time consuming process and can only work

to preventive adverse changes but it does not reverse deficits that have already occurred. No research has been done previously to investigate the possible link between nicotine and SIRT1 functions. **The central hypothesis of this dissertation is that chronic activation of high affinity nicotinic receptors protects the brain from adverse effects of aging through mechanisms that are similar to those that act in caloric restriction.**

We evaluated this hypothesis by investigating four specific aims:

1) Examine the effect of loss of high affinity nicotinic receptors using the β2-/- mouse, on cortico-hippocampal regions on anatomical changes in aging mouse brain, and determine CR-related longevity gene expression. , The β2-/- mouse has been proposed to be a neurodegenerative model, because these mice exhibit an accelerated aging phenotype. The objective of this aim was to confirm the aging phenotype in our β2-/- mice in middle age male mice, and to determine whether lack of endogenous receptor activation changes expression of genes that are correlated with CR-induced longevity.

2) Evaluate the effect of loss of high affinity nicotinic receptors on cortico-hippocampal regions on neuronal plasticity and interneuron population in aged β2-/- and control mouse brains. β2-/- mice lack high-affinity nAChRs and exhibit deficits in spatial learning and memory, and increased neurodegeneration during ageing including decreased cortical thickness, decreased hippocampal volume, and increased neuronal densities. These anatomical alterations could result from decreased connectivity due to loss of synapses and decreased dendritic arborizations, or result from overt neuronal loss. Synaptic loss has been found in the brains of both mouse models of and human patients

with several neurodegenerative diseases. β2-/- mice have a tendency to exhibit decreased basal dendrite size and decreased process complexity in almost all cortical areas, and β2-containing nAChRs might be involved in dendritic morphogenesis.

Loss of GABAergic neuron occurs at a late stage of AD. Chronic dosing with nicotine in rats has been shown to increase the number of GABAergic neuron in the hippocampal area (unpublished data). Thus, loss of high affinity nicotinic receptor could result in decreased numbers of GABAergic interneurons. The objective of this specific aim was to determine whether loss of high affinity nicotinic receptor changes neuronal plasticity or the GABAergic neuronal population.

3) Assess the effect of short-term high affinity nicotinic receptor activation through nicotine exposure on memory and CR-related longevity gene expression in the brain of young adult mice. Nicotine has high affinity for β2-containing nAChRs (Zanardi et al., 2002) and nicotine is more accessible than other receptor-specific agonists, so we used nicotine as the agonist for β2-containing nAChRs. This specific aim not only tested the memory improving effect of nicotine, it also assessed the responses of longevity gene expression in the brain to different doses of nicotine in young adult mice in a short period of time.

4) Determine the effect of long-term high affinity nicotinic receptor activation by nicotine exposure on memory and CR-related longevity gene expression in the aging mouse brain as compared to the effects of caloric restriction. The objective of this fourth specific aim was to test whether long-term nicotine exposure or nicotinic receptor activation reduced or slowed memory and cognitive decline of aging brains as has been

observed with CR, and determine whether any improvement was correlated with activation of CR-related longevity genes. The effect of long-term nicotine exposure (4 months) was determined for rodents for the first time in this study. Although chronic (but not long-term) nicotine administration has been proved in rats to be neuroprotective and improve memory and cognitive function, it was unknown whether such long term exposure sustains or reverses the previously observed effects. It was also crucial to compare the effects of long-term nicotine administration with caloric restriction, because we hypothesized that they share similar mechanisms. We also tested the neuroprotective effect of caloric restriction and nicotine exposure on the normal aging brain to evaluate whether any benefits that were observed also could be applied to normal physiological aging or were benefits only restricted to pathological conditions.

CHAPTER II

REGULATED EXPRESSION OF NEURONAL SIRT1 AND RELATED GENES BY AGING AND NEURONAL B2-CONTAINING NICOTINIC CHOLINERGIC RECEPTORS†

SUMMARY

Longevity genes attenuate the aging process, but their expression in the brain during aging remains unknown. Loss of the majority of heteromeric brain nicotinic acetylcholine receptors (nAChRs) results in premature brain aging, and altered regulation of longevity genes could be involved. Using in situ hybridization, the expression of SIRT1, Ku70, Nampt, p53, FoxO3, and UCP5 was determined in neocortex and hippocampus of young adult 3-month and middle-aged 18-month-old wild-type (WT), and age-matched mice lacking β2-containing (β2*) heteromeric nAChRs (β2-/-). Age-related structural changes were detected in WT mice. In particular, cortical thickness was decreased but neuronal density increased, and hippocampal volume increased with age. In contrast, young β2-/- mice exhibited increased cortical neuronal density, and with age, cortical thickness decreased more dramatically, and hippocampal volume did not increase. Thus, young β2-/- mice exhibited cortical signs of aging, and aging was accelerated at 18 months.

---

†Reprinted with permission from "Regulated expression of neuronal SIRT1 and related genes by aging and neuronal β2-containing cholinergic receptors" by Huang PS, Son JH, Abbott LC, and Winzer-Serhan UH (2011) Neuroscience 196:189-202, Copyright 2011 by Elsevier Ltd.

The longevity genes probed exhibited similar expression patterns in frontal brain structures, with strong expression in hippocampus, medial habenula (MHb) and cortex. In WT mice, age significantly decreased expression of all genes except SIRT1 in cortical structures, and a similar pattern was detected in the MHb. Genotype had no effect on expression in young adults in either cortex or MHb, but increased mRNA expression of SIRT1, Nampt, and Ku70 was detected in cortex, hippocampus and MHb of aged β2-/- mice compared to WT mice. This is the first study to determine age-related expression of survival genes in forebrain areas. Although, structural changes indicative of accelerated aging are evident in young β2-/- mice, the data suggest that nAChRs do not directly regulate expression of survival genes. However, loss of β2* nAChRs could result in augmented cellular stress which indirectly increases expression of SIRT1, Nampt, and Ku70 as an adaptive response to provide protection against neurodegeneration.

INTRODUCTION

Nicotine exerts neuroprotective effects and improves cognitive performance via activation of neuronal nicotinic acetylcholine receptors (nAChRs) (Socci et al., 1995; Zarrindast et al., 1996; Picciotto and Zoli, 2008b). Neuronal nAChRs are ligand-gated cation channels (Karlin, 2002), composed of various combinations of α and β subunits that form either homomeric or heteromeric receptors (Cooper et al., 1991; Sargent, 1993a). The heteromeric α4β2 pentamer is the most abundant neuronal nAChR subtype in the central nervous system, widely distributed in mammalian brain, including cortical

structures, and pharmacologically characterized by its high affinity for nicotine (Picciotto et al., 1998).

In humans, loss of high affinity nicotinic binding sites is a major histological change observed in normal brain ageing and excessive loss is linked to several neurodegenerative diseases that also exhibit dementia (Hellstrom-Lindahl and Court, 2000). Aged (22- to 24-month-old) mice lacking this predominant form of high-affinity β2* nAChRs (β2-/- mice) exhibit increased neurodegeneration with deficits in spatial learning and memory compared to age matched wild type (WT) control mice (Zoli et al., 1999). This suggests that the aging process is accelerated in the brains of β2-/- mice, and that age-related changes may already occur in middle-aged (18-month-old) animals.

In rodents, caloric restriction slows the ageing process and increases longevity, with SIRT1 being a key regulator(Agarwal and Baur, 2011). SIRT1 is connected to a signaling network that involves a number of longevity factors such as Nampt, Ku70, FoxO3 and p53. The silent information regulator 2 (Sir2) protein found in yeast is a nicotinamide adenine dinucleotide (NAD)-dependent deacetylase and is positively linked to longevity (Kaeberlein et al., 1999; Imai et al., 2000; Lin et al., 2000). SIRT1 is the mammalian homolog of Sir2, and a key regulator of cellular defenses and survival in response to stress (Brunet et al., 2004; Cohen et al., 2004b). SIRT1 is expressed in the brain, where it is upregulated in mouse models of Alzheimer's disease and amyotrophic lateral sclerosis. This is thought to be a neuroprotective adaptational response (Kim et al., 2007b), because upregulation of SIRT1 can protect neurons against neurodegeneration and neurotoxic insults (Chen et al., 2005a; Kim et al., 2007b).

SIRT1 deacetylates numerous factors that govern a wide range of biological functions (Michan and Sinclair, 2007). The tumor suppressor gene p53 can be deacetylated by SIRT1, thereby inhibiting p53-mediated apoptosis (Luo et al., 2001; Vaziri et al., 2001). SIRT1 can attenuate apoptosis by deacetylating the DNA repair factor, Ku70 (Cohen et al., 2004b). The FoxO family of transcription factors are typical substrates for SIRT1 (Brunet et al., 2004; Nemoto et al., 2004), and their deacetylation increases cellular resistance to oxidative stress and inhibits cell death (Giannakou and Partridge, 2004). Nampt controls the activity of SIRT1 (Revollo et al., 2004). Nampt is induced by stress or nutrient deprivation and increases cellular resistance to damage (Yang et al., 2006a). We also included the mitochondria uncoupling protein 5 (UCP5/BMCP1) in the analysis; UCP5 is highly expressed in the brain (Sanchis et al., 1998), and thought to exert neuroprotective effects by decreasing production of oxygen reactive species (Kim-Han et al., 2001).

Although it is clear that SIRT1 and SIRT1-related genes are important in cell defense and survival, their regulation during aging and whether they are part of neuroprotective pathways associated with high-affinity nAChR activation in the central nervous system are unknown. In this study we show that cortical signs of aging were already present in middle-aged 18-month-old β2-/- mice. Furthermore, we determined the expression patterns of SIRT1 and related longevity genes in young and middle-aged male WT mouse brains, and investigated whether lack of high-affinity nAChRs affected their expression, which might explain the accelerated aging seen in these mice.

EXPERIMENTAL PROCEDURES

Animals and tissue preparation

C57/BL6: β2-/- mice, derived from a colony at Baylor College of Medicine (Houston, TX, USA, originally from the lab of Dr. Arthur L. Beaudet and now available from The Jackson Laboratory, Bar Harbor, MA, USA), were first described by Xu et al. (Xu et al., 1999). A breeding colony was established at Texas A&M University's Laboratory Animal Research and Resource (LARR) facility. Young adult (3-month-old) (n = 8) and middle-aged (18- to 20-month-old) male β2-/- mice (n = 9), and young adult (3-month-old) male WT mice (n = 8) were housed under standard conditions at the College of Medicine Animal Care Facility. Middle-aged (18-month-old) WT male C57/BL6 mice were purchased from the National Institutes of Health (n = 11). All procedures were approved by the Texas A&M University Animal Use Committee and carried out in accordance with the National Institutes of Health Guide for the Care and Use of Laboratory Animals (National Institutes of Health Publication No. 85-23, revised 1996).

Tail biopsies were taken after weaning and genotypes were determined using three-way PCR with the following primers: β2P1: GAG ACT AGT GAG ACG TGC TAC TTC CAT TTG; β2P2: CTC TGA CTG TAA AGG CAG TGG TTG CTA TAG; β2P3: TAG CTA TTG ACG ACG TCT TTA AGA TCC. The genotype results were verified by *in situ* hybridization using a rat β2 antisense cRNA probe (Figure II-1).

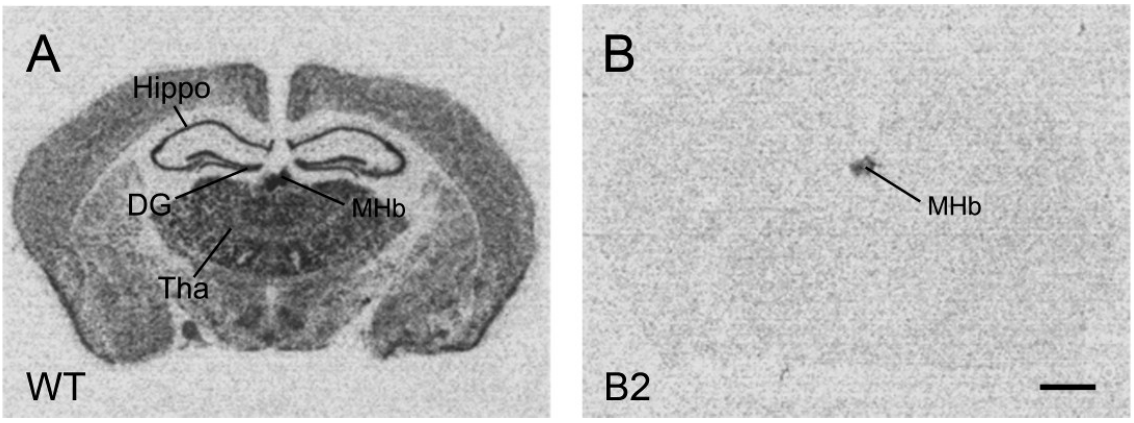

Figure II-1. Expression of β2 nAChR subunit mRNA in WT but not β2-/- mice. Representative images of *in situ* hybridization with β2 nAChR antisense probe in adult wild type (WT) (***A***) and β2-/- (B2) (***B***) mouse brains. In β2 -/- mice, the hybridization signal was undetectable except for hybridization signal in the medial habenula nucleus (MHb), which could be the result of cross-reactivity between the rat β2 probe and mouse β4 mRNA, which is strongly expressed in the MHb. Bregma level -1.82 mm. Hippo, hippocampus. DG, dentate gyrus. Tha, thalamus. MHb, medial habenula nucleus. Scale bar: 1 mm.

All mice were anesthetized using isoflurane (IsoFlo, North Chicago, IL, USA) and euthanized by decapitation. The brains were rapidly dissected and frozen in isopentane at -20°C, and stored at -80°C until used. Using a cryostat, 15 μm thick coronal sections, 150 μm apart, were cut from Bregma level -1.28 mm to -2.21 mm and mounted onto glass microscope slides coated twice with gelatin (Spectrum, Gardena, CA, USA) and also with poly-L-Lysine (Sigma, St. Louis, MO, USA). The sections were post-fixed with 4% paraformaldehyde in 0.1 M phosphate buffer, pH 7.4, for 1 hour at room temperature (RT), washed in 0.1 M phosphate buffer three times, 5 minutes each, air-dried, and stored with desiccant at -20°C until used.

cRNA probe synthesis

Extraction of mouse brain RNA was done using Absolutely RNA Miniprep Kit (Stratagene, La Jolla, CA, USA). Templates for mouse SIRT1, Ku70, Nampt, FoxO3a, p53, and UCP5 were generated by reverse transcription-PCR (SuperScript III First-Strand Synthesis SuperMix for qRT-PCR, Invitrogen, Carlsbad, CA, USA) and subcloned into pPCR-Script Amp SK (+) (Stratagene, La Jolla, CA, USA) (Table II-1).

Table II-1. Primers sequence of genes

Gene	Number	Forward	Reverse
SIRT1 (643 bp)	NM_019812	ACC TCC TGT TGA CCG ATG GA	ATC CTT TGG ATT CCT GCA ACC TGC
Ku70 (724 bp)	AB010282	TAC AAG ATT TGG ACA ACC CAG GCG	ATC AAA CCT GGC TCA TCA AAC CGC
Nampt (910 bp)	AY679720	TTC CCG AGG GCT CTG TCA T	TTG GGA TCA GCA ACT GGG TCC TTA
FoxO3a (810 bp)	NM_019740	ACT CCA TCC GGC ACA ACC T	AGT CTG AAG CAA GCA GGT CTT GGA
p53 (954 bp)	NM_011640	ACC TCA CTG CAT GGA CGA TCT GTT	TCC TCT GTA GCA TGG GCA TCC TTT
UCP5 (523 bp)	AF155812	TCT AAG GGT GAA GTT TGC AAC GGC	AAT GAA GCT GCC AAT CAT GCT CCC

Plasmids were isolated using the QIAGEN Plasmid Maxi Kit (Qiagen, Valencia, CA, USA), linearized by restriction enzymes (Promega, San Luis Obispo, CA, USA) and sequenced to verify the orientation. A plasmid containing the full-length sequence for rat β2 nAChR subunit (2,196 bp) (Dr. J. Boulter, UCLA, CA, USA) was used as a template for the β2 cRNA probe. ^{35}S-labeled cRNA probes were synthesized in sense and

antisense orientations in the presence of ^{35}S-UTP (PerkinElmer Life Science, Boston, MA, USA) with T3 or T7 RNA polymerase (Life Technologies/Ambion, TX) by *in vitro* transcription.

In situ hybridization

Tissue sections were processed for *in situ* hybridization as previously described (Huang and Winzer-Serhan, 2007). Briefly, sections were pre-hybridized with 0.1 μg/ml proteinase K for 30 minutes at RT followed by 0.1 M triethanolamine and 0.25 % acetic anhydride. After overnight (16-20 hours) hybridization at 60°C, sections were treated with RNase A at 37°C for 30 minutes, and washed in 4X, 2X, 1X and 0.5X standard Saline Sodium Citrate (SSC) at RT followed by a hot wash in 0.1X SSC at 65°C for 30 minutes. Slides were dehydrated through graded series of alcohols and air-dried. Sections were apposed to BioMax MR film (Kodak, Rochester, NY, USA) along with [^{14}C]-standards of known radioactivity (Amersham, Code RPA 504L, Batch 21, Buckinghamshire, UK). After film exposure for one (Nampt, FoxoO3a, p53, UCP5) or two days (SIRT1, Ku70), the films were developed in D19 Kodak developer for 4 minutes, rinsed in water, and fixed in Kodak Rapid Fixer for 5 minutes.

Autoradiogram analysis

The hybridization signal of each gene was measured in CA1 and CA3 pyramidal cell layers and the granule cell layer of the dentate gyrus (DG). The entire cerebral cortex and MHb located on individual sections was measured. Quantitative analysis of

autoradiograms (density, nCi/g wet weight) was completed using a PC-based image analysis system (MCID basic, Imaging Research Inc. St. Catherine, Canada; now InterFocus Imaging Ltd, UK). A standard curve (raw optical density vs. nCi/g wet weight) was generated using the [^{14}C]-standards. Quantitative values determined from the autoradiograms were divided by their decay factors to obtain specific values based on the calibration day. Specific hybridization was determined by subtracting values for non-specific hybridization from total values.

Neocortex thickness

Using autoradiographic films from UCP5 cRNA hybridization, Bregma level -1.28 mm to -2.21 mm, images were captured at the level of the barrel fields of the primary somatosensory cortex according to the Mouse Brain Library atlas (Rosen et al., 2000). The thickness of the primary somatosensory cortex was measured at the area directly external to the CA2 of hippocampus from each picture (indicated in Figure II-2A and B) from the external border of layer I to the internal border of layer VI using NIH ImageJ 1.40 (Rasband, 1997-2011). The measurements were calibrated using a ruler imaged by MCID basic (60 pixels per mm).

Relative dorsal hippocampal volume

Tissue sections were stained with thionin (Sigma, St. Louis, MO, USA) and coverslipped. Four sections from each mouse, selected using systematically random sampling, each 150 μm apart, from Bregma level -1.28 mm to -2.21 mm, were

photographed using a microscope with a 4X objective (Nikon Eclipse E400) equipped with a camera (Nikon digital camera DXM 1200). Either the left or right side of the hippocampus was used for area measurements of the entire hippocampus. The measurements were calibrated using scale bars provided by the microscopy software NIS-Elements D 3.10 (165 pixels per mm). The granular cell layer of the DG in the upper and lower blade, and the pyramidal cell layer of CA1 and CA3 (hippocampus proper) were measured using NIH ImageJ 1.40. Volumes were calculated using the following formula based on the Cavalieri Method: volume = area × section thickness (15 μm) × number of skipped sections (10) between measured sections.

Neuron cell density

Frozen sections were warmed to RT and dried thoroughly for 30 minutes. The sections were then stained with ProLong® Gold antifade reagent containing 4'-6-diamidino-2-phenylindole (DAPI) (Invitrogen, Carlsbad, CA, USA), and allowed to dry overnight. DAPI-stained sections were examined using epifluorescence, and images were acquired using a Zeiss Axioplot2 research microscope (Carl Zeiss, Inc., Thornwood, NY, USA) equipped with a three-chip Hamamatsu video camera. Images were taken from seven different brain regions: CA1 and CA3 pyramidal cell layers, the granular cell layer and hilar region of the DG, and layer II/III, IV, and V/VI of the barrel field region of primary somatosensory cortex. Only cells with a large, round, euchromatic nucleus were counted as neurons.

Statistics

The expression of each gene was collected and analyzed independently from each other, because each gene was assessed from a different set of tissue sections. For age comparisons in WT mice gene expression, cortico-hippocampal area data were analyzed using two-way ANOVA (region and age). Data from gene expression in the MHb in WT mice were analyzed using Student's *t*-test (age was the only variable). For genotype comparison of gene expression at a specific age, percent control based on age-matched WT was used, which allowed us to combine data from two repeated experiments. The data were calculated leaving genotype as the only variable and therefore, analyzed using Student's *t*-test. For neuronal cell density, data were analyzed using two-way ANOVA (age and genotype). For cerebral cortex thickness, two-way ANOVA was used (age and genotype). A three-way ANOVA was used for the hippocampal volume study (region, age, and genotype). When a significant interaction was noted in a three-way ANOVA at the level of three variables, each individual category was further analyzed by a two-way ANOVA; when significant interactions were noted in a three-way ANOVA at the level of two variables or in a two-way ANOVA, each individual category was further analyzed by a one-way ANOVA; when no interaction was noted, the ANOVA was followed by a Tukey's post hoc test if the collected model p-value was significant. When a main effect was noted in a two-way ANOVA when the collected model p-value was significant, the p-value of the main effect was further analyzed by a Tukey's post hoc test. All statistics were carried out using PC-based SPSS 15.0. Significance was defined as $p < 0.05$.

RESULTS

Morphological and histological changes in middle-aged β2-/- male mice

Cortical thinning is accelerated in middle-aged β2-/- mice compared to age-matched wild type mice.

Cortical hypotrophy has been reported in the somatosensory cortex of 22 to 24-month-old β2-/- mice compared to age matched WT controls (Zoli et al., 1999). Here we examined changes in 18-month-old (middle-aged) WT and β2-/- mice to determine whether signs of aging were already detectable in this age group. Eighteen-month-old WT mice showed a significant 10.16 % decrease in thickness in primary somatosensory cortex compared to 3-month-old WT mice (two-way ANOVA: main effect of age, $F(1, 21) = 14.49$, $p = 0.001$; main effect of genotype, $F(1, 21) = 0.055$, $p = 0.817$; genotype by age interaction, $F(1, 21) = 0.891$, $p = 0.356$. WT 3-month-old: 1.1 mm, WT 18-month-old: 0.98 mm, Tukey's post hoc test: $p = 0.053$) (Figure II-2A, C and E). There was no difference in cortical thickness between 3-month-old WT and β2-/- mice, but eighteen-month-old β2-/- mice had a more robust 16.45 %, decrease in the same region compared to 3-month-old β2-/- mice (β2-/- 3-month-old: 1.12 mm, β2-/- 18-month-old: 0.94 mm, Tukey's post hoc test: $p = 0.01$) (Figure II-2B, D and E). Cortical thinning, while characteristic for the normal aging cortex, was accelerated in middle-aged β2-/- mice.

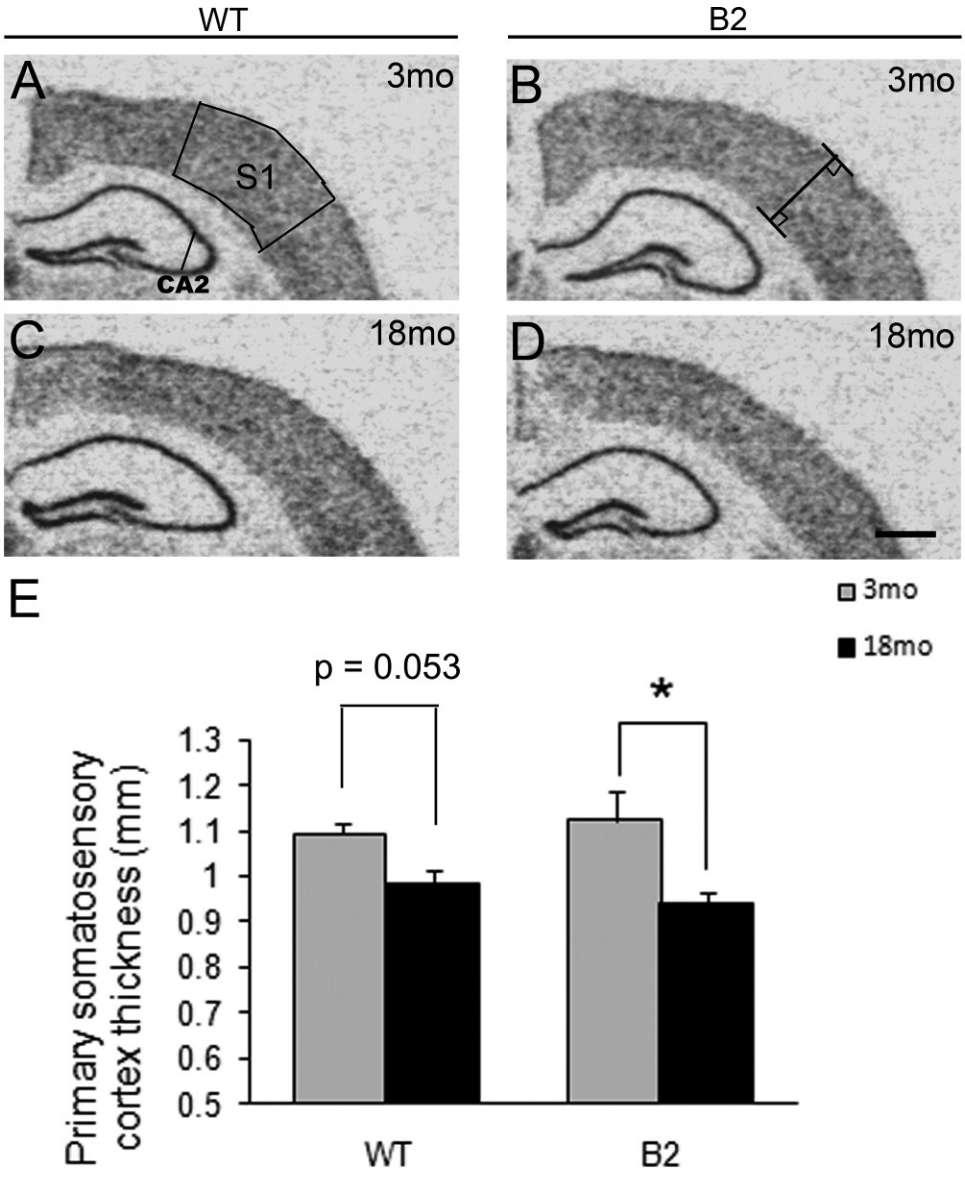

Figure II-2. Primary somatosensory cortex thickness was significantly decreased in middle-aged β2-/- mice. ***A-D***, Representative images of *in situ* hybridization with UCP5 antisense probe in 3-month-old (3mo) WT. Schematic diagrams in ***A*** shows the cortical area in which of thickness measurement (indicated in ***B***) was taken. (***A***), 3-month-old β2-/- (***B***), 18-month-old (18mo) WT (***C***), and 18-month-old β2-/-(***D***) mouse brains, showing the primary somatosensory cortex (S1). Bregma level -1.82 mm. Scale bar: 1 mm. ***E***, Quantification of the primary somatosensory cortex thickness. Error bars: standard error of the mean (SEM). Two-way ANOVA, age vs. genotype, Tukey's post hoc test, * $p < 0.05$.

A reduction in cortical thickness is often accompanied by a change in neuronal cell density. To determine neuronal density in WT and β2-/- mice, DAPI stained nuclei were counted in defined areas (WT 3-month-old, n = 4; WT 18-month-old, n = 11; β2-/- 3-month-old, n = 4; β2-/- 18-month-old, n = 8). In cortical layers II/III, 18-month-old WTs had significantly higher neuronal density compared to 3-month-old WT mice (two-way ANOVA: main effect of genotype, $F(1, 23) = 0.914$, $p = 0.349$; main effect of age, $F(1, 23) = 11.145$, $p = 0.003$; genotype by age interaction, $F(1, 23) = 4.525$, $p = 0.044$; Tukey's post hoc test: $p = 0.005$). However, 3-month-old β2-/- mice exhibited a significantly higher density of neurons compared to age-matched WT mice (Tukey's post hoc test: $p = 0.012$) (Figure II-3A and B), but there was no further increase in density with age in β2-/- mice. In layers V/VI, neuronal density was increased in 18-month-old WT mice compared to 3-month-old WT mice (two-way ANOVA: main effect of genotype, $F(1, 23) = 0.578$, $p = 0.455$; main effect of age, $F(1, 23) = 5.483$, $p = 0.028$; genotype by age interaction, $F(1, 23) = 3.185$, $p = 0.087$; Tukey's post hoc test: $p = 0.025$) (Figure II-3C and D). In young β2-/- mice a trend towards increased neuronal density was detected in layers V/VI compared to young WT mice with no further increase with age. Together these results show that cortical alterations were already present in young adult β2-/- mice prior to any age-related changes seen in WT mice.

Difference in relative dorsal hippocampal volume is due to a smaller granular cell layer in the dentate gyrus of middle-aged β2-/- mice.

The hippocampus is an important area with respect to aging and cognitive function. Although aged rodents exhibit functional hippocampal decline (Deupree et al., 1993) and significant deficits in spatial memory (Barnes, 1987), several studies have indicated that age-related decreases in hippocampal area, volume or cell density do not

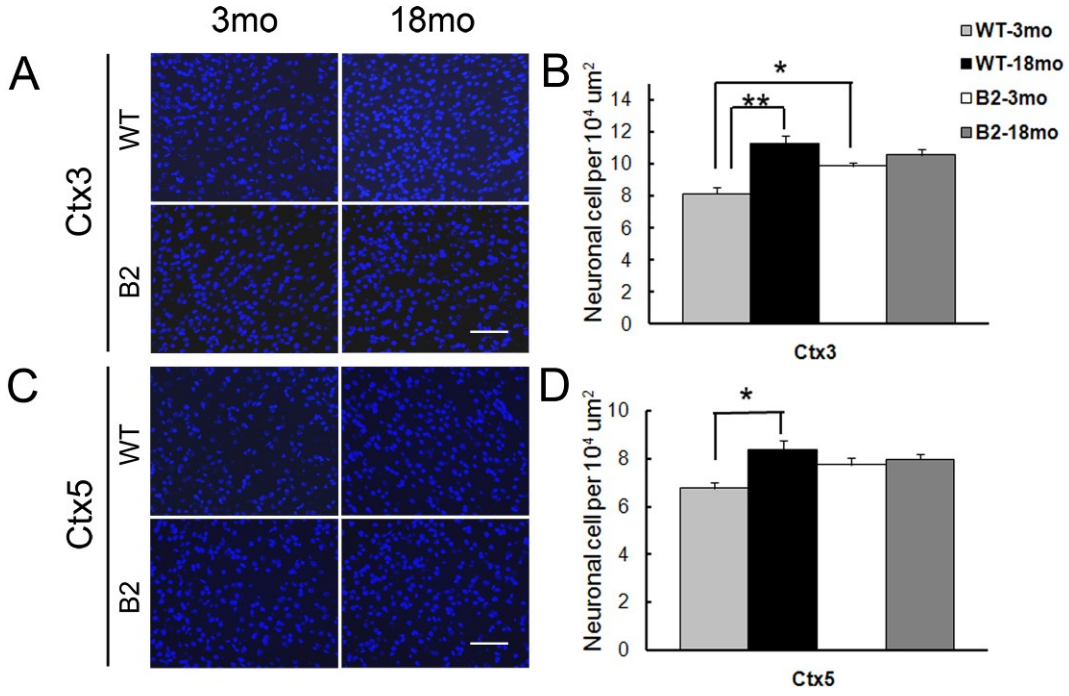

Figure II-3. Neuronal cell density increased in middle-aged WT and young adult β2-/- mice compared to young adult WT mice. Neuronal cell densities were counted in primary somatosensory cortex layer II/III (Ctx3) (***A, B***), and primary somatosensory cortex layer V/VI (Ctx5) (***C, D***). ***A and C***, Representative images of the DAPI stained sections. Bregma level -1.82 mm. Scale bars: 100 μm. ***B and D***, Quantification of neuronal cell density. Error bars: SEM. Two-way ANOVA, age vs. genotype, Tukey's post hoc test, * $p < 0.05$, ** $p < 0.01$.

occur until very old age (Rasmussen et al., 1996; Calhoun et al., 1998; von Bohlen und Halbach and Unsicker, 2002). Since β2-/- mice exhibited premature age-related changes in the cortex, it is possible that signs of aging might already appear in the hippocampus of 18-month-old β2-/- mice. The relative volume of the dorsal hippocampal was determined in young and middle-aged WT (n = 4, n =11, respectively), and β2-/- mice (n = 4; n = 8, respectively). Hippocampal volume increased significantly by 16.6% in 18-month-old WT compared to 3-month-old WT mice, whereas in β2-/- mice, a non-significant trend towards a 11.8 % increase was detected (two-way ANOVA: main effect of genotype, $F(1, 23) = 0.303$, $p = 0.587$; main effect of age, $F(1, 23) = 8.50$, $p = 0.008$; genotype by age interaction, $F(1, 23) = 0.244$, $p = 0.626$. WT 3-month-old: 1.23 mm^3, WT 18-month-old: 1.44 mm^3, Tukey's post hoc test: $p = 0.018$; β2-/- 3-month-old: 1.23 mm^3, β2-/- 18-month-old: 1.38 mm^3, Tukey's post hoc test: $p = 0.161$) (Figure II-4A). To further elucidate whether the age-related change in hippocampal volume also affected the principal cell layers, we measured the volume of the granular cell layer of the DG and pyramidal cell layer of the hippocampus proper (CA1/CA2 and CA3). The DG granule cell layer volume significantly increased by 19.0 % in 18-month-old compared to 3-month-old WT mice. However, in β2-/- mice there was no change in granule cell layer volume in the DG with age (-4 %) (three-way ANOVA (two regions, dentate gyrus granular cell layer and CA pyramidal cell layer, were considered as another variable here): main effect of region, $F(1, 46) = 145.0$, $p < 0.0001$; main effect of genotype, $F(1, 46) = 1.731$, $p = 0.195$; main effect of age, $F(1, 46) = 11.12$, $p = 0.002$; genotype by region interaction, $F(1, 46) = 0.017$, $p = 0.896$; genotype by age interaction, $F(1, 46) =$

3.186, p = 0.081; region by age interaction, F(1, 46) = 2.252, p = 0.14; genotype by region by age interaction, F(1, 46) = 1.288, p = 0.262. WT 3-month-old: 0.087 mm^3, WT 18-month-old: 0.103 mm^3, Tukey's post hoc test: p = 0.022; β2-/- 3-month-old: 0.092 mm^3, β2-/- 18-month-old: 0.088 mm^3, Tukey's post hoc test: p = 0.527) (Figure II-4B). Thus, a significantly larger granule cell layer was detected in 18-month-old WT mice but not β2-/- mice (Tukey's post hoc test: p = 0.007) (Figure II-4B). In contrast, the pyramidal cell layer of the hippocampus proper exhibited significantly increased volume with age in both WT and β2-/- mice (WT 3-month-old: 0.127 mm^3, WT 18-month-old: 0.146 mm^3, Tukey's post hoc test: p = 0.04; β2-/- 3-month-old: 0.125 mm^3, β2-/- 18-month-old: 0.139 mm^3, Tukey's post hoc test: p = 0.049) (Figure II-4C).

Neuronal density was determined in different hippocampal regions and the density was significantly higher in the hilar region of the DG in 18-month-old β2-/- mice compared to age-matched WT mice (two-way ANOVA: main effect of genotype, F(1, 23) = 7.44, p = 0.012; main effect of age, F(1, 23) = 0.081, p = 0.779; genotype by age interaction, F(1, 23) = 0.797, p = 0.381; Tukey's post hoc test: p = 0.003) (Figure II-5C and D). In the pyramidal cell layer of the CA3 region of the hippocampus, 3-month-old β2-/- mice had significantly higher neuronal density compared to 18-month-old β2-/- mice, and there was a trend towards higher density in 3-month-old β2-/- mice compared to age-matched WT mice (two-way ANOVA: main effect of genotype, F(1, 23) = 2.027, p = 0.168; main effect of age, F(1, 23) = 0.714, p = 0.407; genotype by age interaction, F(1, 23) = 6.47, p = 0.018, Tukey's post hoc test: p = 0.012 and 0.066, respectively) (Figure II-5E and F). In contrast, no differences were detected in neuronal cell densities

in the granular layer of the DG and pyramidal layer of CA1 region between young and aged mice or between genotypes (data not shown).

Thus, in WT mice, cortical thickness decreased and neuronal density increased with age, whereas hippocampal volume increased but neuronal density remained the same, suggesting that aging affects the cortex at a younger age than the hippocampus. In contrast, in β2-/- mice cortical thickness decreased more drastically and neuronal density was already significantly higher in 3-month-old β2-/- mice compared to age-matched WT mice. This suggests that loss of β2* heteromeric nAChRs affects the cortex at a young age, perhaps setting it up for higher sensitivity to aging-related insults. In the hippocampus, which seemed unaffected by aging in WT mice, a significant difference in DG granular cell layer volume and increased neuronal density in the hilar region in middle-aged β2-/- mice compared to age-matched WT mice suggested that loss of β2* heteromeric nAChRs accelerated age-related changes in the hippocampus, a trend similar to that found in cortex.

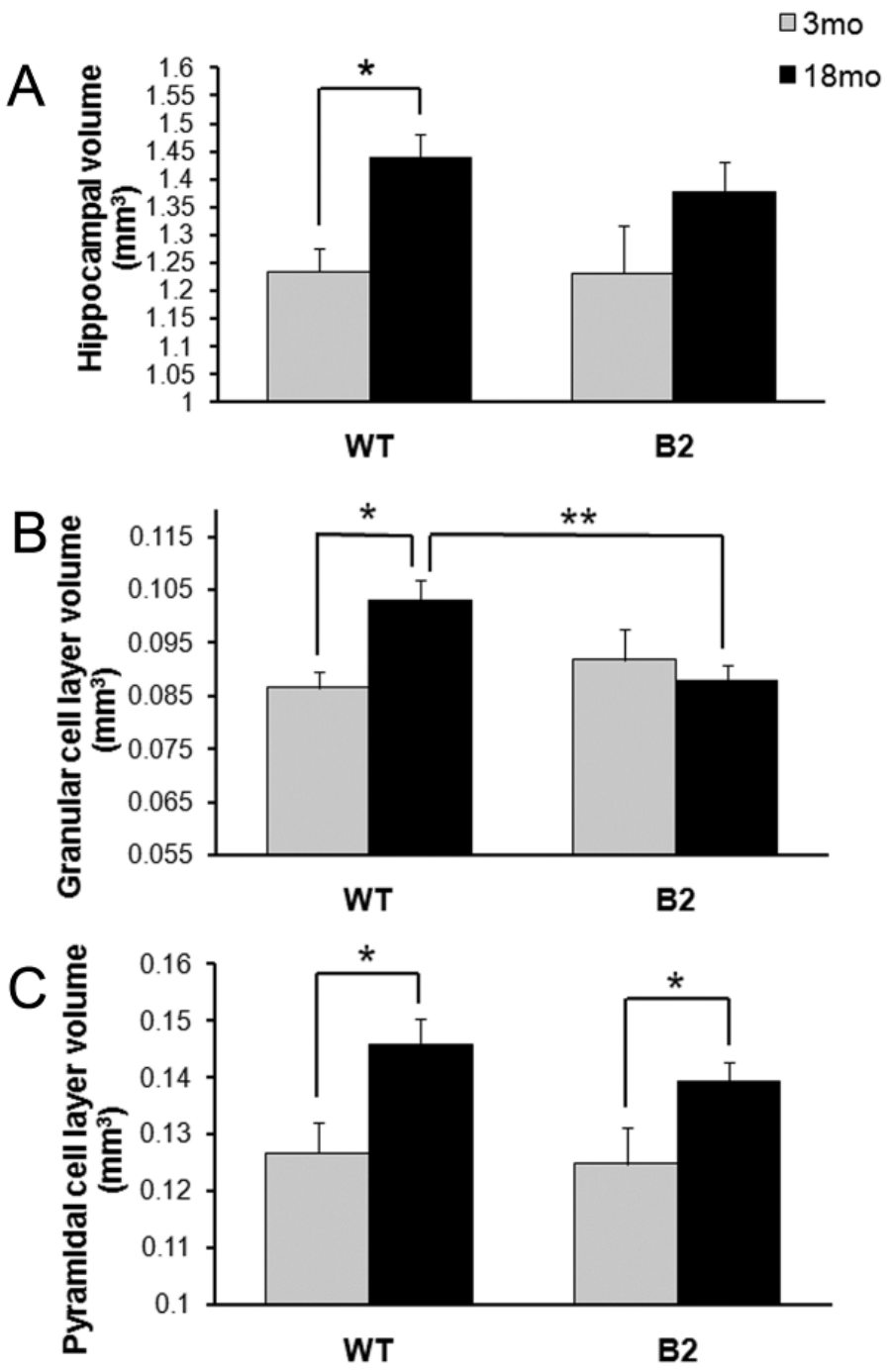

Figure II-4. Relative dorsal hippocampal volume increased with age in wild-type but not β2-/- mice. ***A***, Dorsal hippocampal volume measured from Bregma level -1.46 to -2.06. ***B***, Dentate gyrus granular cell layer volume. ***C***, Volume of hippocampal proper (CA1 and CA3) pyramidal cell layer. Error bars: SEM. Two-way ANOVA, age vs. genotype, One-way ANOVA each for age and genotype, * $p < 0.05$, ** $p < 0.01$.

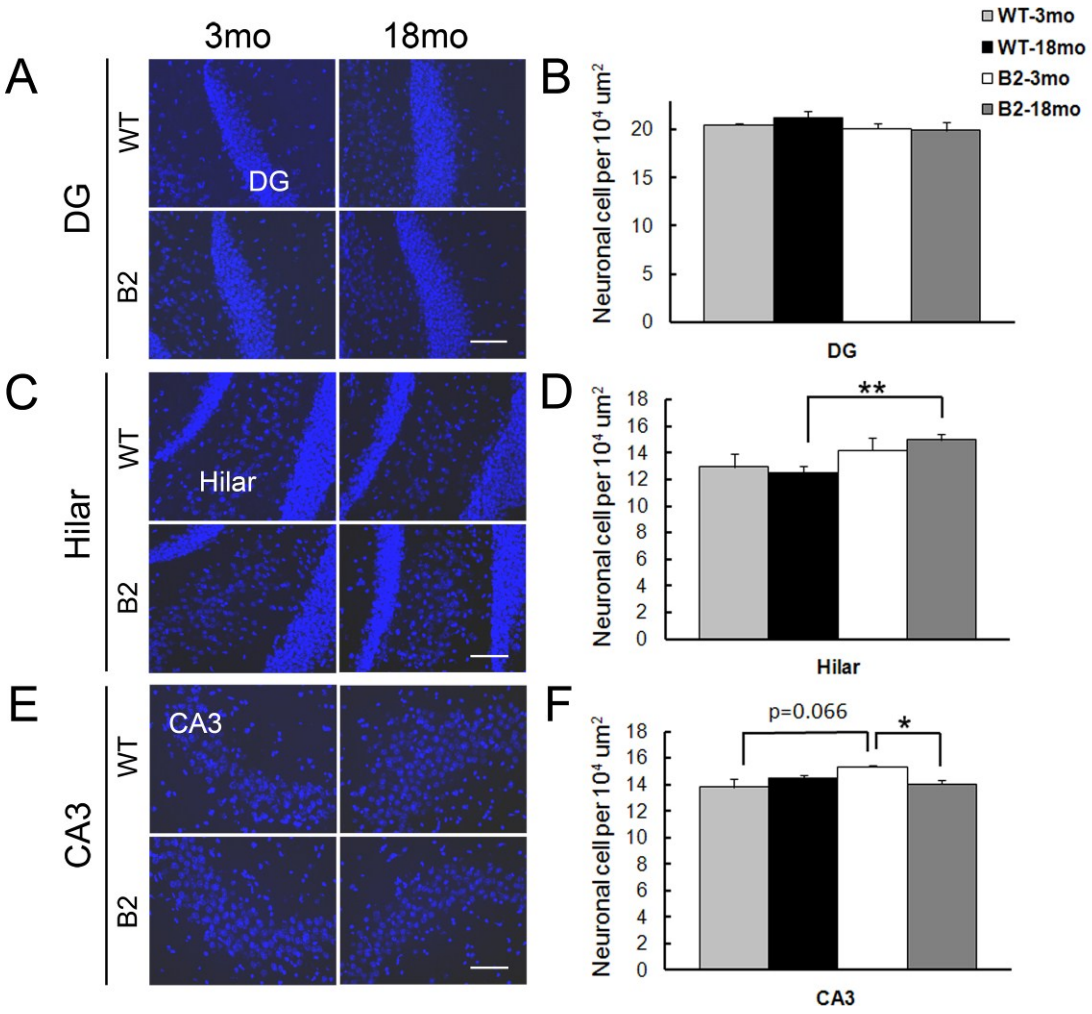

Figure II-5. Neuronal cell density was changed in the hippocampus. Neuronal cell density was measured in the granular cell layer of the dentate gyrus (***A, B***), hilar region of the dentate gyrus (***C, D***), and CA3 pyramidal cell layer of the hippocampus (***E, F***). ***A, C, and E*** show representative images of DAPI stained sections. Bregma level -1.82 mm. Scale bars: 100 μm. ***B, D, and F*** show quantification of neuronal cell density. Error bars: SEM. Two-way ANOVA, age vs. genotype, Tukey's post hoc test, * $p < 0.05$, ** $p < 0.01$.

Most longevity regulatory genes probed in this study are highly expressed in cortical structures and exhibit decreased expression levels with aging

Expression of longevity regulatory genes in adult mouse brain

Several longevity genes are linked to the aging process (Salminen and Kaarniranta, 2009). To determine the mRNA expression pattern of SIRT1 and other related longevity regulatory genes, we performed *in situ* hybridization in sections from 3-month-old WT mice using SIRT1, Nampt, Ku70, p53, FoxO3 and UCP5 antisense and sense cRNA probes to detect specific and non-specific hybridization, respectively (n = 4). Expression levels of mRNAs were quantified in several cortical and hippocampal regions including the granular cell layer of the DG, the pyramidal cell layer of CA1 and CA3 of hippocampus, the MHb and the neocortex. All sense probes exhibited low background hybridization signal indicating low levels of non-specific hybridization (Figure II-6A-C and 6G-I insets). The most intense *in situ* hybridization signal for SIRT1 mRNA was found in the hippocampus and MHb (Figure II-6A). SIRT1 was also broadly expressed in the cerebral cortex with increased expression intensity in layers II/III and V/VI (Figure II-6A). In thalamus and hypothalamus, moderate to low signal was detected with increased SIRT1 mRNA expression in the arcuate, ventromedial, and dorsomedial nuclei (Figure II-6A). Quantitative data demonstrated that the DG exhibited the highest mRNA expression, which was almost twice that of any other region measured, whereas SIRT1 mRNA levels in CA1 and CA3 were comparable to those found in the neocortex (Figure II-6D).

This is the first description of the mRNA expression pattern of Nampt and Ku70 in a rodent brain. The hybridization signal for Nampt was very strong in all fields of the hippocampus, and uniformly distributed moderate signal was observed in the neocortex (Figure II-6B). Higher levels of expression were also found in the claustrum and endopiriform nucleus, and in the MHb. Moderate to low levels were detected in the amygdala, thalamus and hypothalamus (Figure II-6B). Quantitative analysis of cortical structures showed that expression intensities for Nampt were highest in the granule layer of the DG and CA3 pyramidal layer; whereas, expression intensity was significantly lower in the neocortex (Figure II-6E).

Messenger RNA expression levels of Ku70 were high in the hippocampus, moderate in the neocortex and the MHb, and low to moderate in the thalamus and hypothalamus regions (Figure II-6C). Quantitative data showed that Ku70 mRNA was expressed highest in the DG followed by CA3, and CA1, with neocortex expressing the lowest level of mRNA among regions measured (Figure II-6F).

FoxO3 mRNA was strongly expressed in all fields of the hippocampus, neocortex, and piriform cortex in a pattern similar to that obtained with non-isotopic *in situ* hybridization (Hoekman et al., 2006) (Figure II-6G). In the neocortex, expression was strongest in cortical layers II/III and V/VI. In addition, expression of FoxO3 mRNA also was detected in the MHb and evenly distributed in the amygdala, thalamus and hypothalamus (Figure II-6G). Quantitative comparison of cortical structures showed that the highest expression level was found in the granule cell layer of the DG, followed by

similar expression levels in the pyramidal cell layer of CA1 and CA3 and the neocortex (Figure II-6J).

All fields of the hippocampus exhibited high levels of p53 mRNA expression. In the neocortex, p53 mRNA was evenly distributed through all layers, and p53 mRNA was also moderately expressed in the MHb (Figure II-6H). In the amygdala, thalamus and hypothalamus moderate, evenly distributed hybridization signals for p53 were found (Figure II-6H). This expression pattern in adult mouse brain is similar to that reported previously for rat brain (van Lookeren Campagne and Gill, 1998). Quantitative comparison revealed that among regions measured, p53 mRNA expression was highest in the DG, followed by the CA1 and CA3 and lowest in the neocortex (Figure II-6K).

UCP5 mRNA was expressed highly in the principal layers of CA1, CA3 and DG of the hippocampus. In the neocortex, moderate to high levels were detected with slightly increased expression in layers I and VI. Other areas such as the caudate putamen and amygdala also exhibited moderate levels, whereas expression levels were low in thalamus and hypothalamus with the exception of the MHb and a few hypothalamic nuclei, which is similar to the mRNA distribution pattern previously described (Sanchis et al., 1998) (Figure II-6I). Quantitative comparison of UCP5 measured in hippocampus and cortex showed that mRNA expression was highest in the DG, followed by CA1 and CA3 and lowest in neocortex (Figure II-6L).

Decreased expression of longevity regulatory genes in cortical regions of 18-month-old WT compared to 3-month-old WT mice

Although most longevity genes have been implicated to function in aging, it is not known how age affects their expression. Therefore, mRNA expression levels of longevity genes were determined in 18-month-old WT mice and compared to 3-month-old WT mice on a region-matched basis (3-month-old WT, n = 4; 18-month-old WT, n = 5). Except for SIRT1 (two-way ANOVA: main effect of age, $F(1, 28) = 2.05$, $p = 0.163$; main effect of region, $F(3, 28) = 106.4$, $p < 0.0001$; age by region interaction, $F(3, 28) = 0.209$, $p = 0.889$) and Nampt (two-way ANOVA: main effect of age, $F(1, 28) = 3.42$, $p = 0.075$; main effect of region, $F(3, 28) = 97.06$, $p < 0.0001$; age by region interaction, $F(3, 28) = 1.353$, $p = 0.277$) (Figure II-6D, E), the other four genes showed a significant general age effect with 18-month-old WT mice exhibiting lower mRNA expression levels than 3-month-old animals (two-way ANOVA, main effect of age: Ku70, $F(1, 28) = 103.9$, $p < 0.0001$; FoxO3, $F(1, 28) = 4.32$, $p = 0.047$; p53, $F(1, 28) = 16.44$, $p < 0.0001$; UCP5, $F(1, 28) = 5.55$, $p = 0.026$; main effect of region: Ku70, $F(3, 28) = 287.5$, $p < 0.0001$; FoxO3, $F(3, 28) = 63.28$, $p < 0.0001$; p53, $F(3, 28) = 269.2$, $p < 0.0001$; UCP5, $F(3, 28) = 107.9$, $p < 0.0001$; age by region interaction: Ku70, $F(3, 28) = 6.012$, $p = 0.003$; FoxO3, $F(3, 28) = 0.305$, $p = 0.821$; p53, $F(3, 28) = 5.691$, $p = 0.004$; UCP5, $F(3, 28) = 0.496$, $p = 0.688$) (Figure II-6F and J-L). Ku70 had the strongest age-related effect, and the cortical regions examined showed significantly reduced Ku70 hybridization levels in 18-month old mice (Tukey's post hoc test: DG: 22.5%, $p = 0.001$; CA1: 19.1%, $p = 0.002$; CA3: 22.9%, $p = 0.001$; neocortex: 18.7%, $p = 0.001$) (Figure

II-6F). FoxO3 mRNA expression was significantly reduced in the neocortex by 20.3% (Tukey's post hoc test: $p = 0.018$) (Figure II-6J), and this reduction was significant in layers V/VI (15.7%) and a strong trend in layers II/III (14%) (two-way ANOVA: main effect of age, $F(1, 14) = 11.04$, $p = 0.005$; main effect of layer, $F(1, 14) = 28.19$, $p < 0.0001$; age by layer interaction: $F(1, 14) = 0.052$, $p = 0.824$; Tukey's post hoc test: $p = 0.043$ and 0.057, respectively). The strongest reduction in p53 mRNA expression was detected in the DG (18.3%) and CA3 (9.6%) (Tukey's post hoc test: $p = 0.012$ and 0.056 respectively) (Figure II-6K). There was a trend towards decreased UCP5 mRNA expression in CA3 (11.2%) between 3-month and 18-month-old mice (Tukey's post hoc test: $p = 0.079$) (Figure II-6L). Taken together, mRNA levels decreased with age for the longevity regulatory genes Ku70, FoxO3, p53 and UCP5 in the cortico-hippocampal area, with an especially significant decline for Ku70, whereas Nampt only showed a trend towards decreased expression in older animals (Figure II-6E).

Increased mRNA levels of SIRT1, Nampt and Ku70 in middle-aged β2-/- mice compared to age-matched WT mice in cortical regions

Because most genes we examined showed decreased mRNA levels in 18-month old WT mice, and 18-month old β2-/- mice exhibited a premature ageing in cortex and hippocampus, we hypothesized that mRNA expression levels would be further decreased in cortical regions of middle-aged β2-/- mice compared to age-matched WT mice. To test this hypothesis, we performed *in situ* hybridization with the same set of genes on 3- and 18-month-old β2-/- mice (WT 3-month-old, n = 7; WT 18-month-old, n = 11; β2-/-

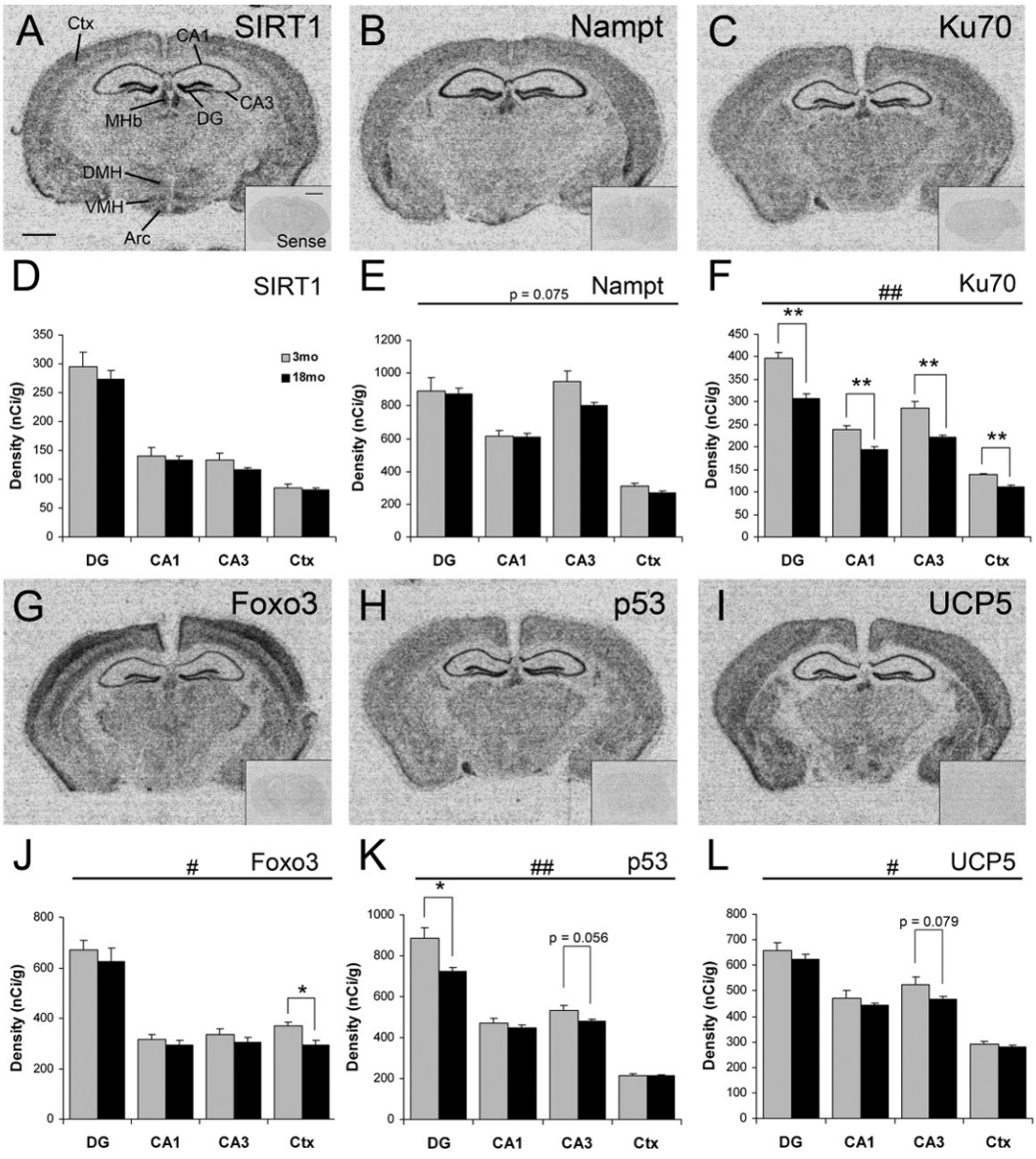

Figure II-6. Ku70, FoxO3, p53 and UCP5 mRNA expression levels were decreased in cortico-hippocampal regions in middle-aged wild-type mice. ***A-C and G-I***: Representative autoradiographic images of *in situ* hybridization for SIRT1 (***A, D***), Nampt (***B, E***), Ku70 (***C, F***), FoxO3 (***G, J***), p53 (***H, K***), and UCP5 (***I, L***) derived with antisense probes in 3-month-old WT mice. Insets: sense probes. Bregma level -1.82 mm. Scale bar: 1 mm. Scale bar of inset: 2 mm. ***D-F and J-L***, Quantification of mRNA expression intensities of each gene in the granular cell layer of the dentate gyrus (DG), pyramidal cell layer of CA1 and CA3 of the hippocampus, and the neocortex (Ctx). Error bars: SEM. Two-way ANOVA, age vs. region, # general age effect $p < 0.05$, ## general age effect $p < 0.01$, Tukey's post hoc test, * $p < 0.05$, ** $p < 0.01$.

3-month-old, n = 7; β2-/- 18-month-old, n = 8). *In situ* hybridization patterns were identical between WT and β2-/- young and adult mice suggesting that there were no qualitative changes in mRNA distributions in response to loss of β2* heteromeric nAChRs. For quantitative analysis, mRNA expression levels were analyzed in the granular cell layer of the DG, pyramidal cell layer of CA1 and CA3 of the hippocampus and neocortex. In young adult β2-/- mice, mRNA expression levels were not significantly different from WT mice for any of the genes tested, although there were trends towards higher Nampt mRNA expression in CA1 and lower Ku70 mRNA expression in the DG of 3-month-old β2-/- mice compared to WT mice (Student's *t*-test, $p = 0.061$ and 0.066, respectively) (Figure II-7A, C and E).

In middle-aged β2-/- mice, mRNA expression levels were comparable to age-matched WT mice for p53, FoxO3, and UCP5 ($p > 0.05$). However in 18-month-old mice, SIRT1 mRNA expression intensity was significantly affected by genotype demonstrating increased mRNA expression in the DG and CA3 (Student's *t*-test, $p = 0.024$ and 0.039 respectively) (Figure II-7B). Nampt mRNA expression was significantly increased in middle-aged β2-/- compared to age-matched WT mice in CA3 (Student's *t*-test, $p < 0.001$) (Figure II-7D). Eighteen-month-old β2-/- mice also exhibited increased mRNA levels of Ku70 compared to age-matched WT mice. The up-regulation of Ku70 mRNA levels was significant in all cortical regions tested including the DG, CA1 and CA3 of the hippocampus and neocortex (Student's *t*-test, DG: $p = 0.012$, CA1: $p = 0.04$, CA3: $p = 0.017$, neocortex: $p = 0.007$) (Figure II-7F).

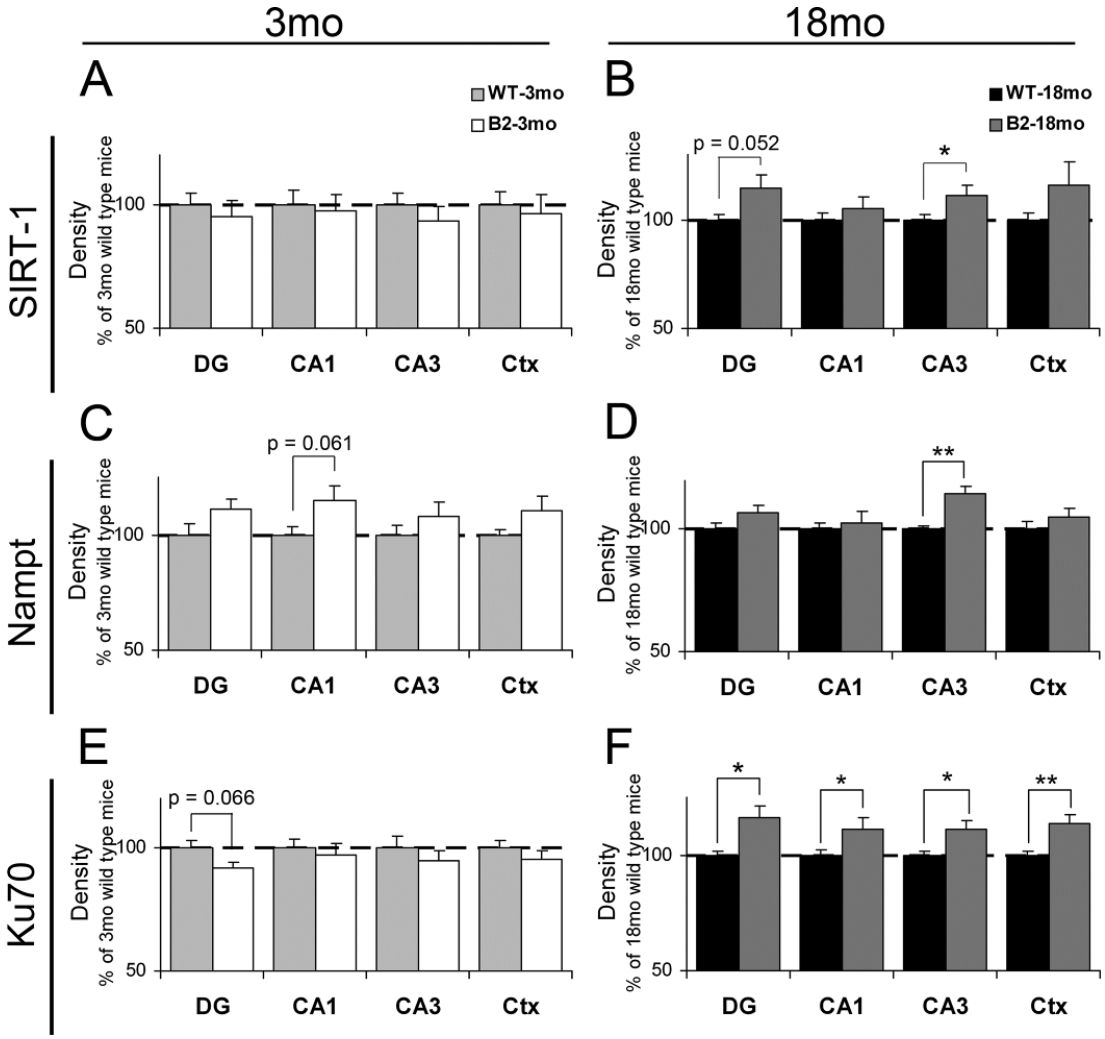

Figure II-7. SIRT1, Nampt, and Ku70 mRNA expression levels were increased in cortico-hippocampal regions in middle-aged β2-/- compared to age-matched wild-type mice. Quantification of mRNA expression of SIRT1 (***A, B***), Nampt (***C, D***), and Ku70 (***E, F***) in 3-month-old (***A, C, and E***) and 18-month-old (***B, D, and F***) WT and β2-/- mice. Regions measured included granular cell layer of the dentate gyrus (DG), CA1 and CA3 pyramidal cell layer of the hippocampus, and neocortex (Ctx). Data were presented as % control of WT at both ages. Error bars: SEM. Student's *t*-test, * $p < 0.05$, ** $p < 0.01$.

Similar changes of longevity regulatory gene expression levels in MHb

The MHb, a brain area with strong expression of nAChRs (Quick et al., 1999; Grady et al., 2009), also exhibited medium to high signals of hybridization for all longevity regulatory genes probed (Figure II-6). Therefore, we determined if similar age- and phenotype-related changes in gene expression levels took place, compared to those seen in cortical structures. The mRNA levels between 3-month-old and 18-month-old WT mice (3-month-old WT, n = 4; 18-month-old WT, n = 5) and between β2-/- mice and age-matched WT (WT 3-month-old, n = 7; WT 18-month-old, n = 11; β2-/- 3-month-old, n = 7; β2-/- 18-month-old, n = 8) were measured and compared in the MHb. In agreement with our cortico-hippocampal data, significant age-related decreases in expression intensities were found for Nampt, Ku70, p53 and UCP in middle-aged compared to young WT mice (Student's *t*-test, Nampt: 16.2%, p = 0.027; Ku70: 22.3%, p = 0.042; p53: 28.1%, p = 0.01; UCP5: 17.9%, p = 0.01) (Figure II-8A). Only SIRT1 and FoxO3 mRNA expression exhibited no change. In 3-month old mice, phenotype did not affect the expression intensity in the MHB of any gene tested (data not shown). At 18 months of age, most longevity regulatory genes showed increased mRNA levels in β2-/- mice compared to age-matched WT except for FoxO3 and UCP5 (Student's *t*-test, SIRT1: p = 0.042; Nampt: p = 0.042; Ku70: p = 0.023; p53: p = 0.047) (Figure II-8B).

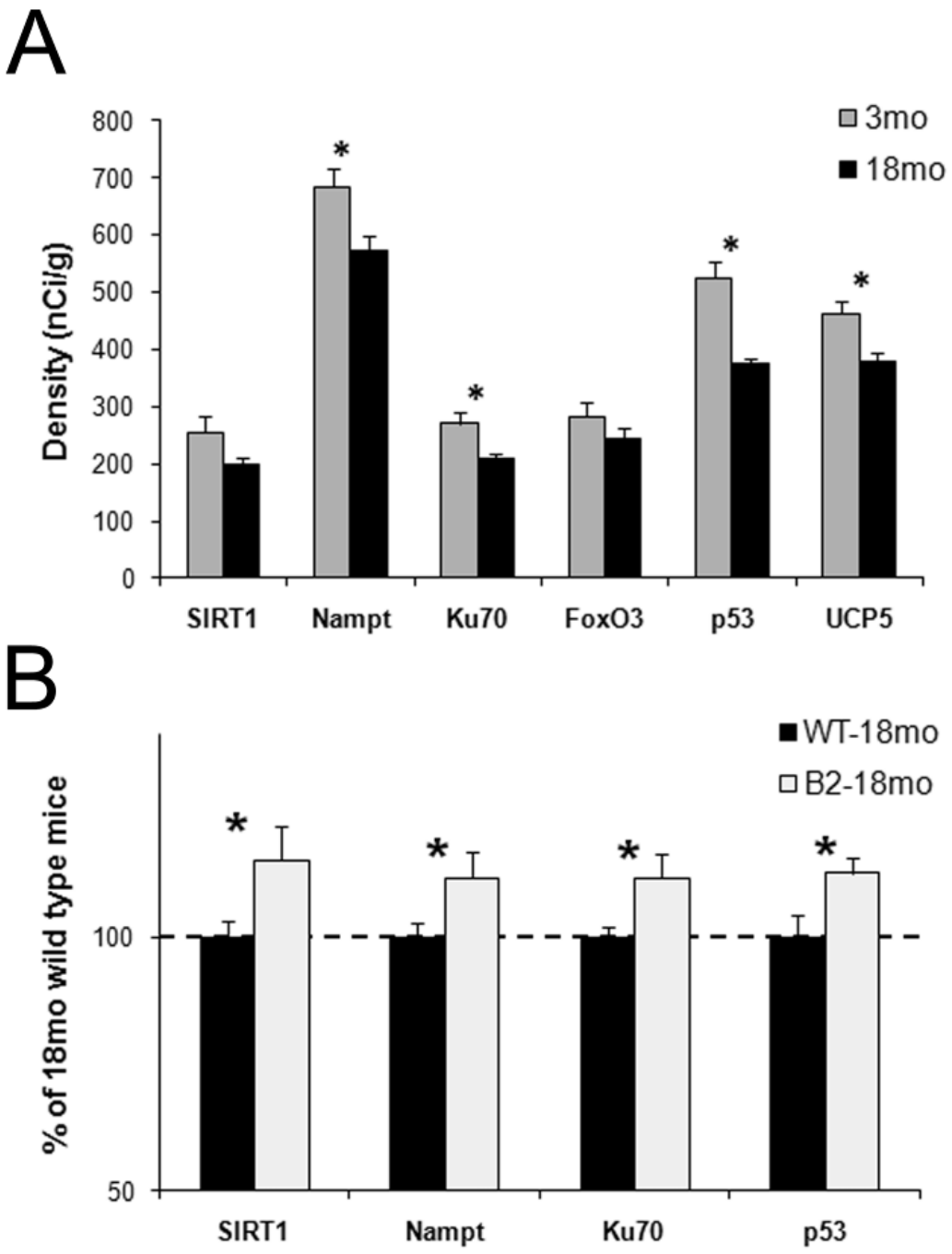

Figure II-8. Changes of survival gene expression observed in medial habenula (MHb) are similar to those in cortico-hippocampal areas. ***A***, Quantification of mRNA expression levels in the MHb of 3-month- and 18-month-old wild-type mice. ***B***, Comparison of mRNA levels of SIRT1, Nampt, Ku70 and p53 in 18-month-old WT and 18-month-old β2-/- mice. Error bars: SEM. Student's *t*-test, * $p < 0.05$.

DISCUSSION

Anatomical changes in middle-aged WT and β2-/- mice

The nicotinic cholinergic system is critically involved in the aging process, and its impairment is often correlated with human dementia (Picciotto and Zoli, 2008b). A previous study had shown that mice lacking high affinity heteromeric β2* nAChRs exhibit enhanced age-related cortical atrophy in 22- to 24-month old mice (Zoli et al., 1999). In this study we show that an age-related decline in cortical thickness is already enhanced in middle-aged, 18-month-old β2-/- mice, and that anatomical alterations in the cortex in the form of increased neuronal density can be detected in young, 3-month-old, β2-/- mice. Thus, lack of β2* heteromeric nAChRs affects anatomical features in young adults, prior to a functional cognitive decline (Zoli et al., 1999). The increase in neuronal density at an early age in β2-/- mice suggests a decrease in synaptic connectivity, and the age-related decrease in cortical thickness without further increase in cell density likely reflects increased neuronal loss in the neocortex of β2-/- mice. This finding is supported by similar results in β2-/- mice exhibiting enhanced neuronal loss of spiral ganglion neurons underscoring the importance of β2* nAChR to prevent early neuronal aging not only in the brain but also in peripheral neurons (Bao et al., 2005). However, it is possible that the observed differences, in particular those that indicate a small although significant difference between young and middle-aged WT mice were the result of different housing conditions and/or colonies, since the middle-aged WT mice were obtained from an outside source.

In the hippocampus, there was an age-related increase in hippocampal volume in WT mice in all hippocampal fields. Additional experiments indicated that the hippocampal volume increases up to 12 months of age in WT mice and remained constant thereafter (data not shown). This significant increase in dorsal hippocampal volume was not detected in β2-/- mice. Specifically, the volume increased in CA1 and CA3 regions of the dorsal hippocampus but not in the DG. The DG is a known site for cell proliferation throughout adulthood, where new cells primarily differentiate into granular neurons and form axonal connections with the major hippocampal subfields (Stanfield and Trice, 1988; Cameron et al., 1993; Hastings and Gould, 1999). These results suggest that initially the DG develops normally in β2-/- mice, but adult neurogenesis is either decreased, survival of newly generated neurons is impaired, or both. These results are supported by the observations that in young β2-/- mice the rate of proliferation in the DG and the survival of newly born cells are not affected (Mechawar et al., 2004). However, in older animals hippocampal neurogenesis is significantly lower in β2-/- mice compared to age-matched WT mice (Harrist et al., 2004). Taken together, functional β2* heteromeric nAChRs seem to be important for synaptic integrity, neuronal survival, and adult neurogenesis, although, the underlying mechanisms remain unknown.

Expression of survival genes in young and middle-aged WT mice

In this study we described expression patterns for six different survival genes: SIRT1, Nampt, Ku70, p53, FoxO3, and UCP5, which is the first time mRNA

distributions for Nampt, Ku70 and p53 have been described in adult mouse brain. SIRT1 mRNA, which was expressed throughout the forebrain, was not changed in middle-aged animals compared to young mice in either cortex hippocampus or MhB, and thus was the only gene that was completely unaffected by aging in cortical structures. This finding is in line with other reports that SIRT1 mRNA levels remain unchanged despite significantly increased protein levels in response to fasting (Kanfi et al., 2008; Ramadori et al., 2008) suggesting that SIRT1 protein levels are not necessarily correlated with gene expression.

Nampt is the rate-limiting component in the biosynthesis pathway of NAD. Studies indicate that an age-related decline in Nampt-regulated NAD synthesis could contribute to reduced SIRT1 activity and subsequently affect neuronal viability (van der Veer et al., 2007; Borradaile and Pickering, 2009). Nampt, which was strongly expressed in the hippocampus, especially in the DG and CA3, exhibited a trend ($p = 0.075$) towards decreased expression in middle-aged WT mice. Thus, decreased Nampt expression and activity in middle-aged and especially senescent animals could affect SIRT1 function thereby reducing SIRT1-mediated protection, which could result in decreased vitality of the aging brain.

Ku70, which can be co-immunoprecipitated with the deacetylase SIRT1 (Cohen et al., 2004a), mediates DNA repair and maintenance of mitochondrial integrity. Decreased acetylation of Ku70 results in increased binding to and repair of double-stranded DNA (Smith and Jackson, 1999). Ku70-/- mice have increased developmental cortical apoptosis due to decreased repair of double-strand DNA breaks created by

oxidative damage (Narasimhaiah et al., 2005). This crucial function of Ku70 might also play a critical role in the mature brain, and in particular in metabolically active areas such as hippocampus, cortex and MHb where strong Ku70 mRNA expression was detected. Ku70 mRNA expression was negatively correlated with aging in all cortical and hippocampal areas and in the MHb, and exhibited the most dramatic and widespread decline of all genes investigated. A similar negative correlation of Ku70 expression with age has been detected in aged but cycling, non-neuronal cells (Ju et al., 2006; Prall et al., 2007). Decreased expression of Ku70 would leave neurons vulnerable to oxidative DNA damage, which increases with age (Lovell and Markesbery, 2007). This effect might be even more dramatic considering that NAD-dependent SIRT1 function might be reduced in the aging brain due to decreased levels of NAD. An increase in Ku70 acetylation would reduce its activity, which could further increase vulnerability of aged neurons to toxic insults.

FoxO3 forms a complex with SIRT1 in response to stress, leading to enhanced stress resistance in mammalian dividing cells (Brunet et al., 2004). There was striking overlap between the mRNA expression pattern of SIRT1 and FoxO3 suggesting that those genes are associated, and could form SIRT1/FoxO3 complexes in neurons, similar to those seen in non-neuronal cells. The age-related decrease of FoxO3 mRNA expression in hippocampus and cortex detected here suggest a reduced ability to form FoxO3/SIRT1 complexes, which could have implications for neuronal survival. However, future studies need to determine if, indeed, FoxO3 and SIRT1 form complexes in cortex or hippocampus and if complex formation is altered during aging.

Our study detected substantial expression of p53 mRNA in hippocampus, cortex and MHb at a time of very little cell cycling or cell death in young adults, and an age-related decline of expression levels (Buss et al., 2006; Sibille et al., 2007). Whether p53 mRNA is translated into protein in the CNS, and is involved in cell division or cell death remains unknown. High expression of p53 has also been detected in the developing rat brain (van Lookeren Campagne and Gill, 1998), and disruption of p53 causes abnormal brain development in mice (Armstrong et al., 1995). Thus, in addition to its widely known role in apoptosis, p53 might have an alternative function as a regulator of gene targets that stabilize non-dividing cells like neurons. Furthermore, its apoptotic function might be diminished in the brain because of deacetylation of p53 by SIRT1. Deacetylation decreases binding of p53 to its target sequences and represses transcriptional activity, thereby suppressing p53-mediated apoptosis (Bitterman et al., 2002). Since SIRT1 is expressed in the same brain areas and most likely in the same neurons, SIRT1 could shift the function of p53 to cell protection rather than cell death. If this is the case, then p53 expression might be beneficial in the mature brain, and age-related decreased expression together with reduced expression of Ku70 and FoxO3, could further contribute to decreased neuronal vitality of neurons.

UCP5 also is expressed in the adult brain (Andrews et al., 2005). Uncoupling activity results in reduced oxidative stress and decreased mitochondrial membrane potential with subsequently reduced cell death (Liu et al., 2006). This process could contribute to the proposed neuroprotective function of UCPs, which might be particularly important in high energy consuming areas such as hippocampus, cortex and

MHb (Kim-Han et al., 2001), where UCP5 is robustly expressed. The expression of UCP5 mRNA in the hippocampus, cortex and MHb decreased with age. This could increase oxidative stress, but also decrease calcium regulation which might influence synaptic plasticity and neurotransmission, and subsequently reduce neuronal survival (Andrews et al., 2005).

Taken together, the expression of the longevity gene SIRT1 and several of its target genes are robust in cortex, hippocampus and MHb of young adult mice. However, decreased expression of several genes is evident in middle-aged, 18-month-old mice. The similar regulatory pattern between cortical structures and the MHb suggest a similar regulation of gene expression in different brain regions, and might also apply to other areas not included in this analysis. The combination of decreased Nampt, FoxO3, Ku70 and UCP5 expression could render the brain more vulnerable to insults and neural damage prior to overt functional cognitive decline, and could contribute to the aging process.

Expression of survival genes in β2-/- mice

β2-/- mice showed increased age-related atrophy in cortex and hippocampus, and alterations in cortical and hippocampal structures were already detected in young adults underscoring the importance of normal heteromeric nAChRs function in deterring early aging in the adult brain. Heteromeric nAChRs are also involved in the regulation of body weight (Huang and Winzer-Serhan, 2007), and can be tied to the insulin/IGF-1 signaling pathway (Sugano et al., 2006), which has been implicated in the regulation of survival

genes by caloric restriction (Cohen et al., 2004b). Although, insulin/IGF-1 signaling might be deregulated in β2-/- mice, and could contribute to the accelerated brain aging, there was no difference between genotypes in any of the genes analyzed in young adult β2-/- and WT mice. This suggests that these genes are not directly affected by loss of β2* nAChRs in young animals. In contrast, middle-aged β2-/- mice exhibited increased Ku70 mRNA expression and although spatially restricted, increased expression levels of Nampt and SIRT1 compared to WT mice. Together these data suggest that the early onset of brain aging in β2-/- mice is not the result of decreased expression of survival genes, and indicates an alternative mechanism by which heteromeric nAChR activation provides neuroprotection. However, in older animals, loss of nAChRs in β2-/- mice could potentially increase neurotoxic stress, which then could result in increased expression of certain survival genes such as Ku70, Nampt and SIRT1, in an attempt to provide neuroprotection similar to that seen with caloric restriction (Kim et al., 2007b). In support of this explanation, lack of serotonin 1B receptors which also results in early onset brain aging, is accompanied by increased expression of SIRT5 mRNA expression in cortex (Rosen et al., 2000).

CHAPTER III

LACK OF HIGH AFFINITY NICOTINIC ACETYLCHOLINE RECEPTORS DECREASES NUMBER OF GABAERGIC INTERNEURONS BUT NOT SYNAPTIC DENSITY IN THE HIPPOCAMPAL REGION OF MIDDLE-AGED MICE

SUMMARY

Loss of high affinity nicotinic acetylcholine receptors (nAChRs) in β2 knockout (β2-/-) mice has been correlated with accelerated neurodegeneration during aging, including, decreased cortical thickness, decreased hippocampal volume, and increased neuronal densities. These anatomical alterations could result from decreased connectivity due to loss of synapses or decreased dendritic arborization, or result from loss of neurons. In this study, we performed Golgi-Cox staining to investigate spine density and dendritic arborization, and we used immunohistochemistry (IHC) to localize synaptic markers: synapsin I and PSD95 for presynaptic vesicles and postsynaptic densities, respectively, and a marker for GABAergic neurons, glutamic acid decarboxylase (GAD) 67, to study synaptic and inhibitory interneuron densities. For Golgi-Cox staining, brains from 18-month-old male β2-/- and wild type (WT) mice were fixed and stained in Golgi-Cox solution at room temperature in the dark for 4 months and 80 μm coronal brain sections were cut. The number of primary dendrites, somatic area, apical spine density, and basal spine density were determined. For IHC, 12 μm coronal sections were cut using perfused brains from 18-month-old male WT and β2-/-

mice and stained with antibodies specific for GAD67, synapsin I, and PSD95. Golgi staining revealed that the number of primary dendrites, somatic area, apical spine density, and basal spine density for pyramidal cells in neocortical layers II/III were identical between WT and β2-/- mice. Mean gray values for synapsin I and PSD95 IHC staining were measured. No differences were found in any region of the hippocampus indicating that loss of high affinity nAChRs did not affect synaptic density in this area. Numbers of GAD67 positive neurons per area were determined in the hippocampus. The cell density of inhibitory interneurons in the hippocampus showed a general genotype effect in all three regions, CA1, CA3, and the dentate gyrus (DG), with β2-/- mice displayed significantly lower GAD67 cell density compared to aged-matched WT mice (two-way ANOVA, CA1: $p = 0.04$; CA3: $p = 0.006$; DG: $p = 0.014$). Significant differences were specifically observed in the CA1 molecular layer ($p = 0.024$), CA3 oriens ($p = 0.043$), and DG molecular layer ($p = 0.013$). Experiments were done to evaluate the synaptic and GABAergic interneuron density in different layers of the neocortex and characterize the GABAergic subpopulation most affected by loss of high affinity nAChRs. Thus far, the data suggest that loss of endogenous activation of heteromeric nAChRs has little effect on synaptic connections, but strongly impairs survival of hippocampal GABAergic neurons.

INTRODUCTION

Loss of nicotinic binding sites, especially in cortico-hippocampal regions, is one of the major histological changes observed in normal brain ageing as well as

neurodegenerative diseases related with dementia such as AD. Pentameric nAChRs are ligand-gated cation channels formed by various combinations of α and β subunits. The α7- and α4β2-containing receptors are the most abundant and widely distributed in mammalian brains.

Activation of neuronal nAChRs by nicotine and nicotinic agonists exerts neuroprotective effects. β2 subunit knock-out mice (β2-/- mice) lack high-affinity nAChRs and exhibit deficits in spatial learning and memory, and increased neurodegeneration during ageing including decreased cortical thickness, decreased hippocampal volume, and increased neuronal densities. These anatomical alterations could result from decreased connectivity due to loss of synapses or decreased dendritic arborization, or result from loss of neurons.

Synaptic loss has been found in both mouse models and human patients with several neurodegenerative diseases (Hof and Morrison, 2004; Shankar, 2010; Jindahra et al., 2012; Marcello et al., 2012; Pienaar et al., 2012). β2-/- mice have a tendency towards decreased basal dendritic size and complexity in almost all cortical areas, and β2 containing nAChRs might be involved in dendritic morphogenesis (Ballesteros-Yanez et al., 2010).

Loss of GABAergic neurons occurs during the later stages of AD. GABAergic interneurons play important roles in controlling the timing of pyramidal cell firing, synchronizing network activity, and the generation of cortical rhythms. They also seem to play an important role in responding to dynamic changes in excitation, increasing the dynamic range of cortical circuits, controlling sensory receptive fields and plasticity, and

maintaining the excitatory and inhibitory balance necessary for the transfer of information while preventing runaway excitation (McBain and Fisahn, 2001; Pouille and Scanziani, 2001; Wehr and Zador, 2003; Markram et al., 2004; Trevelyan et al., 2006; Klausberger and Somogyi, 2008; Haider and McCormick, 2009). GAD mediated GABA synthesis occurs in the cytosol, and GABA is transported into synaptic vesicles by the vesicular GABA transporter. Triggered by an action potential, vesicular GABA is released in a Ca^{2+}-dependent manner (Gonzalez-Burgos et al., 2011). In parvalbumin (PV) neuron terminals, PV may act as a Ca^{2+} buffer that binds residual Ca^{2+} after activation of the Ca^{2+} sensor that triggers GABA release (Gonzalez-Burgos et al., 2011). Malfunction of these neurons has been implicated in a number of diseases ranging from epilepsy to schizophrenia, anxiety disorder and autism (Cossart et al., 2001; Noebels, 2003; Levitt et al., 2004; Cobos et al., 2005; Gonzalez-Burgos and Lewis, 2008). Chronic dosing with nicotine in rat neonates increases the number of GABAergic neurons in the hippocampal area (unpublished data from Dr. Ursula H. Winzer-Serhan, Department of Neuroscience and Experimental Therapeutics, Texas A&M Health Science Center, Bryan, TX). Thus, loss of high affinity nicotinic receptors could result in decreased numbers of GABAergic interneurons.

In this study, we performed Golgi-Cox staining to investigate dendritic spine density. We also used IHC for synaptic markers: synapsin I and PSD95 for presynaptic vesicles and postsynaptic densities, respectively, and as a marker for GABAergic neurons, GAD67, to study synaptic and inhibitory interneuron densities.

EXPERIMENTAL PROCEDURES

Animals and tissue preparation

Male C57BL/6: +/+ (wild type) and β2-/- mice were group housed in a room that was on a 12-hour light/dark cycle. All mice were given food and water *ad libitum* until they reached an average age of 17 months. For Golgi-Cox staining (n = 6), mice were anesthetized using isoflurane and decapitated. Brains were dissected into right and left hemispheres and put directly into Golgi-Cox solution. For immunohistochemistry staining (n = 6), mice were anesthetized with an intraperitoneal injection of ketamine/xylazine and transcardially perfused with Tyrode's saline followed by 4% paraformaldehyde. Brains were removed, cryoprotected in 20% sucrose overnight and rapidly frozen. Coronal sections through the rostral hippocampi were cut (12μm) and mounted on gelatin coated glass microscope slides. Adjacent sections on the same slide were separated by 15 sections. Tissue sections were stored at -70°C until used. All procedures were approved by the Texas A&M University Animal Use Committee and carried out in accordance with the National Institutes of Health Guide for the Care and Use of Laboratory Animals (National Institutes of Health Publication No. 85-23, revised 1996).

Golgi-Cox staining

Each pair of half brains sat in 50 to 100 ml of filtered 0.8% potassium chromate, 1% potassium dichromate, 1% mercuric chloride Golgi-Cox solution in the dark at room

temperature for 5 months. Each half brain was rinsed in deionized water, briefly immersed in 70% ethanol and then encased in paraffin. Thick 75-100 μm coronal sections through the region of the rostral hippocampus were cut using a sliding microtome. Sections were then reacted with 5% ammonium hydroxide for 20 minutes, dehydrated, and mounted onto plain glass microscope slides using permount.

Immunohistochemistry staining

Antigen retrieval was carried out for 15-30 minutes, in 10 mM trisodium citrate buffer at 80°C. Subsequently the sections were processed for standard immunohistochemistry using diaminobenzidine as the chromagen (Abbott and Jacobowitz, 1999). GAD67: mouse monoclonal, 1:20,000 (Chemicon); parvalbumin: mouse monoclonal, 1:20,000 (Chemicon); synapsin I: rabbit polyclonal, 1:10,000 (AbCam). PSD95: rabbit polyclonal, 1:5000 (AbCam).

Data analysis

For Golgi-Cox, sections were examined by light microscopy using a microscope (Nikon Eclipse E400) equipped with a camera (Nikon digital camera DXM 1200) and an oil-100X objective. With the investigator blind to the genotype, 6 to 8 cortical layer II/III pyramidal cells from each animal were selected for analysis. Dendritic lengths and somatic areas were measured using ImageJ 1.43S (Rasband, 1997-2011). Again, with the investigator blind to the genotype, for GAD67 and parvalbumin, cell counts that were carried out in specific regional areas were converted into cell densities. Cells were

counted using the 10X objective. Photomicrographs of each section analyzed were taken using the 4X objective. Areas were measured using ImageJ 1.43S. For synapsin I and PSD95, four sections per animal (both sides) were photographed using the 4X objective for the hippocampus, and the 10X objective for the somatosensory cortex. Exposure conditions were kept constant during photographing. Using NIH-imageJ 1.43S, pictures were converted to 8 bit and inverted, and the mean gray value and modal gray value were measured (0 = pure black; 255 = pure white). For the hippocampus, measurements were done at the CA1 stratum oriens, CA1 pyramidal cell layer, CA1 stratum radiatum, CA1 molecular layer, CA3 stratum oriens, CA3 pyramidal cell layer, CA3 molecular layer (combined with striata lucidum and radiatum), dentate gyrus (DG) molecular layer, DG granular cell layer, and DG hilus region (Fig. IV-1). For the somatosensory cortex, measurements were done within a 300 μm wide column and separated into layer II & III, IV, V, and VI. Mean gray values were measured using ImageJ 1.43S.

Statistics

SPSS 14.0 was used for data analysis. Two-way ANOVAs (genotype vs. region) followed by the Tukey's HSD post hoc test was used for GAD67, PV, synapsin, and PSD95 immunohistochemistry analysis. The Student's *t*-test was used for somatic area, dendritic number, and dendritic spine density analysis. $\alpha = 0.05$.

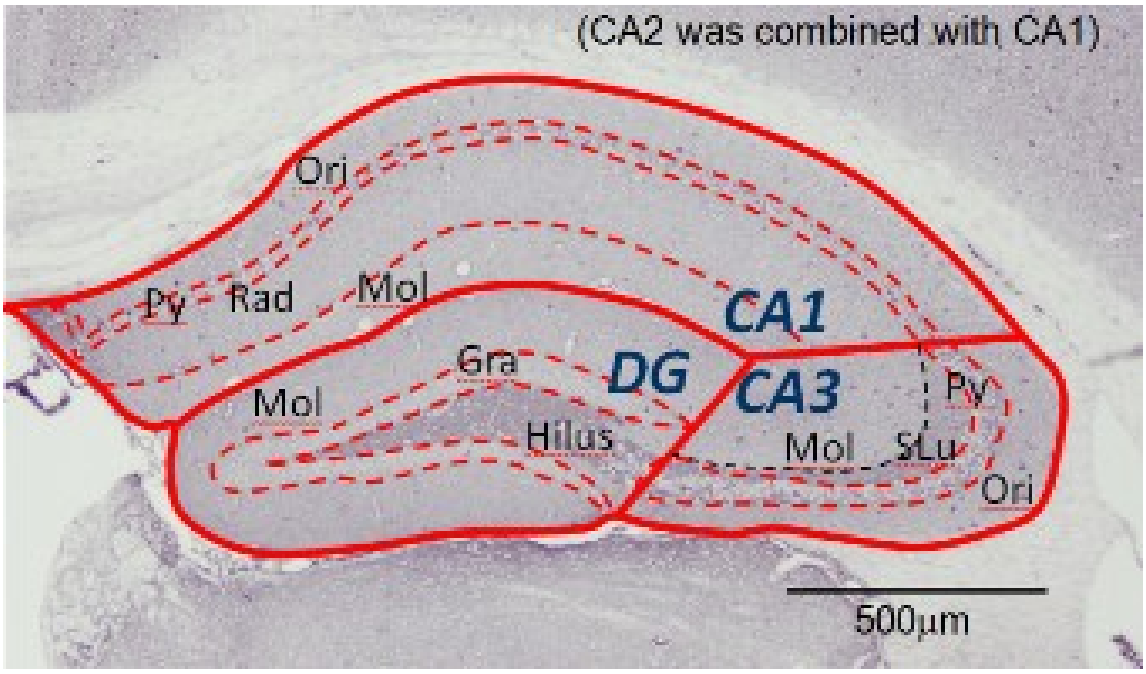

Figure III-1. Anatomy of mouse hippocampal cross section.

RESULTS

GAD67 labeled GABAergic interneurons were examined in middle-aged β2-/- and wild type mice. In the hippocampus, all three areas (CA1, CA3 and DG) displayed significant decreases in GAD67 positive cell density in β2-/- mice as compared to age-matched wild type (Fig. III-2). In the hippocampal CA1 area, analysis using two-way ANOVA (subregion vs. genotype) indicated a general genotype effect ($p = 0.04$), with the molecular layer showing a significant difference between the two genotypes after running Tukey's HSD post hoc test ($p = 0.024$) (Fig. III-2B). In the hippocampal CA3 region, analysis using a two-way ANOVA indicated a general genotype effect ($p = 0.006$), with the stratum oriens layer showing a significant difference between the two

genotypes after running the Tukey's HSD post hoc test ($p = 0.043$) (Fig. III-2C). In the DG, the two-way ANOVA also indicated a general genotype effect ($p = 0.014$), with the molecular layer showing significant difference between genotypes, after running the Tukey's HSD post hoc test ($p = 0.013$) (Fig. III-2D). However, in the somatosensory cortex no difference was found between the genotypes (Fig. III-2E).

The decrease in GABAergic cell density could be accounted for by the possible decreased presence of parvalbumin expressing interneurons, so parvalbumin labeled GABAergic interneurons were investigated in middle-aged β2-/- and wild type mice (Fig. III-3). Unlike GAD67, except for hippocampal CA1 region, none of other regions showed any difference in parvalbumin cell densities between the two genotypes. In the hippocampal CA1, the two-way ANOVA indicated a strong interaction between genotype and subregion ($p < 0.001$), so the subregions were further analyzed separately using Student's *t*-test. Only the pyramidal cell layer showed a decrease in parvalbumin immunopositive cell density in β2-/- mice as compared to age-matched wild type mice (Fig. III-3B). Levels of pre- and post-synaptic markers measured by synapsin I (Fig. III-4) and PSD95 (Fig. III-5) respectively using immunohistochemistry did not change in the cortico-hippocampal region in middle-aged β2-/- mice as compared to wild type mice. There also was no difference between middle-aged β2 knock-out mice and wild type mice with respect to the number of primary dendrites, the soma area, and the dendritic spine density of cerebral cortex layer III pyramidal cells (Fig. III-6).

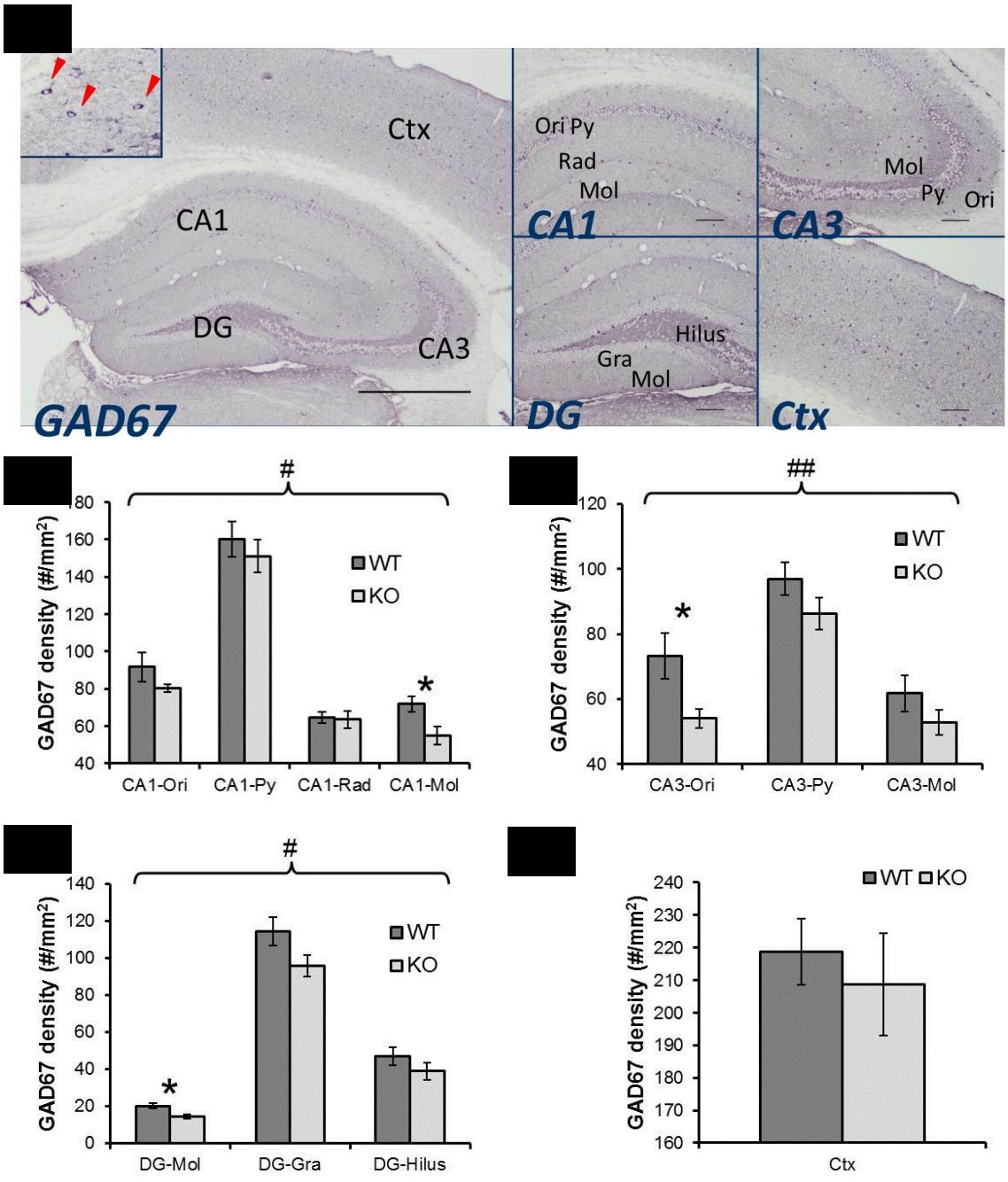

Figure III-2. GAD67 labeled GABAergic interneurons were investigated in middle-aged β2-/- and wild type mice. Hippocampus: two-way ANOVA, region vs. genotype; neocortex: Student's *t*-test. WT, n = 6; KO, n = 5. # general genotype effect $p < 0.05$, ## general genotype effect $p < 0.01$, * Post-hoc Tukey's HSD test $p < 0.05$. Scale bars: insets-10 μm; whole regions- 500 μm; subregions- 100 μm.

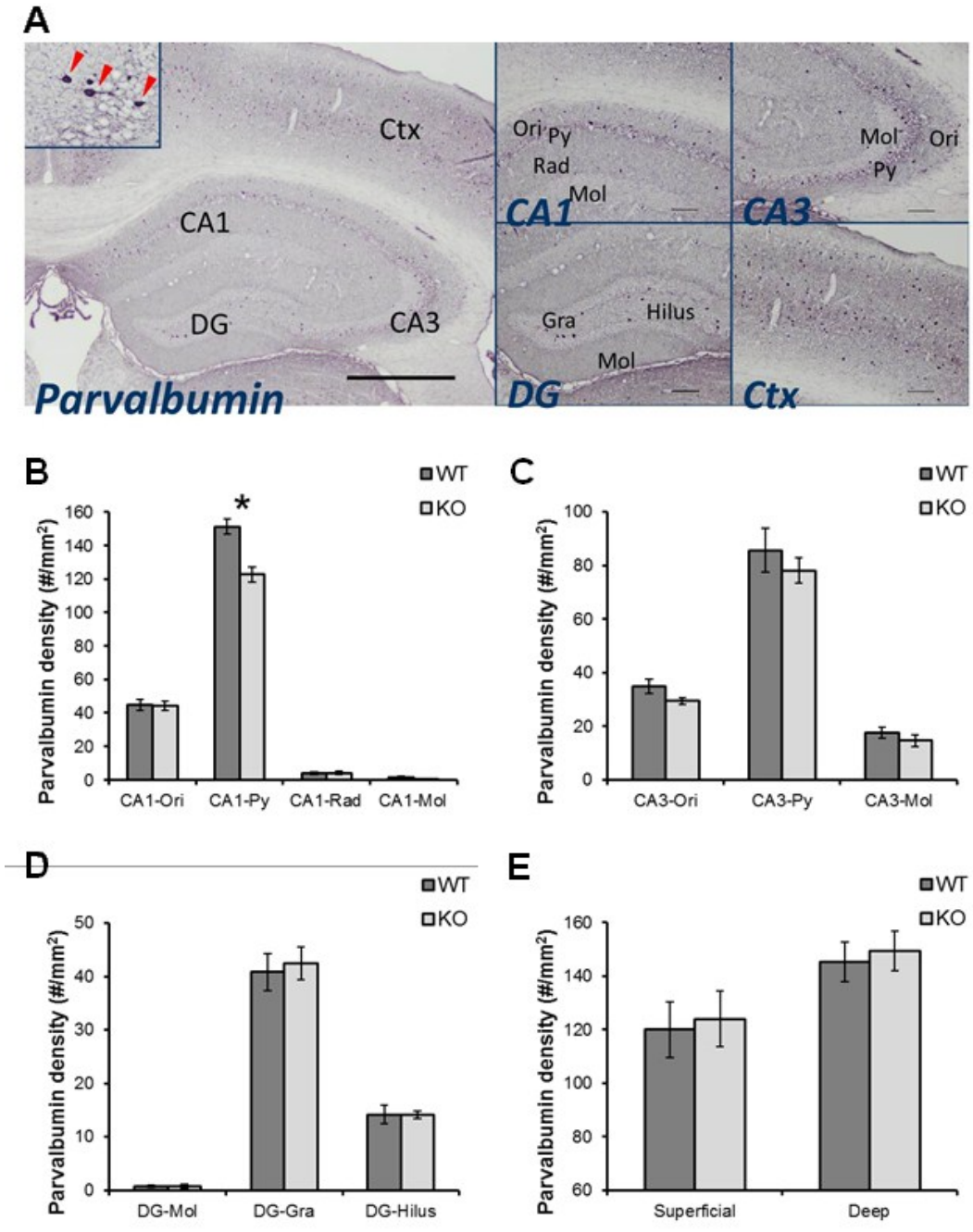

Figure III-3. Parvalbumin labeled GABAergic interneurons were investigated in middle-aged β2-/- and wild type mice. Hippocampus: two-way ANOVA, region vs. genotype; neocortex: Student's *t*-test. WT, n = 6; KO, n = 5. # general genotype effect $p < 0.05$, ## general genotype effect $p < 0.01$, ***** Post-hoc test $p < 0.05$. Arrowheads in inset indicate parvalbumin positive neurons. Identify abbreviations used in the figure. Scale bars: insets-10 μm; whole regions- 500 μm; subregions- 100 μm.

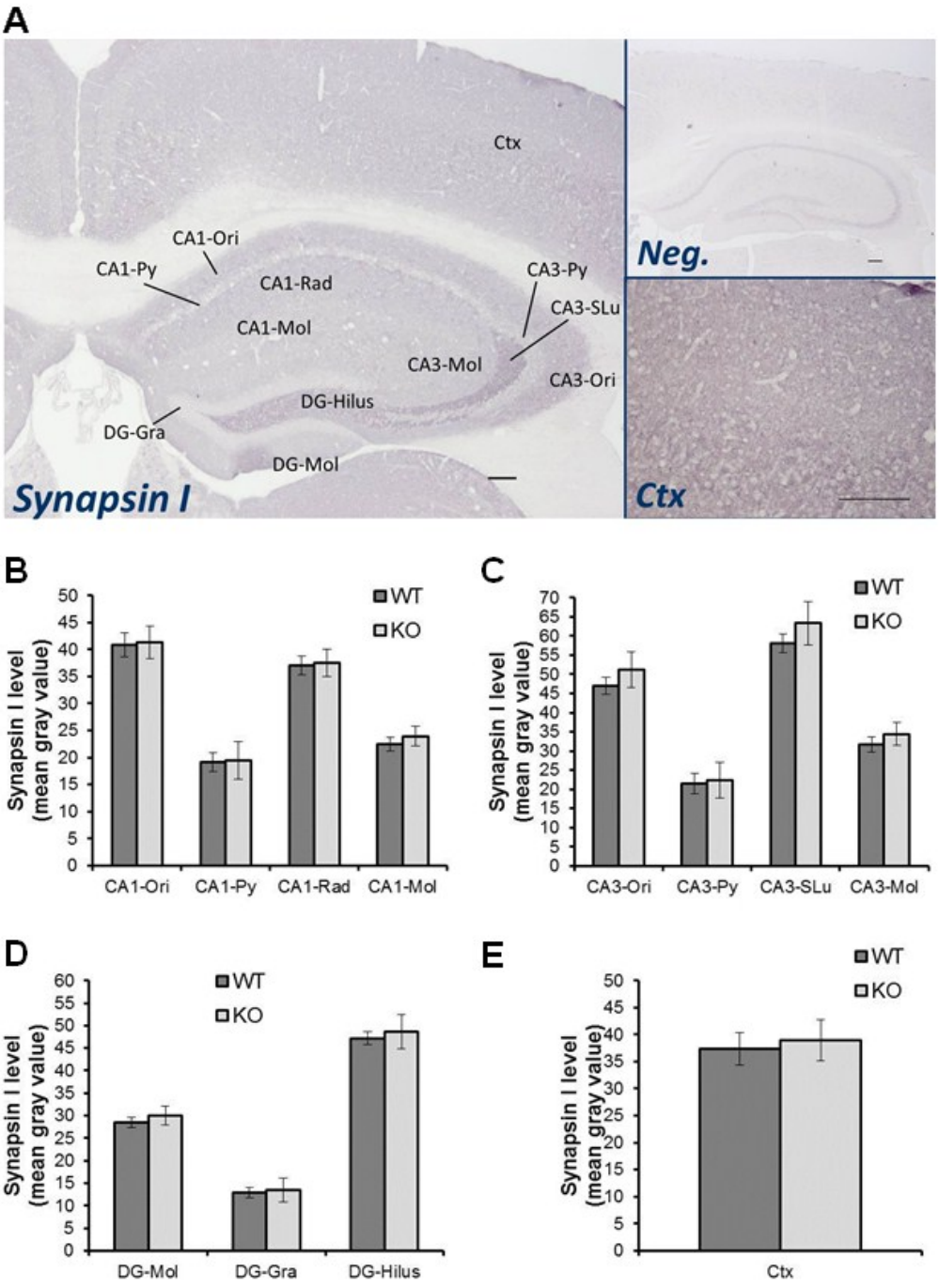

Figure III-4. Levels of pre-synaptic markers that were measured by synapsin I using immunohistochemistry. Hippocampus: two-way ANOVA, region vs. genotype; neocortex: Student's *t*-test. WT, n = 6; KO, n = 5. DG, dentate gyrus; Ori, oriens layer; Py, pyramidal cell layer; Rad, stratum radiatum; Mol, molecular layer; SLu, stratum lucidem; Gra, granular cell layer; Ctx, neocortex; Alv, alveus. Scale bars: 100 μm.

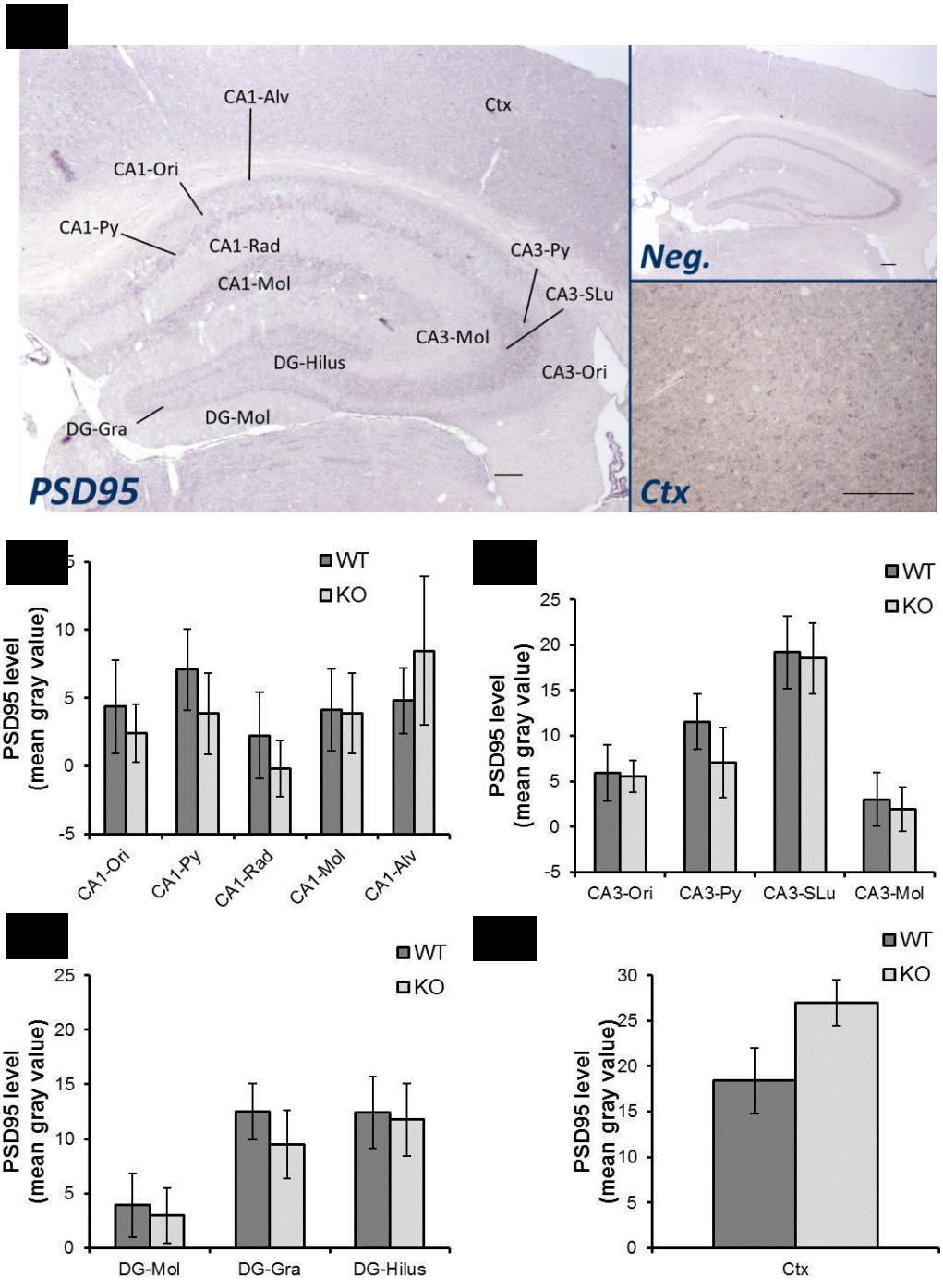

Figure III-5. Levels of post-synaptic markers measured by PSD95 using immunohistochemistry. Hippocampus: two-way ANOVA, region vs. genotype; neocortex: Student's *t*-test. Wild type mice = WT, n = 6; B2-/- mice = KO, n = 5. Scale bars: 100 μm.

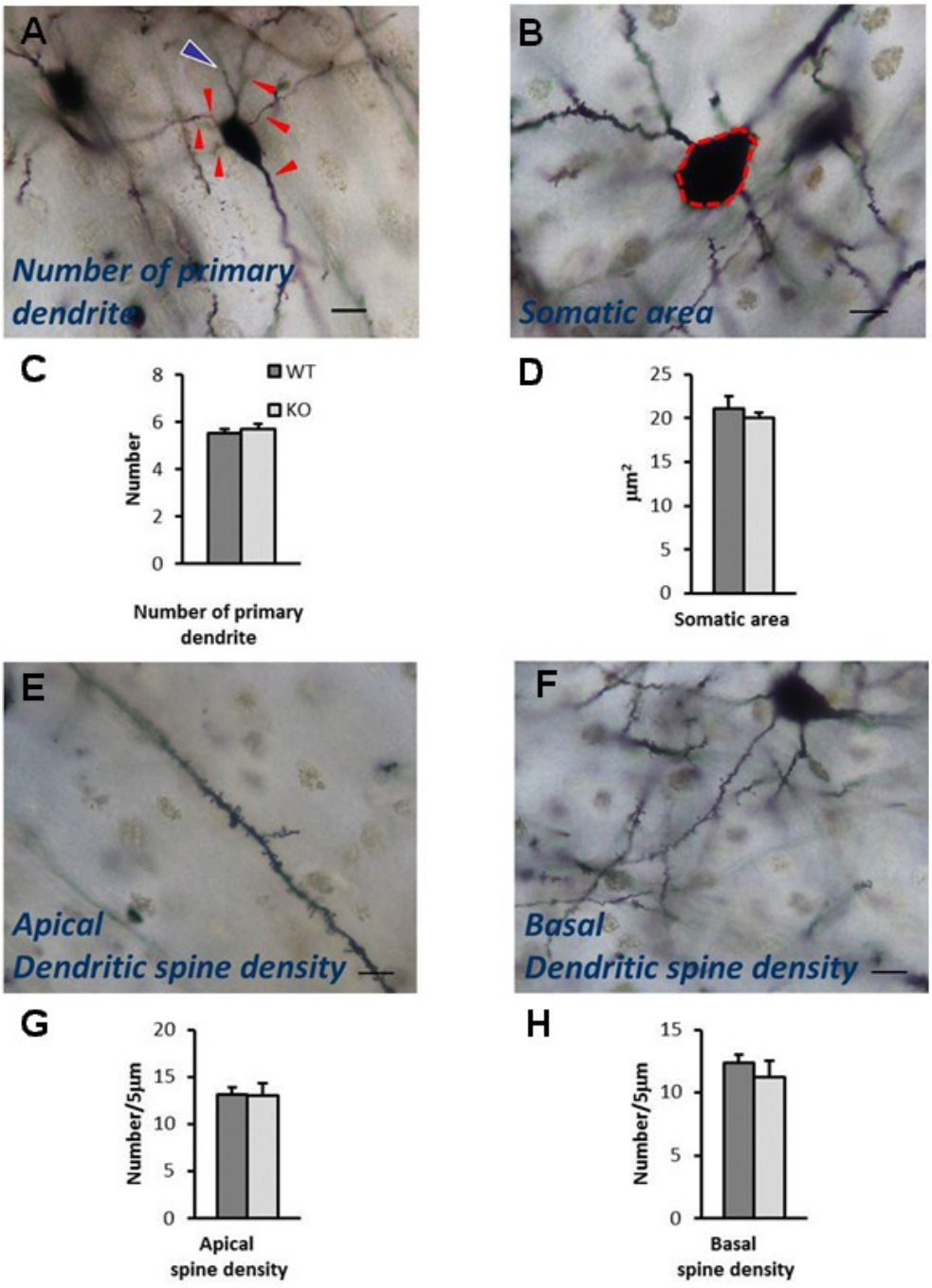

Figure III-6. No differences were observed between middle-aged β2 knock-out mice and wild type mice with respect to the number of primary dendrites, the soma area, and dendritic spine density for neocortex layer III pyramidal cells. Student's *t*-test, n = 6. Red arrowheads: primary dendrites; blue arrow head: axon; dashed line: measured soma area. Scale bars: 10 µm.

DISCUSSION

GABAergic interneurons represent 10-20% of all neocortical neurons in rodents (Rudy et al., 2011). GABAergic neurons have the capacity to synthesize GABA from glutamate via the enzymatic activity of GAD, for which there are two gene products with different molecular size: GAD65 and GAD67 (Soghomonian and Martin, 1998). These two GAD isoforms differ with respect to a number of properties, but their specific functions are still not fully understood (Soghomonian and Martin, 1998). However, GAD65 and GAD67 are differentially expressed in GABAergic terminals in a cell type-specific manner. The ratio of GAD67/GAD65 expression has been shown to vary significantly with respect to different types of terminals (Fish et al., 2011). Though the differential functional roles of GAD67 and GAD65 are still poorly understood, in mice, GAD67 deficiency has been associated with major developmental defects. GAD67-/- animals are born with several deficits including cleft palate, and this knockout has proven lethal and with ~ 90% reduction of total GABA concentration in brain tissue (Asada et al., 1997; Ji and Obata, 1999). In contrast, GAD65-/- mice are able to survive into adulthood, displaying only a ~20% reduction in total brain GABA concentration (Asada et al., 1996). GAD65-/- mice also display increased susceptibility to epileptiform seizures (Asada et al., 1996; Kash et al., 1997), increased anxiety (Kash et al., 1999), and altered fear conditioning (Sangha et al., 2009). Importantly, when GAD67 is reduced but not totally absent, there is marked impairment in the maturation of cortical GABAergic synaptic connections (Chattopadhyaya et al., 2007). GAD65 and GAD67 both comprise ~50% of total GAD protein in the mouse neocortex while the proportions

of GAD protein in human cortex are unknown (Sheikh et al., 1999). Our results indicated that loss of endogenous activation of heteromeric nAChRs strongly impairs survival of GAD67 positive hippocampal interneurons in middle-aged mice. This is in line with the unpublished previous results that chronic dosing with nicotine in rat neonates increases the number of GABAergic neurons in the hippocampal area.

Numerous studies of rodent brain tissue have suggested that among GABAergic interneurons, the Ca^{2+}-bonding protein PV and the neuropeptide somatostatin (SST) are particularly useful, because they define non overlapping groups of interneurons in the cortex and account for 40% and 30% of GABAergic interneurons in the somatosensory cortex, respectively (Gonchar and Burkhalter, 1997; Kawaguchi and Kubota, 1997; Ascoli et al., 2008; Lee et al., 2010; Miyoshi et al., 2010; Xu et al., 2010). The other ~ 30% of the total population are ionotropic serotonin receptor 5HT3a (5HT3aR) neurons, which are exclusively on GABAergic neurons and this GABAergic neuronal population does not overlap with PV and SST expressing interneurons (Morales and Bloom, 1997; Ferezou et al., 2002; Puig et al., 2004; Rudy et al., 2011).

Subtypes of hippocampal interneurons were differentially affected by the loss of β2-nAChRs. While GAD67 positive cells were decreased in all areas of the hippocampus in our experiments, the PV positive neurons only decreased in the CA1 pyramidal layer in middle-aged β2-/-mice, suggesting that PV positive neurons in the CA1 pyramidal layers were more susceptible to chronic nicotine treatment than PV positive cells in other areas. The decreased in GAD67 positive cells in other areas than CA1 pyramidal layers in the hippocampus was due to the SST or 5HT3aR expressing

GABAergic neurons. The reasons for CNE differential regulations in GABAergic subtypes in difference areas need further study.

Our data indicated that both pre-and post-synaptic marker levels did not change in response to loss of high affinity nAChRs. Using Golgi stain, there was no change in somatic area, number of primary dendrite and dendritic spine density in response to loss of high affinity nAChRs. It has been shown that acute nicotine treatment significantly increases synapsin I activity, which is mediated by β2-nAChRs, but not total protein level (Jackson et al., 2009). Prenatal nicotine exposure significantly increased PSD95 levels at postnatal day1, but it is not known whether this effect is mediated by β2-nAChRs (Wang et al., 2011). Nicotine exposure also has been shown to increase spine density in both the nucleus accumbens and prefrontal cortex (Brown and Kolb, 2001; Gonzalez et al., 2005). Our results indicated that the spine density was not changed in pyramidal cells in cortical layer III of somatosensory cortex. Some studies have found that nicotine exposure will increase branching in the motor cortex, but other more recent studies have found no effect on the adjacent somatosensory cortex (Brown and Kolb, 2001; Gonzalez et al., 2005). These suggest that neurons in the somatosensory cortex may have more resistance toward loss of endogenous nAChRs activation than other brain areas such as the nucleus assumbens and prefrontal cortex.

Together, the data suggest that loss of endogenous activation of heteromeric nAChRs has little effect on synaptic connections, but strongly impairs survival of hippocampal GABAergic neurons.

CHAPTER IV

EFFECTS OF CHRONIC ORAL NICOTINE ON FOOD CONSUMPTION, ANXIETY AND EXPRESSION OF SIRT1 AND RELATED GENES IN YOUNG ADULT MOUSE BRAIN

SUMMARY

Nicotine exerts numerous effects on energy metabolism, anxiety and cognitive performance by activating neuronal nicotinic acetylcholine receptors (nAChRs). Nicotine's anorectic action results in lower body weight and body mass index. Caloric restriction (CR) has beneficial effects and activates expression of a series of longevity genes like SIRT1. Therefore, we hypothesized that nicotine exposure would decrease food intake and also increase expression of longevity genes. Young adult (3-month-old) C57BL/6 male mice were dosed for three weeks with 300 μg/ml nicotine in drinking water containing saccharin. ^{125}I-epibatidine binding sites were measured using receptor autoradiography in brain slices from nicotine- and control-treated mice. Increased nAChR binding, a hallmark of chronic nicotine exposure (CNE), was detected in the neocortex ($p = 0.055$) and hippocampus ($p = 0.019$) indicating that relevant levels of nicotine reached the brain. CNE significantly decreased average daily food intake ($p = 0.005$), and reduced daily weight gain ($p = 0.063$), resulting in lower body weight ($p = 0.043$). Nicotine's effect on cognitive function was evaluated using a modified elevated plus maze (EPM) and an object recognition test, and no significant differences due to treatment were observed. Nicotine's anxiolytic effect was determined in an open field

test. The results revealed a significantly lower thigmotaxis index ($p = 0.021$) and less margin time ($p = 0.025$) in the nicotine-treated mice compared to control mice indicating decreased anxiety. Finally, using isotopic *in situ* hybridization with cRNA probes for several genes associated with CR, we found that mRNA levels for SIRT1 ($p = 0.014$), Nampt ($p = 0.023$), and Ku70 ($p = 0.002$) were significantly increased in cortico-hippocampal areas in the brains of nicotine-treated mice compared to controls, with Ku70 exhibiting the most robust change. However, mRNA expression levels for FoxO3, p53, and the neurotrophic factors NT-3 and BDNF remained unchanged. These data indicate that three weeks of oral nicotine self-administration is anxiolytic, decreases caloric consumption, increases nAChR binding sites, and expression of SIRT1 and several of its target genes.

INTRODUCTION

Nicotine is the major psychoactive ingredient in tobacco smoke (Hajek et al., 1988) and interacts with neuronal nicotinic acetylcholine receptors (nAChRs). NAChRs are pentameric ligand gated cation channels that are either homomerically or heteromerically formed by different subunit combinations. Among these combinations, heteromeric $\alpha4\beta2$ nAChRs have high affinity for nicotine, and are the most widely expressed nicotinic receptors in the mammalian brain together with homomeric $\alpha7$ nAChRs, which have lower affinity for nicotine. The combined effects of nicotine influence behaviors such as food intake, anxiety and cognitive performance (Cooper et al., 1991; Sargent, 1993b; Picciotto et al., 1998). The neuroprotective effects of nicotine

and its agonists have been widely reported both *in vivo*, and *in vitro* (Picciotto and Zoli, 2008a). Preclinical studies indicate that nicotine and its agonists can protect neurons from excitotoxicity, and other insults including amyloid beta induced neuronal toxicity. Thus, nicotinic agonists including nicotine might prevent neuronal death due to neurodegeneration, which is particularly important in neurodegenerative diseases such as Alzheimer's disease (AD) and Parkinson's disease (PD) (Owman et al., 1989; Socci and Arendash, 1996; O'Neill et al., 1998). Furthermore, epidemiological studies have shown that smoking is negatively correlated with PD and AD (Fratiglioni and Wang, 2000), suggesting that nicotine, the major psychoactive ingredient in tobacco smoke, may prevent or delay the development of AD and PD.

Cholinergic deficits are characteristic for AD, and decreased numbers of nAChRs have been detected in postmortem brain slices from AD patients (Whitehouse et al., 1986; Whitehouse et al., 1988). Several studies have demonstrated that smoking increases nAChRs in the brains of smokers, most likely due to chronic nicotine exposure, which results in receptor upregulation (Perry et al., 1999; Mukhin et al., 2008). In addition, experiments have shown that nicotine and nicotinic agonists, when given acutely, can improve memory and cognitive function (Wilson et al., 1995; Rezvani and Levin, 2001; Levin and Rezvani, 2002). Thus, medicinal use of nicotine or related nAChR agonists could have beneficial therapeutic effects, by increasing nAChRs in the brain, protect against neuronal degeneration caused by a number of different insults, and improve cognitive function, and hence, protect the brain against age-related cognitive decline and neurodegeneration. Therefore, despite its abuse potential, nicotine and

nicotinic receptor agonists have been evaluated for their therapeutic potential, especially during aging or to repair brain injury (Nordberg et al., 2002; White and Levin, 2004; Aleisa et al., 2006; Weiss et al., 2007; Srivareerat et al., 2009).

However, it should be noted that nicotine not only acts in the CNS it also interacts with nAChRs in the peripheral nervous system (PNS) and enteric nervous system (ENS). In the PNS, nAChRs are major regulators of the sympathetic and parasympathetic functions, and enteric nAChRs regulate gastrointestinal motility (Torocsik et al., 1991; Wessler et al., 1992). In addition, nicotine is an addictive drug that stimulates dopamine release and activates the reward pathway in the CNS (Kleijn et al., 2011; Zhang et al., 2012). Thus, if nicotine were to be used therapeutically, a low dose of nicotine would need to be administered to avoid PNS- and ENS-related side effects, and to reduce the potential for abuse.

Nicotine also has an anorectic action and subsequent decreases in body weight and body mass index following nicotine use have been documented both in human and experimental animals (Wager-Srdar et al., 1984; Hajek et al., 1988; Bellinger et al., 2003). Caloric restriction (CR) is a regimen that extends lifespan in all mammalian species studied so far including rodents and primates (Picard and Guarente, 2005; Wolf, 2006). It is believed that the longevity effect of CR is mediated by SIRT1, a nicotinamide adenine dinucleotide-dependent deacetylase (Cohen et al., 2004b; Tang and Chua, 2008). It is becoming apparent that SIRT1 is a key regulator of cell defenses and survival in response to stress in mammals, and upregulation of SIRT1 can protect neurons against neurodegeneration and neurotoxic insults (Chen et al., 2005b; Kim et al.,

2007a). In aged mice lacking high affinity nAChRs, the expression levels of SIRT1 and its regulator and substrate, Nampt and Ku70 respectively, are increased, and this is thought to be a stress response due to lack of endogenous neuroprotection via heteromeric nAChR activation (Huang et al., 2011). However, little is known about SIRT1 expression or other CR-related genes in response to nicotine. Although no direct relationship has been reported between brain-derived neurotrophic factor (BDNF), neurotrophin-3 (NT-3) and SIRT1, studies have shown that BDNF and NT-3 levels are upregulated by CR in rats (Duan et al., 2001; Kumar et al., 2009), and chronic exposure to nicotine in adults and neonatal rats also has been shown to increase both BDNF and NT-3 expression levels too (Son and Winzer-Serhan, 2009).

Considering the similarities between the actions of nicotine and CR, nicotine's anorexic effects could play a significant part in its neuroprotective function by activation of growth factor expression and CR-related genes. In this study we determined a low but effective, centrally acting dose of nicotine administered orally via drinking water to mice, and evaluated the consequences on behavior and gene expression on SIRT1 and related genes, and on NT3 and BDNF.

EXPERIMENTAL PROCEDURES

Animals and drug administration

Young adult male C57BL/6 mice, originally obtained from the Jackson Laboratory, were used in this study. A breeding colony was established at Texas A&M

University's Laboratory Animal Research and Resource facility. At three months of age, mice were individually caged and randomly assigned to different dosing groups (n = 5).

Table IV-1. Nicotine free base provided in 2% saccharine drinking water of each treatment group.

Treatment day		Day 1	Day 2	Day 3	Day 4	Day 5	Day 6	Day 7	Day 8-23[a]
Dosage (μg/ml)	**Control**	0	0	0	0	0	0	0	0
	Low	20	20	20	20	20	20	20	20
	Medium	20	40	60	80	100	100	120	120
	High	20	40	80	120	160	200	250	300

[a] Mice were euthanized on day 23 of treatment.

Mice received 2% saccharine (saccharin sodium salt hydrate, > 98%) (Sigma, St. Louis, MO, USA) in their drinking water two weeks prior to actual dosing with nicotine to establish their individual daily drinking volume. (-)-Nicotine (hydrogen tartrate) (Sigma) was administered in water containing 2% saccharine as previously described (Ribeiro-Carvalho et al., 2009). Four final nicotine concentrations were tested: control - 0 μg/ml (0 mg/kg/day), low - 20 μg/ml (approximately 5 mg/kg/day, free base), medium - 120 μg/ml (approximately 30 mg/kg/day, free base), and high - 300 μg/ml (approximately 55 mg/kg/day, free base). Animals in the medium and high dose groups initially received 20 μg/ml of nicotine on day 1 and the concentrations were gradually increased until the final concentrations were reached on day 7 and day 8, respectively

(Table IV-1). Animals were treated until day 23. On day 20 to 22, all mice were subjected to behavior tests and then euthanized on day 23. Access to food was *ad libitum*. Food intake and body weight were monitored every three days from day 1 to day 19 and normalized to the first measurement of each individual animal. All procedures were approved by the Texas A&M University Animal Use Committee and carried out in accordance with the National Institutes of Health Guide for the Care and Use of Laboratory Animals (National Institutes of Health Publication No. 85-23, revised 1996).

Open field

To test locomotor, exploratory and anxiety behaviors, on day 20 of nicotine treatment, mice were placed individually in an open field (length × width × height: 20 × 20 × 30 cm) (Versamax animal activity monitor and analyzer, AccuScan Instruments, Columbus, OH, USA) equipped with vertical and horizontal beam sensors. The apparatus was constructed using transparent Plexiglas, located in a quiet room, and environmental cues including lighting and experimenter were kept constant during testing. Mice were accustomed to the experimental room for 5 minutes, and then placed in the open field for 30 minutes. Activity was recorded every minute. The open field chamber was cleaned with 50% ethanol between mice. Horizontal activity, total distance, movement time, rest time, stereotype counts, stereotype time, margin distance, margin time, center distance, center time, rearing activity, and rearing time were automatically recorded.

Elevated plus maze

Cognitive functions were tested in an modified elevated plus maze (EPM) test as described previously (Biala and Kruk, 2009). The EPM apparatus was made of Plexiglas, which was painted matte black from the outside. The maze consisted of two open arms (without walls) facing opposite, and another two enclosed arms (15.25 cm high walls on three sides with one end left open) facing opposite so that they formed a plus shape as previously described (Walf and Frye, 2007). Each arm was 30 cm long and 5 cm wide. The whole maze was elevated 40 cm off the ground, located in a quiet room illuminated by a central dim red light, and environmental cues were kept constant during testing. All mice were accustomed to the experimental room for 5 minutes before acquisition and retention trials. The maze was cleaned with 50% ethanol between mice. On day 20 of nicotine treatment, mice were individually subjected to an acquisition trial. Each mouse was placed at one end of one open arm facing away from the central platform and allowed to move from the open arm to either of the enclosed arms. A successful entry was considered when all four limbs were in the enclosed arm. If a mouse did not enter an enclosed arm within 90 seconds, it was placed in one of the enclosed arms and allowed to explore for another 60 seconds. On the next day (24 hours later, day 21), all mice were subjected to a retention trial in the same manner, and the time to successful entry was recorded as T2.

Object recognition

One-trial object recognition was performed on day 22 of nicotine treatment to study recognition memory as previously described (Bevins and Besheer, 2006) with minor changes. A transparent Plexiglas chamber (length × width × height: 20 × 40 × 30 cm) (AccuScan Instruments) coated outside with white bench protector (VWR, West Chester, PA, USA) was setup in a quiet room where the environmental cues including lighting were kept constant during testing. Mice were allowed to familiarize with the chamber individually for 5 minutes. Two identical sample objects (medium heavy duty black binder clips, 3.2 × 5.5 cm, OfficeMax) were placed in the back left and right corners of the chamber. The test animal was placed at the center of the chamber facing the front opposite to the sample objects with its nose pointing to either side and allowed to explore for 5 minutes. After a two-hour interval, one of the sample objects was replaced by a novel object (standard wooden clothes pin, 8.5 × 1 cm). The mouse was placed back into the chamber as described, and allowed to explore for 2 minutes. The chamber was cleaned with 50% ethanol between mice, and 3 minutes passed before the next test. A video camera (DIGITAL IXUS 50, Canon, Japan) was setup right above the apparatus so that the entire area including objects was recorded. Direct contact scoring was done by a blind investigator using XNote Stopwatch (free evaluation version, http://www.stopwatch-timer.com, dnSoft Research Group, accessed in 2011). The total time test animals spent on exploring objects (both sample and novel), and the time ratio (novel/total time) were analyzed and calculated.

Tissue preparation

All mice were anesthetized using isoflurane (IsoFlo, North Chicago, IL, USA) and decapitated on day 23. Approximately 1 ml of trunk blood was collected from each mouse, kept on ice, and centrifuged at 4°C 3000 rpm for 20 minutes. One hundred to 300 μl of serum was collected from each mouse and sent to Bioanalytical Core Laboratory Service Center (Department of Pharmaceutics, School of Pharmacy, Virginia Commonwealth University, Richmond, VA, USA) for analysis of nicotine and cotinine levels. The brains were rapidly dissected, frozen on powdered dry ice, and stored at -80°C until used. For *in situ* hybridization, 14 μm thick coronal sections, 196 μm apart, were cut using a cryostat from Bregma level -1.70 mm to -2.30 mm and thaw-mounted onto glass microscope slides coated with gelatin (Spectrum, Gardena, CA, USA) and poly-L-Lysine (Sigma). The sections were post-fixed with 4 % paraformaldehyde in 0.1 M phosphate buffer, pH 7.4, for 1 hour at room temperature (RT), washed in 0.1 M phosphate buffer three times, 5 minutes each, air-dried, and stored with desiccants at -20°C until used. For epibatidine binding, sections were collected the same way but mounted on glass microscope slides coated twice with gelatin only. Sections were then boxed with desiccant, left at 4 °C overnight, and stored at -80°C until used.

Epibatidine binding

Epibatidine binding was performed as previously described with minor changes (Huang and Winzer-Serhan, 2006b). Tissue sections were warmed to RT and pre-incubated 5 minutes in Tris-HCl buffer (50 mM Tris-HCl, 120 mM NaCl, 5 mM KCl,

2.5 mM $CaCl_2$, 1 mM $MgCl_2$, pH 7.4). Sections were then incubated with 0.4 nM [^{125}I]-Epibatidine (PerkinElmer Life Science NEX358, Boston, MA, USA, specific activity: 2200 Ci/mmol) for 1 hour at RT. For non-specific binding, sections were incubated with the presence of 400 μM (-)-nicotine hydrogen tartrate. Sections were washed in ice-cold Tris-HCl buffer twice for 1 minute, followed by 10 seconds in cold double-distilled (dd)H_2O, and dried under air stream for 1 hour. Sections were dried at RT overnight before exposure to BioMax MR Film (Kodak, Rochester, NY, USA). After 1-day of exposure, films were developed in D19 Kodak developer for 4 minutes, rinsed in water, fixed in Kodak Rapid Fixer for 5 minutes, and air-dried.

cRNA probes synthesis and *in situ* hybridization

Templates for the synthesis of cRNA probes were generated from mouse SIRT1, Ku70, Nampt, FoxO3a, p53, and rat NT-3 as previously described (Son and Winzer-Serhan, 2009; Huang et al., 2011). A pBSks plasmid containing a 750-base region complementary to rat BDNF mRNA (kindly provided by Dr. Carl Cotman, UC Irvine, CA) was used (Berchtold et al., 1999). The template for rat GAPDH is commercially available (Applied Biosystems/Ambion, TX). ^{35}S-labeled cRNA probes were synthesized in antisense orientation in the presence of ^{35}S-UTP (PerkinElmer Life Science) with T3 or T7 RNA polymerase (Applied Biosystems/Ambion) by *in vitro* transcription.

The method for *in situ* hybridization was described earlier (Winzer-Serhan et al., 1999). Briefly, tissue sections were pre-hybridized with 0.1 μg/ml proteinase K for 10

minutes at RT followed by 0.1 M triethanolamine and 0.25 % acetic anhydride. After overnight (16-20 hours) hybridization at 60°C, sections were treated with RNase A at 37°C for 30 minutes and washed in standard Saline Sodium Citrate (SSC) followed by a hot wash in 0.1X SSC at 65°C for 30 minutes. Slides were dehydrated through graded series of alcohols and air-dried. Sections were exposed to BioMax MR film along with [^{14}C]-standards (Amersham, Code RPA 504L, Batch21, Buckinghamshire, UK), and the films were developed as described in receptor binding section.

Autoradiogram analysis

Quantitative analysis of autoradiograms was done using a PC-base image analysis system, MCID basic (InterFocus Imaging Ltd, Haverhill, Suffolk, UK). For receptor binding, raw optical density (ROD) was measured in the hippocampus (combined measures in the molecular layers of the DG and the stratum lacunosum molecular of the CA1 in hippocampus proper), thalamus (the post thalamic nucleus and the ventral posteriomedial thalamic nucleus), and cerebral cortex (the deeper layer IV-V of the visual and somatosensory cortex). For the analysis of the hybridization signal, a standard curve (ROD vs. nCi/g wet weight) was generated using [^{14}C]-standards and ROD values were converted to nCi/g wet weight. Measurements were taken in the pyramidal cell layer of the CA1 and CA3, and in the granular cell layer of the DG of the hippocampus, and in the entire cerebral cortex located on individual sections. All hybridization signals were normalized to the level of GAPDH of the same region. All

anatomical structures were located according to the Mouse Brain Library atlas (Rosen et al., 2000).

Statistical analysis

SPSS 14.0 was used for statistical analysis. Significance was defined as $p \leq 0.05$. For food intake and body weight changes, repeated measurements were used for between-subject effects after nicotine reached the highest dose in all groups (day 8), and Student's *t*-tests were used to determine significant differences at each time point between nicotine and control groups. For open field, object recognition and EPM, Student's *t*-tests were performed to compare between nicotine and control groups. For receptor binding and gene expression, Student's *t*-tests and two-way analysis of variance (ANOVA) (region vs. treatment) were used, respectively. After performing the two-way ANOVA, the Tukey HSD was used as a post hoc test when needed. All data were presented as average ± SEM.

RESULTS

Dose of nicotine in drinking water and blood nicotine and cotinine levels

Nicotine and cotinine were not detected in the serum of control mice (< 2 ng/ml and < 1 ng/ml, respectively). In the low and medium nicotine group (20 μg/ml and 120 μg/ml, respectively), mice had undetectable levels of nicotine (< 2 ng/ml). Cotinine levels ranged from of 3.2 to 25.0 ng/ml with an average of 11.7 ng/ml in the low nicotine

group, and from 2.0 to 586.9 ng/ml with average of 151.8 ng/ml in the medium nicotine group. In mice exposed to high levels of nicotine (300 μg/ml) nicotine levels ranged from 0 to 21.1 ng/ml with an average of 6.2 ng/ml, and cotinine ranged from 41.4 to 578.1 ng/ml with an average of 192 ng/ml.

There was no difference in food intake and body weight between controls and low- and medium-nicotine-treatment groups (food intake: repeated measurements, between-subject effect, $p = 0.52$; body weight: repeated measurements, between-subject effect, $p = 0.88$). In addition, numbers of nAChR receptor binding sites measured in cortex, hippocampus and thalamus, showed no significant difference between controls and low and medium doses of nicotine (cortex: one-way ANOVA, $p = 0.63$; hippocampus: one-way ANOVA, $p = 0.56$; thalamus: one-way ANOVA, $p = 0.45$). Thus, together the results indicated that the low and medium doses may not be high enough to exert a central effect in mice. Only the high dose of nicotine resulted in significant differences in these measures, therefore, going forward, the high dose group is referred to as the "nicotine group", and is the only nicotine treatment group that was compared to control mice in detail.

Food intake and body weight changes

Food intake and body weight were monitored every three days. Food intake at the first measurement was the same between control- and nicotine-treatment groups (control: 3.61 ± 0.14 g/day; nicotine: 3.75 ± 0.07 g/day), so subsequent measurements were normalized to the first measurement for each individual mouse, and comparisons

were made between groups starting from day 8, when the total dose of nicotine was reached (300 μg/ml), and carried out to day 19. To avoid fluctuations in food intake and body weight caused by behavioral testing on day 20 to 23, data from days 20 to 23 were not included, but nicotine treatment continued. The average food intake was significantly lower in nicotine-treated compared to control mice (control: 4.30 ± 0.26 g/day; nicotine: 3.79 ± 0.13 g/day; repeated measurements, between-subject effect, $p = 0.005$) (Fig. IV-1). Due to variability in daily food intake, differences were only significant on day 11-13 (control: 4.62 ± 0.15 g/day; nicotine: 4.06 ± 0.20 g/day; Student's *t*-test, $p = 0.011$) and day 17-19 (control: 4.98 ± 0.19 g/day; nicotine: 4.51 ± 0.14 g/day; Student's *t*-test, $p = 0.001$) (Fig. IV-1). Overall, nicotine-treated mice decreased their food intake by about 12% compared to controls, which was equal to an 88% calorically reduced diet for 12 days (day 8 to day 19).

Similar to food intake, body weights on the first day of treatment were identical between groups (control: 26.59 ± 1.00 g; nicotine: 26.39 ± 0.70 g), so subsequent measurements were normalized to the weight of each individual animal on the first day of body weight measurement. Body weights in control mice continuously increased over the treatment period, whereas body weights for nicotine-treated mice did not change. With the beginning of the full-dose nicotine treatment, after day 8, control mice gained on average 0.16 ± 0.04 g/day, resulting in a higher body weight at the end of the treatment. In contrast, nicotine-treated mice exhibited a slight loss of 0.02 ± 0.07 g/day, which result in a lower body weight at the end of the treatment as compared to control mice (weight gain, repeated measurements, between-subject effect, $p = 0.063$) (Fig. IV-

2B). This resulted in a significant, 4% difference in body weight between treatment groups at the end of the treatment period (control: 27.59 ± 0.83 g; nicotine: 26.39 ± 0.51 g; body weight, repeated measurements, between-subject effect, p = 0.043) (Fig. IV-2A).

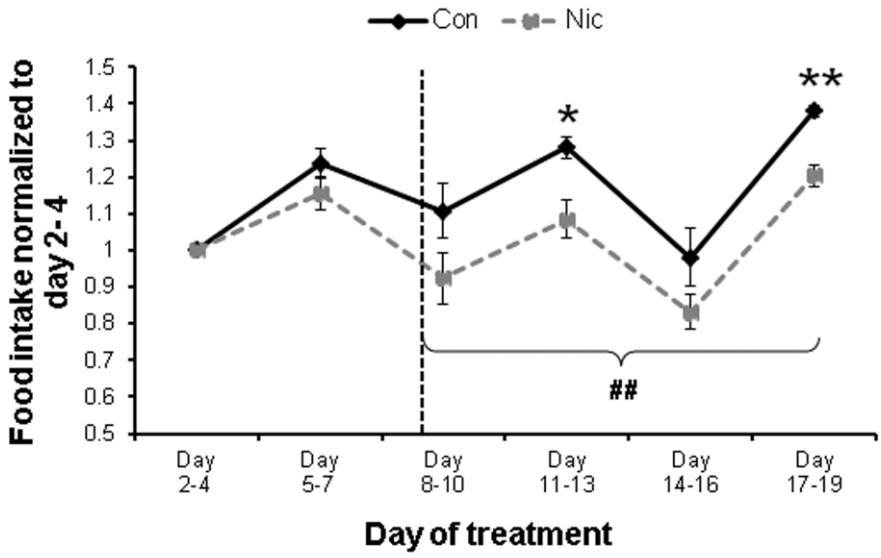

Figure IV-1. Nicotine-treated mice decreased their food intake compared to controls. Measurements from each mouse were normalized to their first measurements (day 2-4) and analyzed. Measurements were taken every three days until day 19. The dash line indicates the day nicotine administration reached the full dose (day 8). Con, control group. Nic, nicotine-treated group. Error bars: SEM. Repeated measurements, between-subject effect, ## $p < 0.01$. Student's *t*-test, compare between control and nicotine group, * $p < 0.05$, ** $p < 0.01$.

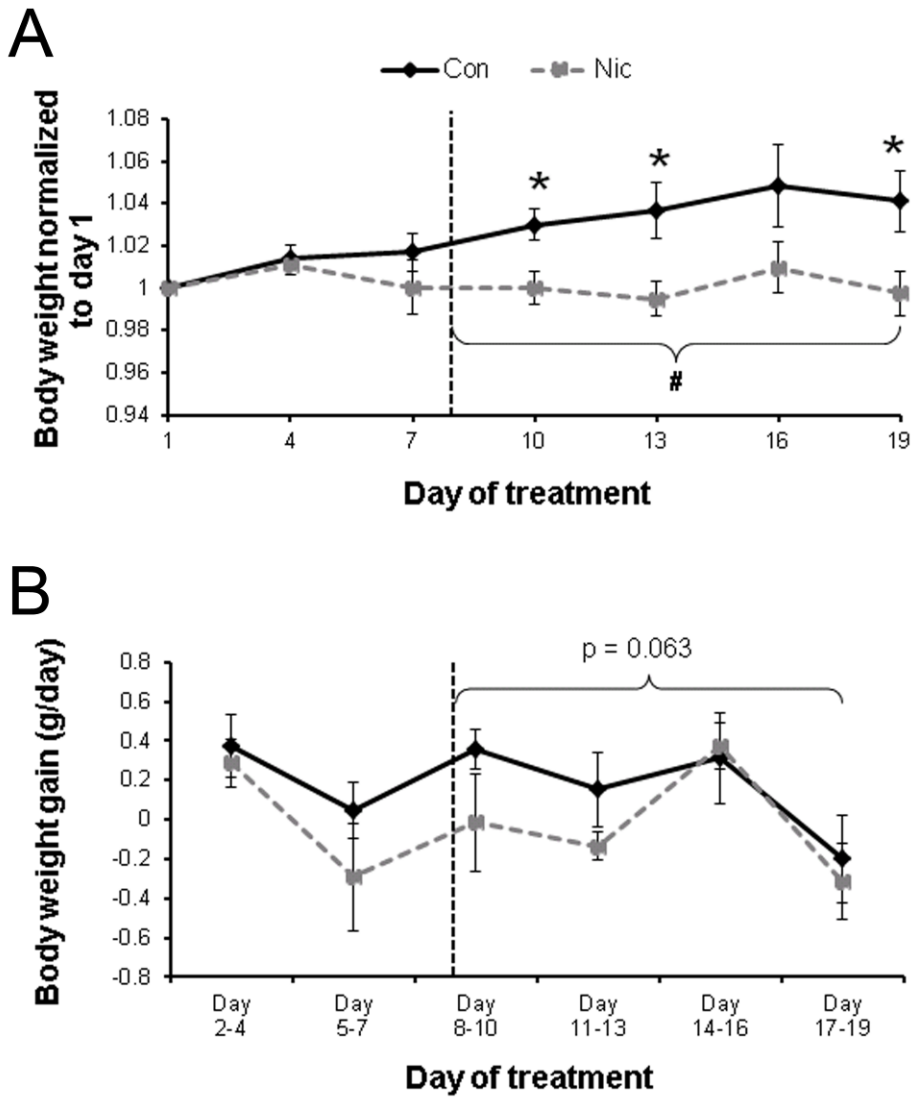

Figure IV-2. Nicotine-treated mice did not gain as much weight as controls (***B***), which results in a lower body weight in the nicotine-treated mice (***A***). Body weight measurements from each mouse were normalized to their first measurements (day 1) and analyzed. Measurements were taken every three days until day 19. The dash line indicates the day nicotine administration reached the full dose (day 8). Con, control group. Nic, nicotine-treated group. Error bars: SEM. ***A***, Repeated measurements, between-subject effect, # $p < 0.05$. Student's *t*-test, compare between control and nicotine group, * $p < 0.05$. ***B***, Repeated measurements, between-subject effect, $p = 0.063$.

Locomotor activity, anxiety and memory behavioral tests

On treatment day 20, mice were subjected to a 30 minute-open field test to assess locomotor activity, exploratory and anxiety behaviors. Twelve parameters were analyzed (see material and methods: open field). Of those, only margin and center time showed significant differences between treatment groups. All other parameters were not affected, indicating that locomotor activity and exploratory behavior were not impaired nor increased by chronic nicotine treatment. Mice were in the open field for 30 minutes, during which control mice spent 78% of the time at the margins, which was significantly longer than nicotine-treated mice which spent only 64% of the time at the margins (30 minutes overall, Student's *t*-test, $p = 0.025$) (Fig. IV-3A). When analyzed by 10 minute intervals, control mice spent significantly more time at the margins of the field than nicotine-treated mice during the first and second intervals (first Interval: control: 425 ± 17 sec, nicotine: 352 ± 24 sec, Student's *t*-test, $p = 0.037$; second Interval: control: 496 ± 19 sec, nicotine: 392 ± 35 sec, Student's *t*-test, $p = 0.031$), but differences diminished during the last interval when nicotine-treated mice spent more time at the margins (control: 475 ± 36 sec; nicotine: 411 ± 20 sec) (Fig. IV-3A). There was no difference in the margin distance or total distance traveled between groups; however, thigmotaxis (margin distance / total distance), thought to be an index of anxiety in mice (Simon et al., 1994), was significantly higher in control than nicotine-treated mice in the second 10 minutes interval (control: 0.71 ± 0.04; nicotine: 0.59 ± 0.03; Student's *t*-test, $p = 0.021$) (Fig. IV-3B).

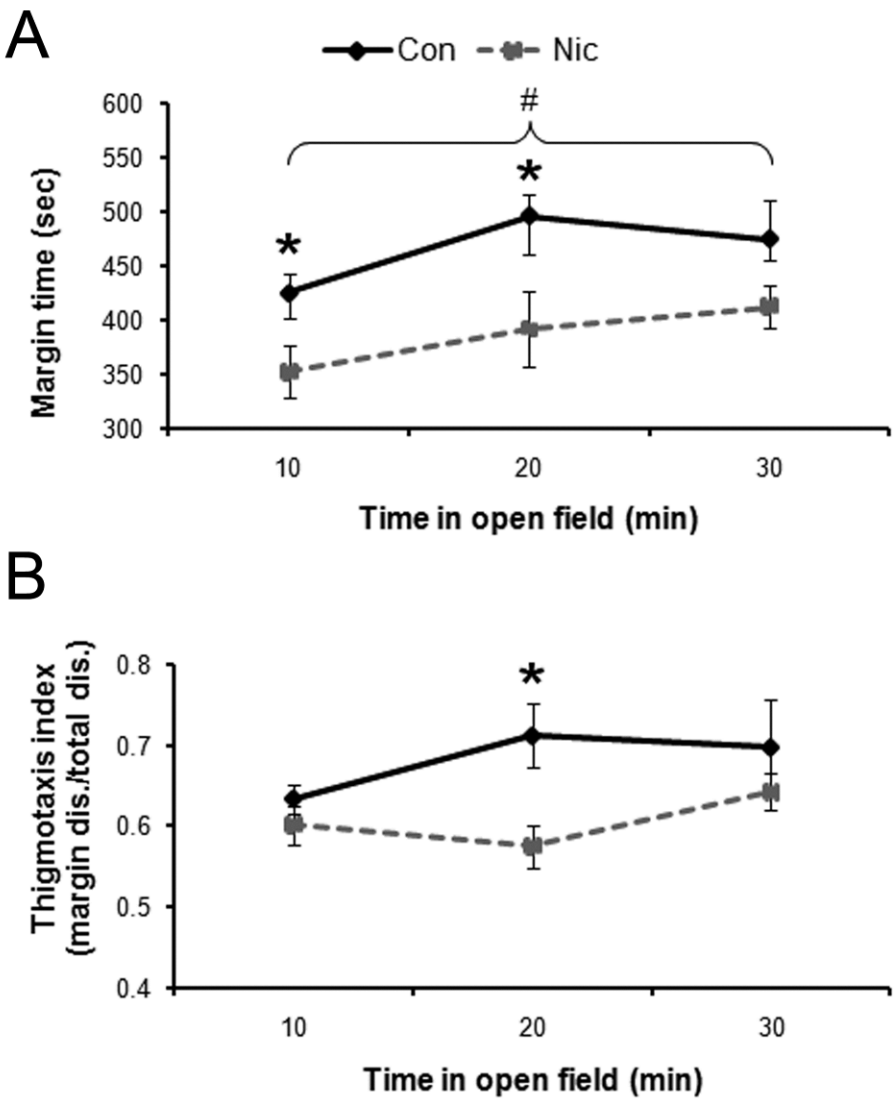

Figure IV-3. Anxiety levels were reduced in nicotine-treated mice as compared to controls indicated by margin time (***A***) and thigmotaxis index (***B***) in the open field test. ***A***, Margin time is presented as second (sec). ***B***, Thigmotaxis index is margin distance divided by total distance. Time in the open field was divided into three 10 minutes (min) intervals. Con, control group. Nic, nicotine-treated group. Error bars: SEM. Student's *t*-test, compare between control and nicotine group, * p-value of individual 10-minute interval < 0.05, # p-value of the whole 30 minutes < 0.05.

For memory and cognitive function, mice were tested in a modified EPM and an object recognition test, but neither test showed significant differences between treatment groups (modified EPM, T2: control: 21.2 ± 3.83 sec, nicotine: 22.2 ± 4.13 sec. Student's t-test, p = 0.86; object recognition, time ratio: control: 0.49 ± 0.09, nicotine: 0.66 ± 0.11. Student's t-test, p = 0.265).

Epibatidine binding

Receptor autoradiography using ^{125}I-Epibatidine binding was performed to evaluate nicotinic receptor binding sites after chronic treatment to validate nicotine exposure in the brain (Corringer et al., 2006). Non-specific binding was negligible and the binding pattern was the same as previously reported with strong binding in the thalamic dorsal lateral geniculate nucleus, medial habenula, and fasciculus retroflexus, moderate binding in neocortical structures and low levels of binding in the hippocampus (Perry and Kellar, 1995; Huang and Winzer-Serhan, 2006a) (Fig. IV-4). In the hippocampus, low numbers of binding sites were with increased binding in the dorsal hippocampal commissure, alveus, lacunosum molecular layer, and the molecular layer of the dentate gyrus (Fig. IV-4A). In the hippocampus, relative ^{125}I-Epibatidine binding levels measured as ROD values were determined in stratum lacunosum molecular of the CA1, and the molecular layer of the dentate gyrus in control- and nicotine-treated animals. ^{125}I-Epibatidine binding was significantly higher in nicotine-treated mice than in controls (control: 0.39 ± 0.010; nicotine: 0.42 ± 0.003; Student's *t*-test, p = 0.019) (Fig. IV-4B). Moderate ^{125}I-Epibatidine binding was detected in the neocortex with more

intense binding in layers IV to VI compared to layers II/III (Fig. IV-4A). Relative ^{125}I-Epibatidine binding levels were measured in visual and somatosensory cortex in layers IV to VI from control- and nicotine-treated animals. The numbers of ^{125}I-Epibatidine binding sites in nicotine-treated mice were higher than in controls (control: 0.48 ± 0.011; nicotine: 0.50 ± 0.007; Student's *t*-test, p = 0.055) (Fig. IV-4B). In contrast, relative binding levels were not affected by nicotine treatment in thalamic areas (control: 0.70 ± 0.024; nicotine: 0.68 ± 0.011) (Fig. IV-4B).

Expression of longevity genes and neurotrophins

The expressions of five CR-related longevity genes were assessed in this study. The expression patterns were the same as previously reported (Huang et al., 2011). The mRNA expression levels were measured in principal layers of hippocampal CA1, CA3 and DG, and in layers II to VI of somatosensory cortex and normalized to GAPDH expression. There was a significant nicotine treatment effect, with nicotine increasing the overall expression levels of SIRT1, Ku70 and Nampt (two-way ANOVA, general treatment effect, p = 0.014, p = 0.002 and p = 0.023, respectively) (Fig. IV-5A, B and C). Post hoc analysis revealed that Ku70 mRNA expression was significantly increased

by nicotine treatment in CA1 (control: 96.1 ± 5.5; nicotine: 120.0 ± 7.0; Student's *t*-test, p = 0.028) (Fig. IV-5B). In contrast, no significant treatment effects were detected for FoxO3 and p53 mRNA expression (Fig. IV-5E, F), although, there was an overall trend detected for FoxO3 with nicotine-treated mice exhibiting higher levels than controls (two-way ANOVA, general treatment effect, p = 0.089) (Fig. IV-5D).

The effects of chronic nicotine exposure on growth factor mRNA expression were determined for BDNF and NT-3. The expression patterns were the same as previously described (Son and Winzer-Serhan, 2009; Di Liberto et al., 2010). Measurements for BDNF were taken in the same areas as for the CR-related longevity genes described above, but NT-3 expression was measured only in CA2 and dentate gyrus since only these areas expressed NT-3 in the mouse brain. There were no significant differences nor trends in expression intensity or expression pattern in response to treatment for either neurotrophins, which correspond to another study showing that chronic oral nicotine has no effect on BNDF levels (Kivinummi et al., 2011) (Fig. IV-5F).

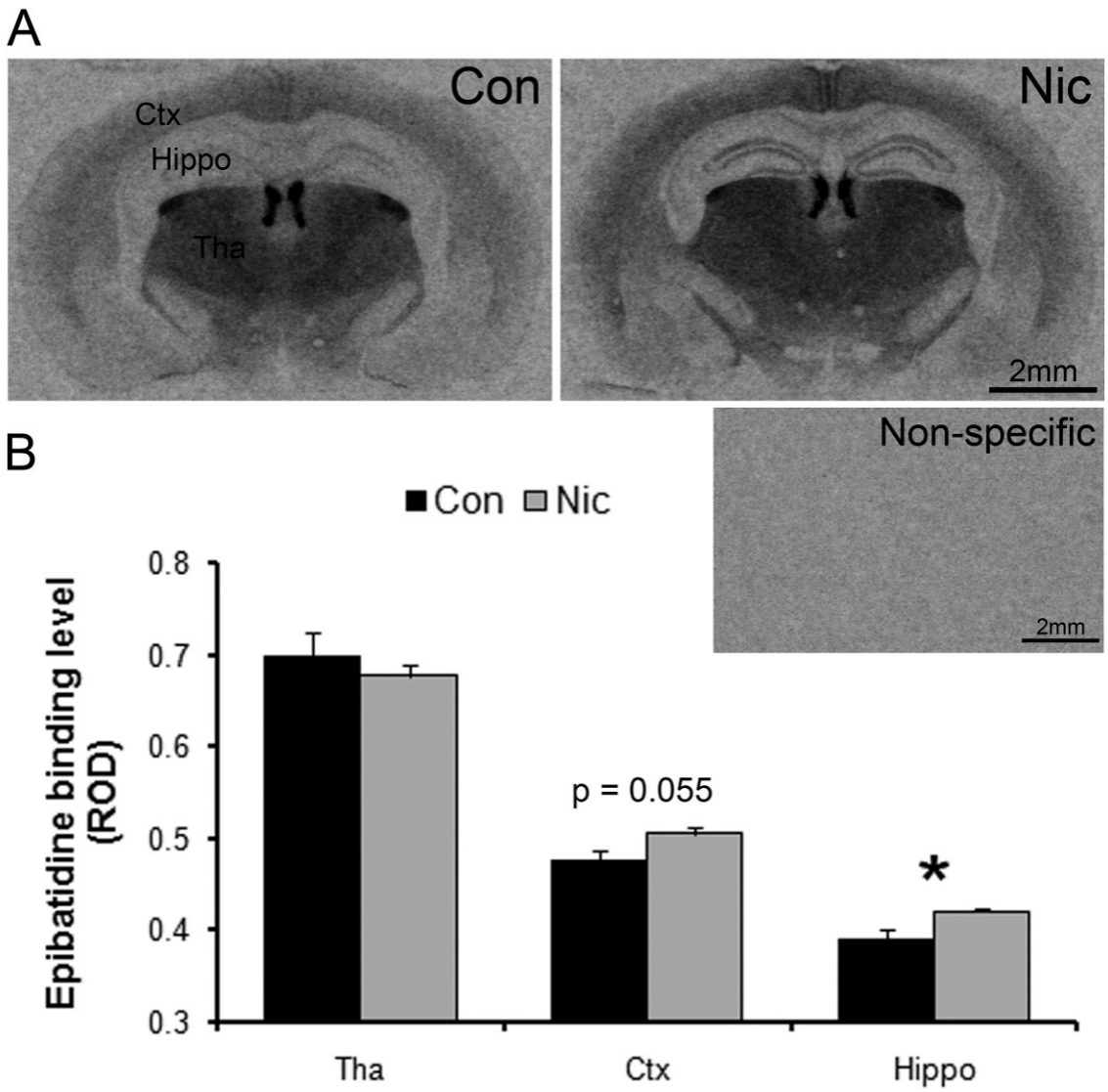

Figure IV-4. Nicotine treatment increased the level of ^{125}I-epibatidine bindings to heteromeric nAChRs in the cortico-hippocampal regions. ***A***, Representative images of receptor autoradiograph. Scale bars: 2 mm. ***B***, Quantitative analysis in the thalamus (Tha), neocortex (Ctx), and hippocampus (Hippo). Binding levels were presented as raw optical density (ROD). Con, control group. Nic, nicotine-treated group. Error bars: SEM. Student's *t*-test, * $p < 0.05$.

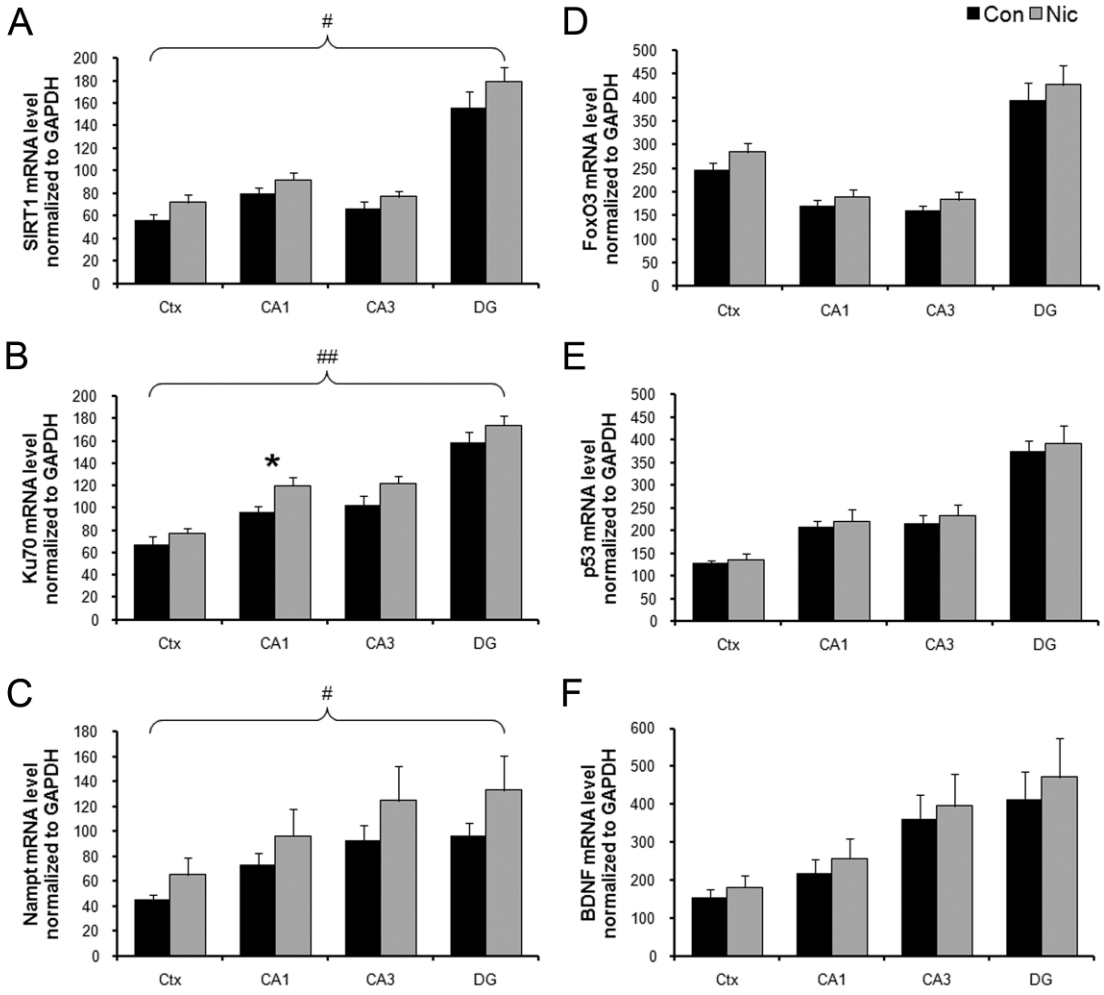

Figure IV-5. SIRT1, Ku70 and Nampt mRNA levels were increased in cortico-hippocampal regions in nicotine-treated mice as compared to controls. Quantification of mRNA levels of SIRT1 (***A***), Ku70 (***B***), Nampt (***C***), FoxO3 (***D***), p53 (***E***), and BDNF (***F***). Regions measured included granular cell layer of the dentate gyrus (DG), CA1 and CA3 pyramidal cell layer of the hippocampus, and neocortex (Ctx). Data were normalized to GAPDH levels of the same areas. Con, control group. Nic, nicotine-treated group. Error bars: SEM. Two-way ANOVA, general treatment effect, # $p < 0.05$, ## $p < 0.01$. Student's *t*-test, * $p < 0.05$.

DISCUSSION

The main purpose of this study was to identify a low dose of nicotine self-administered via drinking water to mice that is safe and effective, and therefore, suitable for long-term treatment. Blood levels of nicotine and cotinine were determined, and, as indications of a centrally acting dose, food intake, body weight gain and number of nicotinic receptor binding sites were measured. Based on these parameters, the highest dose of nicotine in the drinking water (300 μg/ml) was the only dose in this study that resulted in detectable nicotine blood levels, reduced food intake and body weight, and increased numbers of high affinity nAChR binding sites. In addition, we determined the effects of chronic treatment (300 μg/ml) on behavioral measures of anxiety and learning and memory, and expression of SIRT and CR-related genes, and the neurotrophic factors BDNF and NT3.

Dose of nicotine in drinking water and blood nicotine levels

In this study, we treated young adult C57BL/6 male mice for a period of three weeks with three doses of nicotine via drinking water, which is non-invasive, stress-free and requires no additional handling, and therefore, can be used over long-periods of time. It is an established method of chronic self-administration, and is a viable alternative to repeated injections or surgical implantation of minipumps. In addition, administration via drinking water provides the nicotine fluctuations seen in smokers or people using oral nicotine replacement medications such as nicotine gums, sprays or lozenges. However, oral nicotine administration results in reduced bioavailability due to

ion trapping of nicotine in the acidic milieu in the stomach (Hukkanen et al., 2005), slow absorption through the gastrointestinal tract and rapid metabolism in the liver (Le Houezec et al., 1989). Additionally, mice metabolize nicotine more rapidly than rats or humans. Thus, it is difficult to estimate the bioavailability of orally administered nicotine based on the dose (Miller et al., 1977; Pekonen, 1993). Therefore, we initially evaluated different doses of nicotine and measured blood nicotine and cotinine levels. All three doses were well tolerated by the animals with no apparent negative effects on general appearance. In this study, the low and medium doses (20 μg/ml and 120 μg/ml, respectively) resulted in blood nicotine levels that were below the detection limit, and in highly variable blood cotinine levels suggesting, that the doses were too low to provide consistent nicotine exposure. Only the highest dose of nicotine (300 μg/ml) had low but detectable blood nicotine levels with an average of 6.2 ng/ml. This blood nicotine concentration is comparable to levels seen in people using nicotine gum but below that after smoking a cigarette or using oral tobacco products like chewing tobacco or snuff (Hukkanen et al., 2005). Thus, 300 μg/ml provided a low but effective dose in mice that is similar to a low dose in humans treated with nicotine replacement medications. The 300 μg/ml dose resulted in highly variable blood cotinine levels with an average of 192 ng/ml, which is in line with findings from other groups. Research conducted in mice treated with nicotine via drinking water at concentrations of 200 to 500 μg/ml resulted in plasma cotinine levels ranging from 652 to 1450 ng/ml (Pietila and Ahtee, 2000; Brunzell et al., 2003). The large variability of plasma cotinine levels between and within studies is likely due to the relatively short half-life of plasma cotinine in mice (20-40

minutes) compared to other species (rats 5-6 hours and human 19 hours) (Miller et al., 1977; Benowitz et al., 1983; Petersen et al., 1984; Pekonen, 1993), and therefore, does not provide a reliable surrogate measure of blood nicotine levels in mice. Thus, the oral administration route in mice requires large doses of nicotine in drinking water to reach measurable blood levels of nicotine and cotinine that are comparable to low doses detected in humans.

Dosing effects on food intake and body weight

Chronic nicotine reduces body weight and suppress food intake in humans and laboratory animals through activation of nAChR located in brain stem and hypothalamus, thereby activating the central hypothalamic melanocortin system (Mineur et al., 2011). In neonates, even very low doses of nicotine reduce body weight gain, and in humans, people using nicotine replacement therapy during smoking cessation exhibit reduced weight gain (Allen et al., 2005; Huang et al., 2006; Ferguson et al., 2011). Thus, low doses of nicotine activating nAChRs in the CNS affected food intake and body weight. This anorexic effect of nicotine was seen only in our highest nicotine-treatment group whereas low and medium doses had no effect on either food intake or body weight. This result supports the findings from the blood nicotine tests that only the highest dose of 300 μg/ml of chronic nicotine treatment through drinking water results in low but effective nicotine levels. However, decreases in body weight and food intake have not consistently been reported with chronic oral nicotine administration (Sparks and Pauly, 1999), or were only seen after prolonged treatment (Pietila and Ahtee, 2000).

In our experiments, nicotine started to exhibit an effect on food intake and weight gain around the time the highest dose of nicotine was reached. However, as can be seen in Figure 1 and 2, food intake and body weight gain were highly variable on days 14 to 16 of treatment. This corresponded to a period of construction in adjacent rooms in the vivarium. Although we cannot be certain, we believe that the construction noise caused stress for all animals in this study, which might have contributed to the altered feeding behavior during those days, which also affected body weight gain. Thus, different housing conditions or strain sensitivity to stress might explain inconsistencies in the results between our study and those reported by others.

Upregulation of high affinity binding sites

Another hallmark of CNE indicating that relevant amounts of nicotine reach the brain where nicotine can interact with nAChRs, is an increase in CNS heteromeric nicotinic binding sites (Corringer et al., 2006). Chronic nicotine treatment in rodents increases high affinity nicotinic binding sites in cortico-hippocampal regions (Pietila et al., 1998; Sparks and Pauly, 1999; Nuutinen et al., 2005). Human smokers also have greater densities of high affinity nAChRs compared to nonsmokers, most likely due to the action of nicotine on neuronal nAChR numbers (Perry et al., 1999; Mukhin et al., 2008). Using receptor autoradiography, we determined that only the highest treatment dose of nicotine increased ^{125}I-epibatidine binding to heteromeric nAChRs in cortico-hippocampal regions, whereas, low and medium doses had no effect. This finding correlates well with other studies using an oral administration route via drinking water

that reported increased numbers of high affinity nAChR binding sites (Sparks and Pauly, 1999; Nuutinen et al., 2005; Andreasen et al., 2009).

Together, nicotine and cotinine blood levels, food intake, body weight, and receptor binding results indicate that this oral self-administration route is effective in reaching meaningful levels of nicotine in the brain, but that due to the rapid metabolism that occurs in mice, high levels of nicotine need to be administered in the drinking water.

Effects of chronic nicotine exposure on behavioral measures

Nicotine has been shown to have effects on anxiety and depression in both human and animal studies. In humans, smokers experience a lower anxiety level than non-smokers when challenged with stress, and increased anxiety levels during smoking cessation, which suggests that nicotine exposure reduces anxiety (Gilbert et al., 1989; Perkins and Grobe, 1992; Tate et al., 1993). However, in rodents, nicotine's effects on anxiety are complex, and chronic or acute nicotine administration can result in either an anxiolytic or anxiogenic response which depends on several factors such as the dose, regimen and time after drug administration, and behavioral state of the animals (Picciotto et al., 2002). An open field behavior test was used to access locomotion, exploratory activity and anxiety-like behavior in animals receiving the high dose of nicotine and compared to controls. Our results indicated that locomotor and exploratory activities were not changed in response to CNE. However, two parameters suggested that anxiety levels were reduced in nicotine-treated mice. Several animal studies also support an anxiolytic effect of chronic nicotine and nicotinic agonists (Brioni et al.,

1994; Levin et al., 2007), but one study reported no change in anxiety-like behavior in male mice after chronic oral administration (Caldarone et al., 2008). Thus, in agreement with other studies, voluntary oral CNE does not result in increased anxiety, and in fact, might have anxiolytic effect in nicotine-treated male mice.

Several studies provide evidence of improved cognitive function after CNE in mouse models of AD, schizophrenia, attention deficit hyperactivity disorder, and stress-induced memory impairment (Aleisa et al., 2006; Weiss et al., 2007; Srivareerat et al., 2009; Rushforth et al., 2011) as well as in animals without pathological conditions (Levin and Torry, 1996). Therefore, we evaluated learning and memory in a modified version of the EPM which tests the escape latency from the open arm into the enclosed center after one training trail as a measure for spatial memory (Biala and Kruk, 2009), and in the object recognition test, a measure of short-term memory (Bevins and Besheer, 2006). We did not detect a difference in escape time in the modified EPM or in the object recognition test between animals treated with the high dose of nicotine and compared to controls. Thus, in this study, oral CNE did neither improve nor impair cognitive functions, which could be due to the small sample size (n = 5) although, there was not even a trend towards increased or decreased cognitive performance. However, in our study we used young adult male mice without any impairments which are at their optimal level of memory performance, and in line with findings by other, nicotine treatment might not improve cognitive functions in young adults (Aleisa et al., 2006). This also supports Newhouse's theory that results of nicotine stimulation are a reflection of baseline cognitive performance level (Newhouse et al., 2004).

Effects of chronic nicotine exposure on gene expression

This study is the first to examine the possible relationship between the effect of nicotine and the expression of CR-related longevity genes namely SIRT1, Ku70, Nampt, p53, FoxO3, and the neurotrophic factors BDNF, and NT-3. Our previous study showed that β2 knockout mice which lack the predominant heteromeric nAChR subtype in the brain, increased their longevity gene expression in middle-aged 18-month old mice compared to age-matched wild type mice (Huang et al., 2011). This could be an adaptational response due to the accelerated aging, which is observed in these mice, and as seen in other mouse models of neurodegeneration (Zoli et al., 1999; Kim et al., 2007a), or β2-nAChRs could directly influence expression of longevity genes. In this study, we evaluated the effects of CNE on the expression of several of these CR-regulated survival genes to test if chronic activation of nAChRs affects their expression, and expression of the neurotrophic factors BDNF and NT-3 which are regulated by nicotine in adults and during development (French et al., 1999; Son and Winzer-Serhan, 2009; Srivareerat et al., 2009). Increased expression of CR-related genes and neurotrophic factors could be beneficial to maintain healthy brain functions, and prevent insult- or age-related cognitive impairments, and thus could provide a mechanism through which nicotine asserts its positive effects on learning and memory, and reduces premature aging. In particular, increased expression of SIRT1 has been shown to not only protect against neurodegeneration but also play a vital role in normal brain function (Gao et al., 2010).

SIRT1, Ku70, and Nampt exhibited changes in mRNA expression levels in response to CNE in cortico-hippocampal regions whereas mRNA expression of p53 and FoxO3 and of BDNF and NT-3 were not different from controls. Thus, it is possible that there is a molecular link between activation of nAChRs and SIRT1-related longevity genes. Nicotine, by interacting with nAChRs, activates multiple intracellular signaling pathways including PI3 kinase-AKT, JAK2/STAT3 and MEK/ERK (Kawamata and Shimohama, 2011) which could regulate transcription of CR-related genes. CNE results in altered gene expression of numerous genes in several brain tissues, including genes involved in mitochondrial pathways, thus, linking nicotine to cellular metabolism (Wang et al., 2009), which could contribute to the increased expression of SIRT1, Nampt and Ku70 found in this study. However, CNE caused a mild reduction in caloric consumption (88%), and thus, an indirect regulation of CR-related genes though caloric restriction cannot be ruled out. Other studies have shown that CR of 70 – 60% increases expression of SIRT1 in the brain (Qin et al., 2006b). However, it is possible that even a mild reduction in caloric intake could increase expression of SIRT1 and related genes. Further studies need to be done to better understand this action of nicotine and nicotinic agonists on the SIRT1 signaling pathway.

It is not clear why CNE in this study did not affect the expression of the neurotrophic factors, BDNF and NT-3, as seen by others (French et al., 1999; Kenny et al., 2000; Son and Winzer-Serhan, 2009; Srivareerat et al., 2009). Perhaps the dose of nicotine administered via drinking water did not achieve brain levels high enough to

stimulate expression of these genes, or there are species differences between rat and mouse and the previous studies had been done in rats.

Oral self-administration of nicotine via drinking water provides a stress-free route of chronic drug treatment but requires high doses in order to reach biological active levels of nicotine in mice brain. Three weeks of systemic nicotine treatment decreased food intake and body weight gain and increased expression of high affinity nicotine binding sites, all hallmarks of chronic exposure to nicotine. CNE did not impair cognitive functions and had an anxiolytic effect in 3-month-old male mice. CNE increased expression levels of SIRT1, Nampt, and Ku70 in cortico-hippocampal regions. The up-regulation of these genes may contribute to the beneficial neuroprotective effect of nicotine.

CHAPTER V

LONG-TERM NICOTINE AND CALORIC RESTRICTION TREATMENT IMPROVE MEMORY IN MIDDLE-AGED MICE AND DIFFERENTIALLY REGULATE SIRT1, NAMPT AND KU70 GENE EXPRESSION IN CORTICO-HIPPOCAMPAL AREAS

SUMMARY

Nicotine, the major psychoactive ingredient in tobacco smoke, which functions through activating neuronal nicotinic acetylcholine receptors (nAChRs), exerts neuroprotective effects through unknown pathways. In this study we sought to determine if the neuroprotection provided by chronic nicotine exposure shares the same mechanisms as caloric restriction (CR), since both have been shown to be neuroprotective. CR provides neuroprotection through activation of the deacetylase SIRT1, and nicotine could act through a similar mechanism. Fourteen-month-old C57BL/6 male mice were assigned to one of three treatment groups for 4 months: CR mice received 70% caloric restriction and no nicotine; nicotine (NC) mice, received *ad libitum* food and 300 μg/ml of nicotine in water; control (AL) mice, received *ad libitum* food and water. At 18 months of age, CR mice showed a higher level of anxiety than NC and control mice, as detected by increased margin time in the open field test. There was no difference between groups with respect to short-term memory object recognition. In the modified elevated plus maze, which tests long-term spatial memory, both CR and NC mice showed significantly better performance as compared to control mice (p =

0.023). In the Morris water maze, both spatial acquisition and probe trials did not reveal any significant difference between groups, but performers above the median in the NC group displayed a trend to perform better above median performers in the AL group in the probe trial, while the poor performers, below the median, in these groups did not have any difference in their performance. After behavior testing, mouse brains were collected and sectioned for nAChR binding using epibatidine and *in situ* hybridization using cRNA probes for Nampt, SIRT1 and Ku70. Epibatidine binding was increased in NC mice compared to CR mice and AL mice in both neocortex and hippocampus ($p = 0.053$, $p < 0.001$, respectively), demonstrating that nicotine treatment caused upregulation of heteromeric nAChRs in these brain areas but CR did not. CR mice had significantly increased expression levels of SIRT1, Nampt, and Ku70 in the neocortex; whereas in the hippocampus (CA1, CA3, and dentate gyrus). Only Ku70 mRNA expression levels were significantly increased. In contrast, NC mice did not show any difference in gene expression for SIRT1, Nampt or Ku70 in any of the cortico-hippocampal areas examined. These results indicate that long-term CR and nicotine treatment improve memory in aging mice, but they probably accomplish these effects through different mechanisms.

INTRODUCTION

Smoking is negatively correlated with PD and AD. Nicotine is the major psychoactive ingredient in tobacco smoke and is neuroprotective. Loss of nAChRs, especially in cortical regions, is one of the major histological changes in normal brain

ageing and neurodegenerative diseases like AD. In contrast, mice lacking high-affinity nAChRs exhibit accelerated neuronal ageing and early onset of age-related deficits in spatial learning and memory. Thus, chronic nicotine administration, which increases the number of nicotinic binding sites might be beneficial during aging and delay age-related cognitive decline.

Nicotine also decreases appetite and increases energy expenditure, which contributes to the observations that body weight or body mass index are lower in cigarette smokers than in non-smokers. Thus, nicotine administration could result in CR.

CR is a regimen that extends the lifespan in all mammalian species tested and increases the expression of survival genes such as SIRT1, a nicotinamide adenine dinucleotide (NAD)-dependent deacetylase. SIRT1 is expressed in the brain and upregulation of SIRT1 protects neurons against neurodegeneration and attenuates apoptosis by deacetylating the DNA repair factor Ku70. Nicotinamide phosphoribosyltransferase (Nampt), a NAD biosynthetic enzyme, controls the activity of SIRT1. Nampt is induced by stress or nutrient deprivation and increases cellular resistance to damage.

The hypothesis of this study was that long-term nicotine exposure or nicotinic receptor activation improves age-related memory and cognition decline as has been observed with CR, and the improvement is thought to result from activation of CR-related longevity genes. In this study, the effects of long-term nicotine exposure (4 months) were determined for mice. Although chronic (but not long-term) nicotine

administration has been proved on rats to be neuroprotective and improve memory and cognitive function, this study is the first with such a long term exposure to test whether the effects sustain or not. It was also important to compare the effects of long-term nicotine administration with caloric restriction; since we hypothesized that they share similar mechanisms. We also tested the neuroprotective effect of both caloric restriction and nicotine exposure on normal aging process because we believed that the benefits are general and not restricted to any specific disease pathology. In this study we determined if chronic nicotine treatment or CR starting in middle-aged mice, can delay age-related cognitive decline, and if chronic nicotine and CR-treatments share similar mechanisms resulting in beneficial effects in aging animals.

EXPERIMENTAL PROCEDURES

Animals and treatments

A breeding colony of C57BL/6 mice, originally obtained from the Jackson Laboratory, was established at Texas A&M University's Laboratory Animal Research and Resource facility. At 14 months of age, male mice were individually caged, randomly assigned to different treatment groups for 4 months, and tested at 18 months of age (n = 9): control (**AL**) mice – received 2% saccharin in water (saccharin sodium salt hydrate, Sigma, St. Louis, MO, USA) and a control diet (NIH31) *ad libitum*; nicotine treated (**NC**) mice – received 300 μg/ml nicotine free base ((-)-nicotine hydrogen tartrate, Sigma) in 2% saccharin in water and a control diet (NIH31) *ad libitum*; caloric

restriction (**CR**) mice – received 2% saccharin water and a 30 to 40% restricted diet (70 to 60% of AL, by weight, NIH31-fortified). Both the NIH31 and NIH31-fortified diets were purchased from the National Institute on Aging. All groups started to receive 2% saccharin in water two weeks prior to day 1 of the actual treatment regime, to establish their individual daily drinking and food consumption volume. Animals in the NC group initially received 30 μg/ml of nicotine on day 1, and the concentration was gradually increased until the final concentration was reached on day 7. Meanwhile, animals in the CR group started to receive 40% restricted diet (60% of AL). A 40% caloric restriction lasted until day 28, and the amount of food given was then increased to 70% of AL due to the dramatic loss of body weights in the CR mice. All treatments lasted until day 126 (4 months) (Table IV-1). On days 115 to 125, mice were subjected to behavior testing and then euthanized on day 126. Food consumption, water intake and body weight were monitored throughout the dosing period, and the amount of food given to CR mice were subject to change according to the amount of food consumption observe in AL mice. All procedures were approved by the Texas A&M University Animal Use Committee and carried out in accordance with the National Institutes of Health Guide for the Care and Use of Laboratory Animals (National Institutes of Health Publication No. 85-23, revised 1996).

Table V-1. The schedule of CR and NC treatments

Group	Day	1	2	3	4	5	6	7-27	28-126 [a]
CR	% food of AL (by weight)	60	60	60	60	60	60	60	70
NC	Nicotine concentration in 2% saccharin water (μg/ml, free base)	30	50	100	150	200	250	300	300

[a] All mice were sacrificed on day 126.

Behavior tests

Modified elevated plus maze (mEPM)

Long-term spatial memory was tested in a two-trial mEPM on days 115 and 116 as described previously (Biala and Kruk, 2009). The EPM apparatus was made of Plexiglas painted matte black from the outside. The maze consisted of four 30 cm long and 5 cm wide arms: two open arms (without walls) facing opposite, and another two enclosed arms (15.25 cm high walls on three sides with one end left open) facing opposite so that they formed a plus shape (Walf and Frye, 2007). The whole maze was elevated 40 cm off the ground, located in a quiet room illuminated by a central dim red light, and environmental cues were kept constant during testing. All mice were accustomed to the experimental room for 10 minutes before both acquisition (day 115) and retention (day 116) trials. The maze was cleaned with 70% ethanol between mice. In the acquisition trial, mice were individually placed at one end of one open arm facing away from the central platform and allowed to move from the open arm to either of the enclosed arms. A successful entry was considered when all four limbs were in the

enclosed arm. If a mouse did not enter an enclosed arm within 90 seconds it was placed in one of the enclosed arms and allowed to explore for another 60 seconds,. On the next day (24 hours later), all mice were subjected to a retention trial in the same manner, and the time to successful entry was recorded as T2. T2 values on the retention trial were used as an index of memory. The improvement of memory and learning is characterized by decreases in the T2 values.

Open field

All mice were tested in an open field equipped with vertical and horizontal beam sensors for locomotion, exploratory and anxiety behaviors on day 117. The mice were placed individually in an open field (length × width × height: 20 × 20 × 30 cm) (Versamax animal activity monitor and analyzer, AccuScan Instruments, Columbus, OH, USA) equipped with vertical and horizontal beam sensors. The apparatus was constructed from transparent Plexiglas and located in a quiet room. All environmental cues including lighting were kept constant during testing. Mice were accustomed to the experimental room for 30 minutes, and then placed in the open field for another 30 minutes. Activities were recorded every minute and analyzed in 5 minutes segments (6 segments total). The open field chamber was cleaned with 70% ethanol between mice. Total distance, movement time, margin distance, margin time, and center distance were automatically recorded.

Object recognition

Short-term recognition memory was tested in a one-trial object recognition test on day 118 in the manner of "two sample objects with one environment" as described previously (Bevins and Besheer, 2006) with minor changes. A transparent Plexiglas chamber (length × width × height: 20 × 40 × 30 cm) (AccuScan Instruments) covered on the outside with white bench protector (VWR, West Chester, PA, USA) was setup in a quiet room where environmental cues were kept constant during testing. Mice were allowed individually to become familiarized with the chamber for 10 minutes. Two identical sample objects (medium heavy duty black binder clips 3.2 × 5.5 cm, OfficeMax) were placed in the back left and right corners of the chamber. The test animal was placed at the center of the chamber facing the front opposite to the sample objects with its nose pointing to either side and then allowed to explore for 10 minutes. After a one-hour interval, one of the sample objects was replaced by a novel object (standard wooden clothes pin, 8.5 × 1 cm). The mouse was placed back into the chamber as described, and allowed to explore for 3 minutes. The chamber was cleaned with 70% ethanol between mice. Each exploration period was recorded by a video camera (DIGITAL IXUS 50, Canon, Japan) setup directly above the apparatus. Using XNote Stopwatch (free evaluation version, http://www.stopwatch-timer.com, dnSoft Research Group, accessed in 2011), direct contact scoring was done by a blind investigator. The total time test subjects spent exploring the objects (both sample and novel), and the time ratio (novel/total time) were calculated and used as an index of short-term memory.

Morris water maze (MWM)

To assess long-term spatial learning and memory, mice were subjected to the MWM on days 119 to 125 as previously described (Vorhees and Williams, 2006) with minor changes. The maze was made of a stainless-steel circular tank painted white inside (diameter × height: 120 × 50 cm) and divided into four quadrants labeled N (north), E (east), S (south) and W (west), clockwise. An 8 × 8 cm transparent platform was constructed from clear Plexiglas. The tank was filled with a depth of 30 cm room temperature (RT) water. The whole experiment was divided into three parts: the cued trial (day 119), spatial acquisition (days 120-124) and probe trial (day 125). In the cued trial, white curtains were placed around the maze to block any distant visual cues, and the platform was elevated 1cm above the water surface and marked by yellow and red tape. This established a control condition to test the animals' ability to distinguish visual cues and to learn to swim to a cued goal (visible platform marked with yellow and red tape). In this one-day cued trial, each mouse was subjected to 6 training trials with all different start-goal combinations: N-SE, E-NE, S-SW, W-SE, S-NE and N-NW. Each subject was gently placed in the starting position facing the outside perimeter of the maze and allowed swim to the goal platform within 60 seconds. If a mouse failed to swim to the platform within 60 seconds, that mouse was lead to the platform. Once the mouse reached the platform, it was allowed to stay there for another 15 seconds. Animals that could not perform the cued trail were eliminated from the subsequent spatial acquisition and probe trial. The spatial acquisition consisted of 5 consecutive days (days 120-124). On the wall of the tank, colored and shaped cues were given, and

the curtains used in the cued trial were removed. The outer environment including the experimenter was considered as distal visual cues and stayed constant. In the spatial acquisition, the colored tape on the platform was removed, and the platform was submerged 1.5 cm under the water surface and fixed in the center of the SW quadrant, which was designated as the target quadrant. In each spatial acquisition day, each mouse was subjected to 4 training trials that each had different start locations (Table IV-2). Each subject was gently placed at the starting location facing the outside perimeter of the maze and allowed to find the platform within 60 seconds. If a mouse failed to find the platform within 60 seconds, that mouse was lead to the platform. Once the mouse reached the platform, it was allowed to stay on the platform for another 15 seconds to orientate itself. In the last trial, which was the probe trial (day 125), the platform in the target quadrant was removed. All mice were allowed to swim in the maze individually for 30 seconds and then they were removed from the maze. The whole procedure was videotaped using a camera (DIGITAL IXUS 50, Canon, Japan) and manually analyzed using Tracker 3.10 (http://www.cabrillo.edu/~dbrown/tracker, Open Source Physics, accessed in 2011). For the spatial acquisition, three parameters: latency (time to find the platform), path length, and cumulative distance from the platform were acquired for each mouse. Each acquisition was averaged in blocks of four trials and analyzed. In the probe trial, two parameters were acquired for each mouse: time in target quadrant and distance in target quadrant.

Table V-2. Start locations in MWM spatial acquisitions

Acquisition Day	Trial 1	Trial 2	Trial 3	Trial 4
1	N	E	SE	NW
2	SE	N	NW	E
3	NW	SE	E	N
4	E	NW	N	SE
5	N	SE	E	NW
6 (Probe)	NE			

The goal (platform) was located in the SW quadrant during acquisition.

Tissue preparation

Mice were anesthetized using isoflurane (IsoFlo, North Chicago, IL, USA) and decapitated on day 126. The brains were rapidly removed, cut mid-saggitally into two halves, frozen in powdered dry ice, and stored at -80°C until used. One neocortex (cerebral hemisphere) was sectioned into fourteen μm thick coronal sections, 196 μm apart, using a cryostat, starting at Bregma level -1.70 mm and ending at -2.30 mm. For *in situ* hybridization, sections were thaw-mounted onto glass microscope slides coated with gelatin (Spectrum, Gardena, CA, USA) and poly-L-Lysine (Sigma). Sections were then post-fixed with 4 % paraformaldehyde in 0.1 M phosphate buffer, pH 7.4, for 1 hour at RT and stored with desiccant at -20°C until used. For epibatidine binding, sections were mounted on glass microscope slides coated twice with gelatin, left at 4°C overnight with desiccant and stored at -80°C until used. For the other half of the brain, the neocortex and hippocampus were dissected separately on ice for immunoblot analysis. Tissues were mixed with ice-cold RIPA buffer containing protease inhibitor, homogenized using a sonic dismembrator (Thermo Fisher Scientific, MA, USA), incubated on ice for 30

minutes, and then centrifuged at 14000 rpm for 20 minutes at 4°C. The supernatant was collected, mixed with Lamelli buffer and stored at -80°C until used.

Epibatidine binding

Epibatidine binding was performed as previously described (Huang and Winzer-Serhan, 2006b) with minor changes. Tissue sections were pre-incubated 5 minutes in Tris-HCl buffer (50 mM Tris-HCl, 120 mM NaCl, 5 mM KCl, 2.5 mM $CaCl_2$, 1 mM $MgCl_2$, pH 7.4) and then incubated with 0.4 nM [^{125}I]-Epibatidine (PerkinElmer Life Science NEX358, Boston, MA, USA, specific activity: 2200 Ci/mmol) for 1 hour at RT. For non-specific binding, sections were incubated with the presence of 400 μM (-)-nicotine hydrogen tartrate. Sections were washed in ice-cold Tris-HCl buffer twice for 1 minute, followed by 10 seconds in cold ddH_2O, and dried at RT overnight before exposure to BioMax MR film (Kodak, Rochester, NY, USA). After 1-day exposure, films were developed in D19 Kodak developer for 4 minutes and fixed in Kodak Rapid Fixer for 5 minutes.

cRNA probe synthesis and *in situ* hybridization

Templates for the synthesis of cRNA probes were generated for mouse SIRT1, Ku70 and Nampt as previously described (Son and Winzer-Serhan, 2009). ^{35}S-labeled cRNA probes were synthesized in the antisense orientation in the presence of ^{35}S-UTP (PerkinElmer Life Science) and either T3 or T7 RNA polymerase (Applied Biosystems/Ambion) using *in vitro* transcription. The method for *in situ* hybridization

has been described in detail previously (Winzer-Serhan et al., 1999; Huang et al., 2011). In brief, tissue sections were pre-hybridized with 0.1 μg/ml proteinase K for 10 minutes. After overnight (16-20 hours) hybridization at 60°C with ^{35}S-labeled cRNA probes, sections were treated with RNase A at 37°C for 30 minutes and washed. Slides with adhered sections were exposed to BioMax MR film along with [^{14}C]-standards (Amersham, Code RPA 504L, Batch21, Buckinghamshire, UK), and the films were developed as described in the previous **epibatidine binding** section.

Autoradiogram analysis

Quantitative analysis of autoradiograms was carried out using MCID basic (InterFocus Imaging Ltd, Haverhill, Suffolk, UK). For receptor binding, raw optical density (ROD) was measured in the hippocampus (the molecular layers of both dentate gyrus (DG) and the hippocampal proper), thalamus (the post thalamic nucleus and the ventral posteriomedial thalamic nucleus), and cerebral cortex (layers IV-V, of the visual and somatosensory cortex). For analysis of the hybridization signal, a standard curve (ROD vs. nCi/g wet weight) was generated using [^{14}C]-standards and ROD values were converted to nCi/g wet weight. Measurements were taken in the pyramidal cell layer of the CA1 and CA3, in the granular cell layer of the DG of the hippocampus, and in the entire cerebral cortex located on individual sections. All anatomical structures were located according to the Mouse Brain Library atlas (Rosen et al., 2000).

Immunoblot analysis

Both cerebral cortex and hippocampus samples were separated under reducing and denaturing conditions on 7.5% sodium dodecyl sulfate polyacrylamide gel electrophoresis (SDS-PAGE) gels and transferred onto polyvinylidene fluoride (PVDF) membranes. Membranes were incubated overnight with primary antibodies for Ku70 (1:3000, Millipore, Billerica, MA, USA) and β-actin (1:20000). Blots were visualized using appropriate secondary antibodies conjugated to horseradish peroxidase and an enhanced chemiluminescence (ECL) detection system (Pierce, Rockford, IL, USA). Relative protein expression was reported as a ratio to β-actin. Quantification was determined by densitometry using ImageJ 1.43u (Rasband, 1997-2011). All measurements were repeated three times.

Statistics

PASW Statistics 18 was used for statistical analysis. Significance was defined as $p \leq 0.05$. Food consumption, water intake, body weight changes, open field, and spatial acquisition using the MWM were analyzed using repeated measurements for between-subject effects and one-way analysis of variance (ANOVA) for differences between groups at each time point. For object recognition, mEPM, probe trials using the MWM, receptor binding, gene expression, and immunoblot, one-way ANOVA was performed to compare between treatments. When needed the Tukey HSD was used as a post hoc test after one-way ANOVA. All data were presented as average ± SEM.

RESULTS

Body weights of NC mice were significantly lower than controls despite equal amounts of food consumption

A summary of changes in body weights is presented in Figure IV-1A. Body weights of control mice gradually increased throughout the 4 months of the experiment. The average weight gain in control mice was 0.039 ± 0.013 g per day, causing a significantly higher body weight when mice were 18-months-old as compared to when they were 14-months-old (18-month-old AL mice: 41.42 ± 1.60 g, 14-month-old AL mice: 36.16 ± 1.63 g, Student's *t*-test $p = 0.05$). On the other hand, nicotine treatment caused a very subtle loss of body weight of 0.002 ± 0.011 g per day. There was a difference in average weight gain between AL and NC mice (Repeated measurements, test of between-treatments effects $p = 0.001$, Tukey HSD, NC vs. AL $p = 0.08$.) (Fig. IV-1B). The body weights of NC mice when they were 18-months-old were not different from 14-month-old mice (18-month-old NC mice: 37.41 ± 1.73 g, 14-month-old NC mice: 37.91 ± 1.60 g. Student's *t*-test $p = 0.835$). CR caused a dramatic decrease in body weight (0.05 ± 0.012 g per day), and the average weight gain in CR mice was significantly lower than both AL and NC mice (Repeated measurements, test of between-treatments effects $p = 0.001$, Tukey HAS, CR vs. NC $p = 0.023$, CR vs. AL $p < 0.0001$). Body weights of 18-month-old CR mice were significantly lower than 14-month-old CR mice (18-month-old CR mice: 29.12 ± 0.49 g; 14-month-old CR mice: 36.07 ± 0.59 g. Student's *t*-test $p < 0.0001$). Overall, the average body weight of AL

mice during the 4 months treatment was significantly higher than those of both NC and CR mice, and the average body weight of NC mice was significantly higher than that of CR mice (AL: 39.96 ± 1.37 g, NC: 38.67 ± 1.16 g, CR: 29.43 ± 1.25 g. Repeated measurements, test of between-treatments effects $p < 0.0001$, Tukey HSD, CR vs. NC $p < 0.0001$, CR vs. AL $p < 0.0001$, NC vs. AL $p = 0.02$). Treatment for 4 months with either nicotine or CR caused significant lower body weights in these middle-age mice (although in a different degree) when compared to control (AL) mice.

The amount of water intake was also monitored. CR mice significantly drank more than both AL and NC mice during the entire treatment (AL: 5.65 ± 0.43 ml, NC: 4.45 ± 0.27 ml, CR: 12.8 ± 0.62 ml. Repeated measurements, test of between-treatments effects $p < 0.0001$, Tukey HSD, AL vs. CR $p < 0.0001$, NC vs. CR $p < 0.0001$). The NC mice decreased the amount of water that they drank only at the beginning of the treatment period and gradually increased their amount of water intake until the amounts were the same as control mice. Overall there was only a trend of water intake difference between NC and AL mice (AL vs. NC $p = 0.065$) (Fig. IV-1C).

Food consumption by CR mice was controlled to 60% of AL at the beginning of the treatment and then adjusted to 70% of AL starting at day 28. The restricted food consumption caused the body weight of CR mice to decrease. However, the lower body weights in NC compared to AL mice was not caused by a decrease in food consumption since there was no difference in food consumption between AL and NC mice (AL: 5.24 ± 0.46 g/day, NC: 5.49 ± 0.33 g/day, repeated measurements, test of between-treatments effects $p = 0.7$) (Fig. IV-1D).

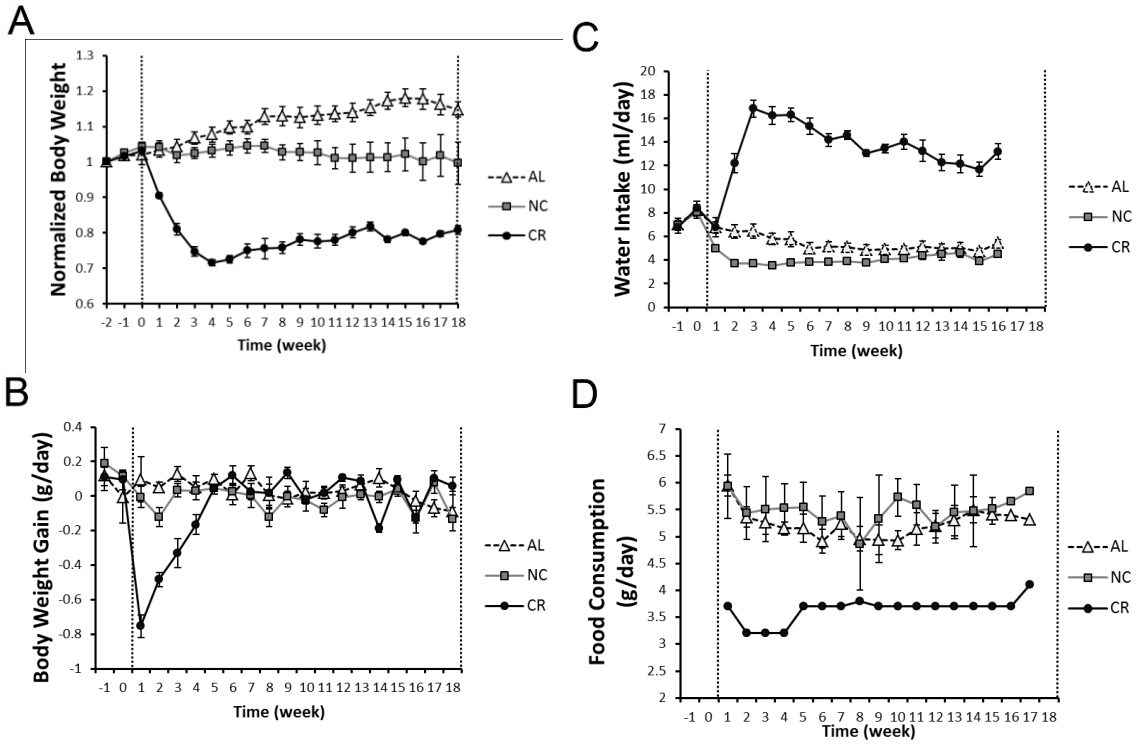

Figure V-1. Body weights of NC mice were significantly lower than control (AL) mice despite of equal amounts of food consumption. ***A***, Body weights were normalized to the first measurement for each individual mouse. Repeated measurements, test of between-treatments effects $p < 0.0001$, Tukey HSD, CR to NC $p < 0.0001$, CR to AL $p < 0.0001$, NC to AL $p = 0.02$. Comparisons between the last time point to the first time point: Student's *t*-test, AL $p = 0.05$, CR $p < 0.0001$, NC $p = 0.835$. ***B***, Body weight gains are presented as g/day. Repeated measurements, test of between-treatments effects $p = 0.001$, Tukey HSD, CR to NC $p = 0.023$, CR to AL $p < 0.0001$, NC to AL $p = 0.08$. ***C***, Water intake is presented as ml/day. Repeated measurements, test of between-treatments effects $p < 0.0001$, Tukey HSD, AL to CR, $p < 0.0001$, NC to CR $p < 0.0001$, AL to NC $p = 0.065$. ***D***, Food consumption is presented as g/day. Comparisons were only made between NC and AL mice, since the food consumption by CR mice was controlled to 60% of AL up to day 28 and 70% of AL after day 28. Repeated measurements, tests of between-treatments effects $p = 0.696$. The left dash line indicates the time when both nicotine and caloric restriction treatments started. The right dash line indicates the time when treatments ended and all mice were euthanized. Each dot represents the measurement of the week. AL, control; NC, nicotine group; CR, caloric restricted group. Error bars: SEM.

Locomotion was not impaired by treatment, but the anxiety level increased in CR mice compared to both AL and NC mice

After 4 months of treatment, each mouse was subjected to a 30-minute open field test for locomotor and anxiety levels. Among the 6 parameters used (total distance, movement time, margin distance, margin time, center distance, and thigmotaxis index), total distance, movement time, margin distance and center distance did not show any difference between treatments indicating that locomotor activity was not impaired by either chronic nicotine treatment or CR. However, CR mice spent significantly more time at the margin of the open field compared to both AL and NC mice in the first and second 5-minute intervals (First 5 minutes: AL: 99.0 ± 18.85 sec, NC: 131.5 ± 18.34 sec, CR: 170.21 ± 12.14 sec. One-way ANOVA $p = 0.041$, Tukey HSD, AL vs. CR $p = 0.033$. Second 5 minutes: AL: 107.4 ± 13.75 sec, NC: 120.4 ± 14.15 sec, CR: 175.3 ± 18.41 sec. One-way ANOVA $p = 0.012$, Tukey HSD, AL vs. CR $p = 0.015$, NC vs. CR $p = 0.045$) (Fig. IV-2). This difference disappeared after 10 minutes in the open field. The longer margin time exhibited by CR mice compared to AL and NC mice in the first 10 minutes indicated a higher anxiety level in CR mice when they entered a new environment. The thigmotaxis, an index of anxiety (margin distance / total distance), also showed that CR mice are more anxious than both AL and NC mice in the first and second 5-minute intervals in the open field (first 5 minutes: AL: 0.45 ± 0.05, NC: 0.48 ± 0.03, CR: 0.59 ± 0.03. One-way ANOVA $p = 0.046$, Tukey HSD, NC vs. CR $p = 0.044$. second 5 minutes: AL: 0.42 ± 0.02, NC: 0.44 ± 0.03, CR: 0.56 ± 0.03. One-way ANOVA $p = 0.007$, Tukey HSD, AL vs. CR $p = 0.011$, NC vs. CR $p = 0.021$). There

were no differences in both margin time and thigmotxis index between AL and NC mice indicating that long-term CNE did not change the anxiety level in mice.

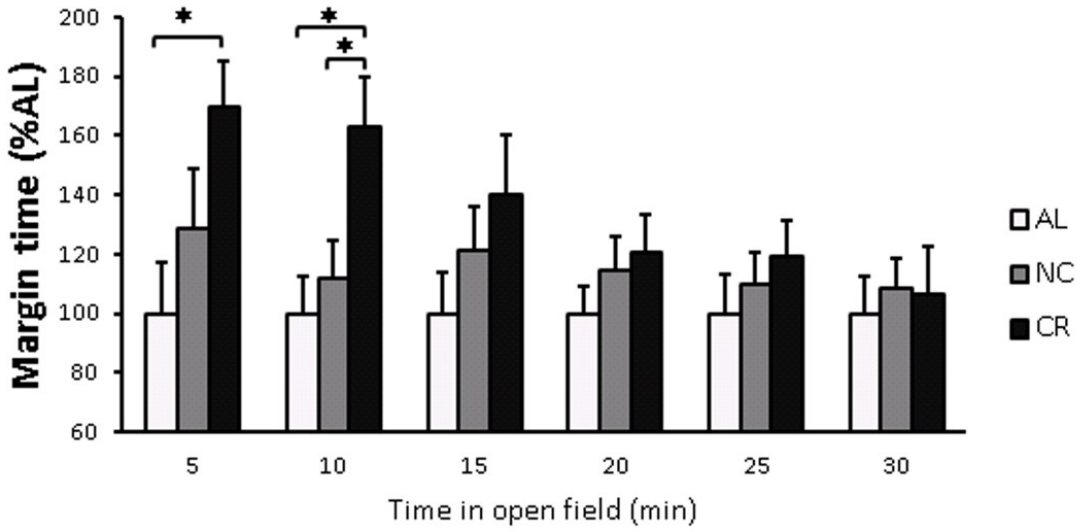

Figure V-2. Anxiety level increased in CR mice compared to both AL and NC mice. Margin time is presented as a percentage of the time spent by control mice. Time in the open field was separated into six segments, five minutes each, and analyzed individually. AL, control; NC, nicotine group; CR, caloric restricted group. Error bars: SEM. One-way ANOVA, Tukey HSD, * $p < 0.05$.

While short-term memory was not impaired by treatment, long-term memory improved in both CR and NC mice

One-hour interval object recognition is a test for short-term learning and memory. After 4 months of treatment, we examined the total time each mouse spent on

exploring objects (novel time + sample time) and the ratio of time that mice spent on exploring the novel object (novel time / total time) after they had explored the sample objects one hour previously. The total exploration time was not different between groups as anticipated, demonstrating that neither of our treatments impaired the interest and ability of these mice to explore objects (AL: 18.63 ± 2.98 sec, NC: 19.71 ± 2.88 sec, CR: 21.12 ± 1.75 sec. One-way ANOVA $p = 0.808$). However, the ratio of time that mice spent on exploring the novel object was not different between groups either indicating that our treatments did not change the short-term memory in these mice (AL: 0.58 ± 0.07, NC: 0.41 ± 0.09, CR: 0.50 ± 0.04. One-way ANOVA $p = 0.259$).

Long-term memory was assessed by mEPM and MWM in these mice at the end of the 4 month treatment period. In mEPM, we examined the time (T2) that each mouse took on the second day to escape from the open arm to one of the enclosed arms of the maze, after they had explored the maze on the first day. Our results showed that both CR and NC mice took significantly less time to find the enclosed arm, indicating an improvement in long-term spatial memory as compared to control (AL) mice (T2, CR: 48.9 ± 11.8 sec, NC: 48.0 ± 10.6 sec, AL: 85.3 ± 4.8 sec. One-way ANOVA $p = 0.023$, Tukey HSD, AL vs. CR $p = 0.043$, AL vs. CR $p = 0.038$) (Fig. IV-3). There was no difference in the times exhibited by NC and CR mice to find the enclosed arm.

In the MWM, mice demonstrated successful learning curves in the five-day spatial acquisition detected using latency, path length, and cumulative distance. No difference between treatment groups was observed for any of the three measurements (Fig. IV-4). In the probe trial, no difference was detected between groups for time spent in the target quadrant or in the percent of the path length located in the target quadrant for all mice tested. We then analyzed performance between mice defined as good versus poor performers. For each treatment group the mice were ranked from the best to worst scores. Good performing mice were defined as the mice that were in the top half of the ranking and the poor performers were the bottom half of the ranking. Good performers in the NC group displayed a trend to perform better than the good performers in the AL group with respect to both parameters (Time in target quadrant: two-way ANOVA $p = 0.075$, Tukey HSD, AL vs. NC $p = 0.076$; percent path length in the target quadrant: two-way ANOVA $p = 0.058$, Tukey HSD, AL vs. NC $p = 0.051$. No differences were observed between CR and NC or between AL and CR groups and the poor performers had no difference at all between groups (Fig. IV-5). This suggested that nicotine might be effective to a subgroup of aging mice.

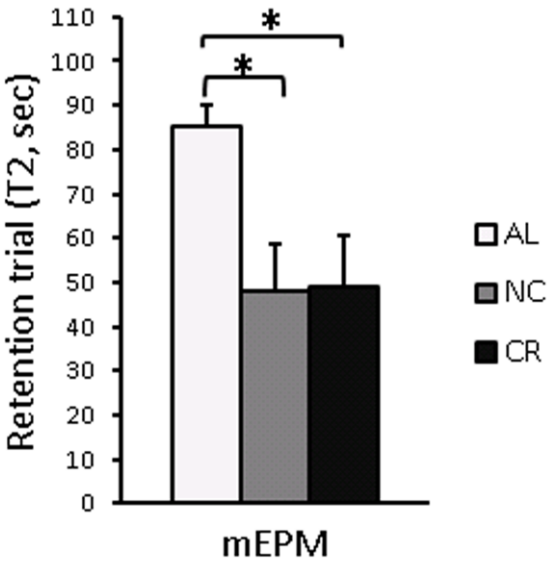

Figure V-3. Modified EPM indicated that long-term memory was improved in both CR and NC mice as compared to AL mice. The time for successful entry into an enclosed arm in the second-day retention trial was recorded as T2, and used as in index of spatial memory and learning ability. mEPM, modified elevated plus maze; AL, control; NC, nicotine group; CR, caloric restricted group. Error bars: SEM. One-way ANOVA, Tukey HSD, * $p < 0.05$.

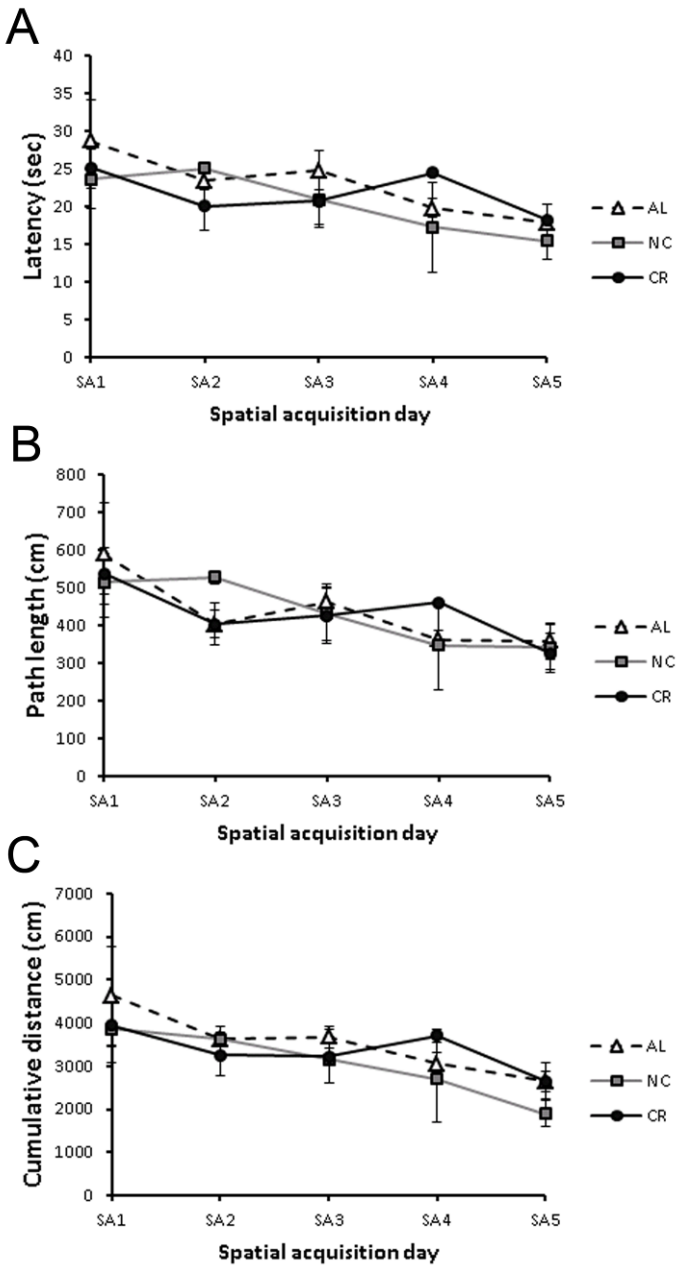

Figure V-4. No difference between groups was detected in the 5-day spatial acquisition in the MWM. Three parameters were examined: ***A***, latency; ***B***, path length, ***C***, cumulative distance. SA, spatial acquisition; AL, control; NC, nicotine group; CR, caloric restricted group. Error bars: SEM.

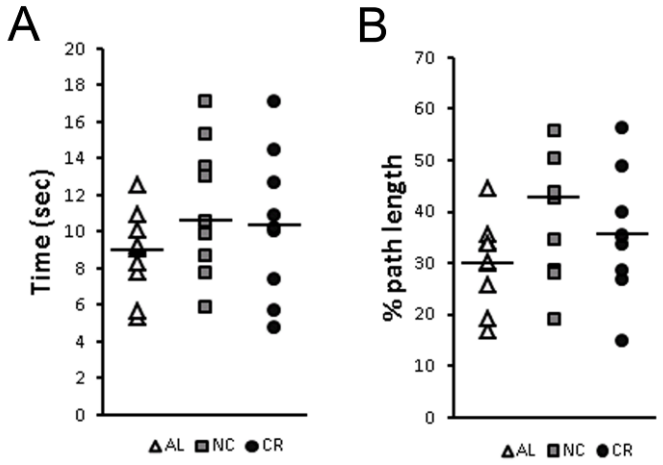

Figure V-5. No difference was detected between groups in the probe trial for the MWM. (***A***) Time in the target quadrant and (***B***) percent path length in the target quadrant were plotted with each individual animal. AL, control; NC, nicotine group; CR, caloric restricted group. Bars indicated the medians for each group.

Heteromeric nAChR binding sites were increased in NC mice in neocortical areas compared to AL and CR mice

Increased heteromeric nicotinic binding sites are hallmark of CNE. In this study, we used ^{125}I-Epibatidine binding levels measured as ROD values to determine the number of heteromeric nicotinic binding sites in the cortico-hippocampal area, thalamus, and the medial habenular nucleus. In the neocortex, binding levels were determined in layers IV to VI of the visual and somatosensory cortex. There was a trend towards higher binding in NC mice as compared to AL mice, and no difference was detected

between CR and AL mice (AL: 0.15 ± 0.012, NC: 0.19 ± 0.011, CR: 0.16 ± 0.011. One-way ANOVA $p = 0.053$, Tukey HSD, AL vs. NC $p = 0.057$) (Fig. IV-6A). In the hippocampus, binding levels were determined in the stratum lacunosum molecular layer of the CA1 and the DG molecular layer. Binding levels in NC mice were significantly higher than both AL and CR mice, and no difference was detected between CR and AL mice (AL: 0.09 ± 0.006, NC: 0.12 ± 0.007, CR: 0.09 ± 0.005. One-way ANOVA $p < 0.0001$, Tukey HSD, AL vs. NC $p < 0.0001$, CR vs. NC $p = 0.001$) (Fig. IV-6B). In the thalamus and medial habenular nucleus, no difference was detected between treatment groups showing that the up regulation of heteromeric nAChRs was specific to cortico-hippocampal areas in response to CNE but not CR (thalamus: AL: 0.23 ± 0.01, NC: 0.24 ± 0.01, CR: 0.23 ± 0.01; medial habenular nucleus: AL: 0.16 ± 0.01, NC: 0.17 ± 0.01, CR: 0.17 ± 0.01) (see Fig. IV-6C and D for thalamus and medial habenular nucleus respectively).

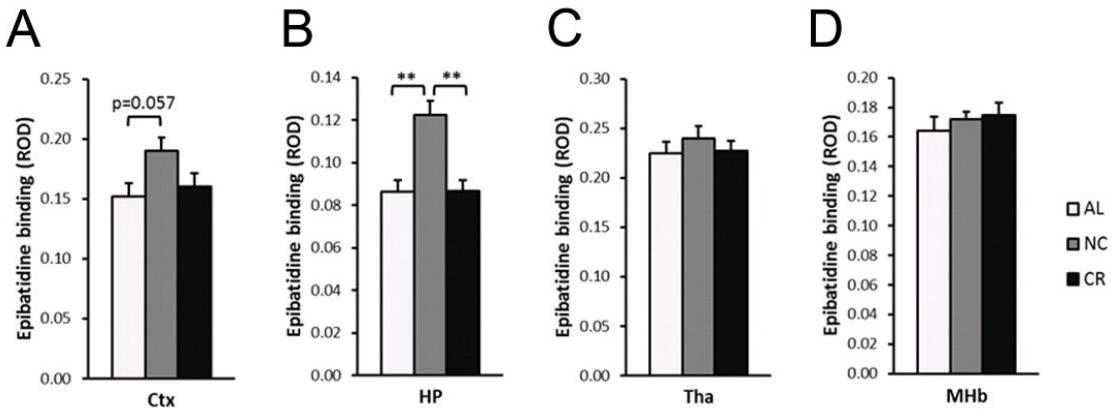

Figure V-6. Heteromeric nAChR binding sites were increased in NC as compared to AL and CR mice in the neocortex (***A***) and hippocampus (***B***) but not thalamus (***C***) and medial habenular nucleus (***D***). Epibatidine binding levels are presented using ROD values. ROD, raw optical density; Ctx, neocortex; HP, hippocampus; Tha, thalamus; MHb, medial habenular nucleus; AL, control; NC, nicotine group; CR, caloric restricted group. Error bars: SEM. One-way ANOVA, Tukey HSD, ** $p < 0.01$.

Messenger RNA levels of SIRT, Nampt, and Ku70 were increased in the cortico-hippocampal areas in response to CR but not NC

Using *in situ* hybridization, mRNA levels of SIRT, Nampt, and Ku70 were determined in the principal layers of hippocampal CA1, CA3 and DG, and in layers II to VI of the somatosensory cortex. A summary of the comparisons is presented in Figure IV-7. After 4 months of treatment, CR significantly increased SIRT1 expression levels generally in the cortico-hippocampal areas when compared to NC mice (Two-way ANOVA (treatment vs. region), test of between-treatments effects $p = 0.006$, Tukey HSD, CR vs. NC $p = 0.005$). There was no difference between CR and AL mice or between NC and AL mice. The difference was specifically detected in the neocortex

using Tukey's HSD post hoc test (One-way ANOVA $p = 0.036$, Tukey HSD, CR vs. NC $p = 0.033$) but not in other hippocampal regions (Fig. IV-7A).

Nampt showed similar changes as SIRT1 in that CR mice significantly increased Nampt expression levels as compared to both AL and NC mice (Two-way ANOVA (treatment vs. region), test of between-treatments effects $p < 0.0001$, Tukey HSD, CR vs. AL $p = 0.022$, CR vs. NC $p < 0.0001$). There was no difference observed in Nampt expression levels between AL and NC mice. The difference was again specifically detected in the neocortex and a trend towards a difference was observed for the DG between CR and NC mice (One-way ANOVA, cortex: $p = 0.034$, DG: $p = 0.085$, Tukey HSD, cortex: CR vs. NC $p = 0.035$, DG: CR vs. NC $p = 0.073$). The CA1 and CA3 regions of hippocampus did not show any differences in Nampt expression between treatment groups (Fig. IV-7B).

Ku70 gene expression showed the most dramatic changes in response to CR. Ku70 mRNA levels were increased in CR mice as compared to both NC and AL mice (Two-way ANOVA (treatment vs. region), test of between-treatments effects $p < 0.0001$, Tukey HSD, CR vs. AL $p < 0.0001$, CR vs. NC $p < 0.0001$), and the differences were significant in all cortico-hippocampal areas measured (One-way ANOVA, cortex: $p = 0.004$, CA1: $p = 0.002$, CA3: $p = 0.008$, DG: $p = 0.003$, Tukey HSD, cortex: CR vs. NC $p = 0.021$, CR vs. AL $p = 0.005$, CA1: CR vs. NC $p = 0.005$, CR vs. AL $p = 0.004$, CA3: CR vs. NC $p = 0.029$, CR vs. AL $p = 0.011$, DG: CR vs. NC $p = 0.007$, CR vs. AL $p = 0.01$). There was no difference between NC and AL mice with respect to Ku70 mRNA expression levels (Fig. IV-7C).

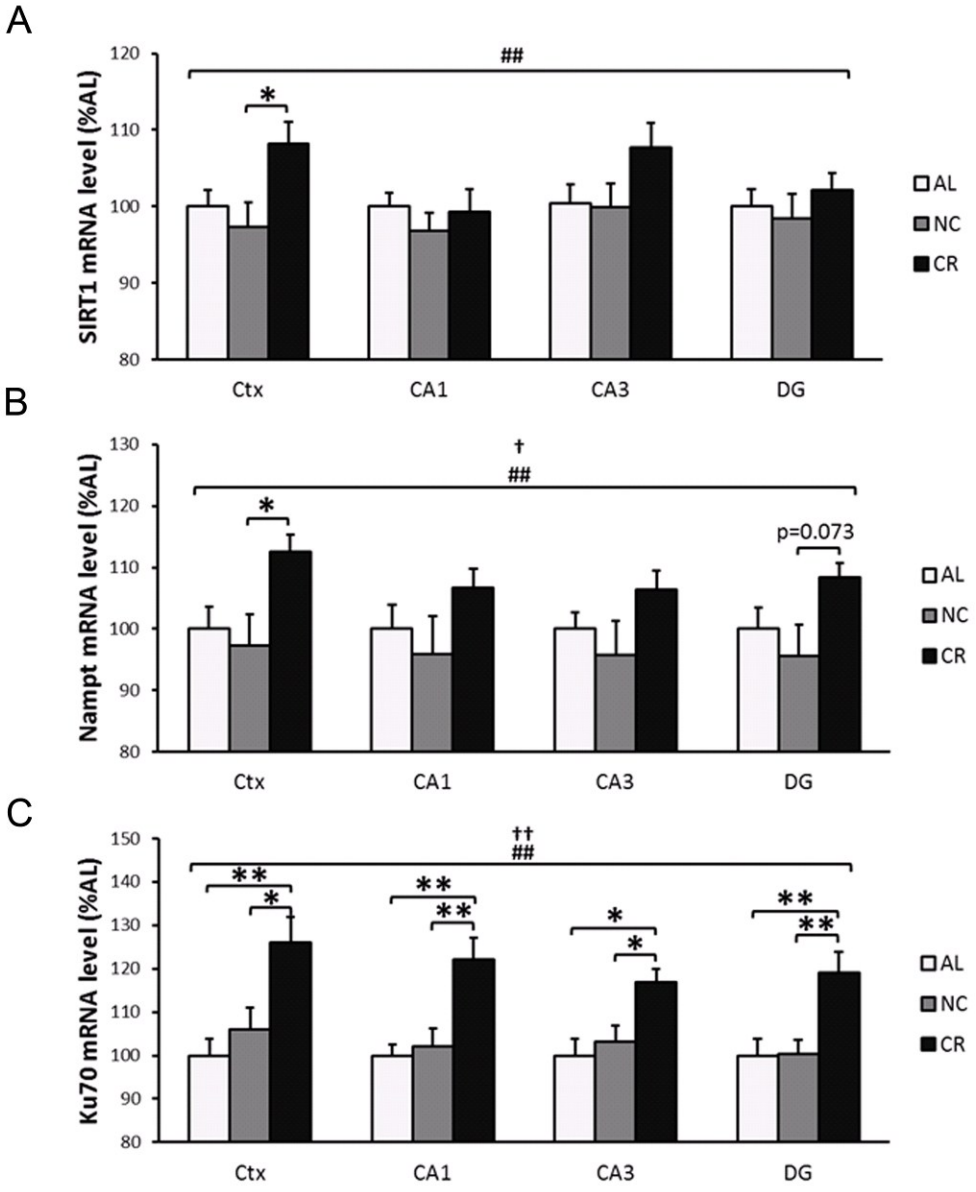

Figure V-7. Messenger RNA levels of SIRT (***A***), Nampt (***B***), and Ku70 (***C***) were increased in cortico-hippocampal areas in response to CR but not NC. *In situ* hybridization levels are presented as a percentage of expression levels exhibited by control mice. Ctx, neocortex; CA1, pyramidal cell layer of hippocampal CA1; CA3, pyramidal cell layer of the hippocampal CA3; DG, granular cell layer of the hippocampal dentate gyrus; AL, control; NC, nicotine group; CR, caloric restricted group. Error bars: SEM. Two-way ANOVA (treatment vs. region), test of between-subjects effects: treatment effect, Tukey HSD, (***A***), CR vs. NC, ## $p < 0.01$; (***B***), CR vs. NC, ## $p < 0.01$, CR vs. AL, † $p < 0.05$; (***C***), CR vs. NC, ## $p < 0.01$, CR vs. AL, †† $p < 0.01$. One-way ANOVA, Tukey HSD, ** $p < 0.01$, * $p < 0.05$.

Despite observed changes in mRNA levels, Ku70 protein levels in cortico-hippocampal areas were not affected by treatment

Because Ku70 mRNA showed the most change in response to the treatments used in this study, we examined protein levels of Ku70 to determine whether the protein levels changed in accordance with the observed changes in mRNA levels. Tissues were dissected into neocortex and hippocampus, and none of these areas showed changes in Ku70 protein levels (Ratio to AL, cortex: CR: 1.27 ± 0.32, NC: 0.93 ± 0.10; hippocampus: CR: 1.2 ± 0.12, NC: 1.1 ± 0.25. One-way ANOVA, cortex: $p = 0.44$, hippocampus $p = 0.68$) (Fig. IV-8).

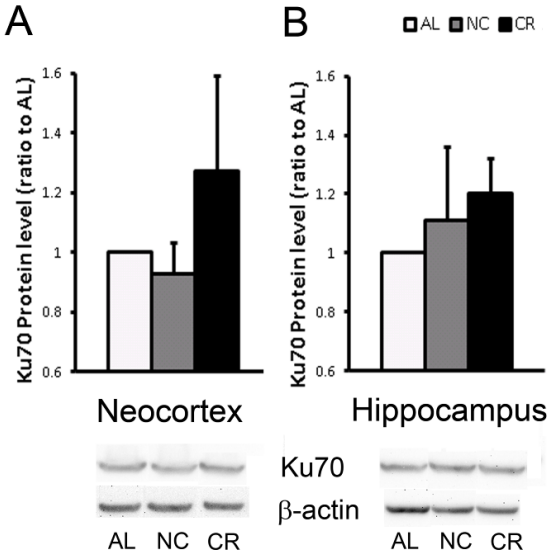

Figure V-8. Despite changes in mRNA levels, Ku70 protein levels in the cortico-hippocampal areas were not affected by either treatment. Protein levels are presented as ratio of protein expression observed in control mice. Representative images of immunoblots from Ku70 and β-actin are shown below. AL, control; NC, nicotine group; CR, caloric restricted group. Error bars: SEM.

DISCUSSION

This study was the first to examine the correlation and compare the effect of nicotine and CR on food consumption, body weight, anxiety level, memory and the expression of CR-related genes: SIRT1, Ku70, and Nampt. Our previous study showed that β2-/- mice, which lack the predominant heteromeric nAChR subtype, increase their longevity gene expression in middle-aged 18-month old compared to age-matched wild type mice (Huang et al., 2011). We believe that this is an adaptational response as seen in other mouse models of neurodegenerative diseases, due to the accelerated aging observed in these mice (Zoli et al., 1999; Kim et al., 2007a), and although the β2-nAChRs do not directly interact with these longevity genes, lack of endogenous nAChR-mediated neuroprotection could create a stressful situation for neurons that could induce up regulation of expression of these genes. We also found that CNE using 300 μg/ml in drinking water has effects on food intake, body weight, anxiety levels and CR related gene expression. In this study, we treated middle-aged C57BL/6 male mice with the high dose of nicotine via drinking water, which was found to be effective in Chapter III, for 4 months, a relatively long period of time in a mouse's life span and compared that exposure with the same time length of time of CR. We observed significant effects on food intake, receptor binding, and anxiety levels. The expression of SIRT1 and related genes was up regulated in the cortico-hippocampal area in the brain in CR mice, but not NC mice. This indicates that long-term chronic nicotine administration does not alter the SIRT1 related signaling pathway like CR does, but has a potential to improved memory and cognitive functions.

One of the goals of this study was to determine the effects of long-term nicotine given orally to mice. This has not been studied previously. We found that long-term CNE resulted in reduced body weight but not food consumption and increased numbers of nAChR binding sites, which are hallmarks of CNE and would indicate an effective dose of nicotine reached the brain. The animals tolerated this dose and route of nicotine well, with no apparent negative effects on general appearance. Nicotine given in drinking water minimizes stress that is caused by daily nicotine injections, especially for long-term studies, and also provides the nicotine fluctuations seen in smokers or people using oral nicotine replacement medications such as nicotine gums, sprays or lozenges. Chronic nicotine reduces body weight and suppresses food intake through the central hypothalamic melanocortin system (Mineur et al., 2011). These anorexic effects were seen only in our short-term nicotine study. However, long-term nicotine treatment did not reduce food consumption but reduced weight gain. This indicated that the reduction of body weight by means of nicotine is not only an effect of less food intake, but also of higher metabolic function. It's also interesting to look into why long-term nicotine does not activate the hypothalamic melanocortin system to suppress food intake as short-term CNE found by others. It is also possible that the inactivation or less responsiveness of the hypothalamic melanicortin system in our long-term study was due to an older age of these mice.

The hallmark of CNE that indicates sufficient amounts of nicotine reached the brain where nicotine interacts with nAChRs, is the increase in heteromeric nicotinic binding sites (Corringer et al., 2006). Four to 7 weeks of chronic nicotine treatment in

rodents increases high affinity nicotinic binding sites in cortico-hippocampal regions (Pietila et al., 1998; Sparks and Pauly, 1999; Nuutinen et al., 2005). Human smokers also have greater densities of high affinity nAChR compare to nonsmokers (Perry et al., 1999; Mukhin et al., 2008). Using receptor autoradiography, we showed that long-term nicotine treatment still increased the level of ^{125}I-epibatidine binding to heteromeric nAChRs in the cortico-hippocampal regions. The binding site upregulation effect by CNE was not adapted by long-term activation. Whether the upregulated nAChRs remain functional or are desensitized needs further investigation. The CR did not increase high affinity nicotinic binding sites.

Behavior tests were used to access locomotion, exploratory activity, anxiety-like behavior, and spatial learning. Our results indicated that locomotor and exploratory activities were not changed by CR or long-term CNE. However, results from the open field test indicated that anxiety levels were increased in CR mice. Long-term nicotine treated mice did not change their anxiety levels when compared to control mice. This showed that the anxiolytic effect of CNE is only seen in short-term treatment. Long-term nicotine administration did not release anxiety. Nicotine's effects on anxiety are complex and depend on the dose, time, and regimen of administration (Picciotto et al., 2002). The positive impact of stress on smoking frequency, smokers yielded a lower anxiety level than non-smokers when challenged with stress, and the increased anxiety level during smoking cessation in human study all suggest that nicotine exposure reduces anxiety levels (Gilbert et al., 1989; Perkins and Grobe, 1992; Tate et al., 1993). Animal studies also support the anxiolytic effect of chronic nicotine and nicotinic

agonists (Brioni et al., 1994; Levin et al., 2007). Our result indicated that this effect did not sustain when the nicotine exposure was long-term or when the mice were at an older age, and CR had an anxiogenic effect to mice. Aging might change the effects of nicotine on the stress system, or the stress system might be less responsive in older mice.

Spatial learning and memory was evaluated in mEPM, object recognition and MWM. The object recognition test was to test short-term memory and no difference was found between treatments. Some studies provide evidence of improved short-term memory after CNE in mouse models of AD, schizophrenia, attention deficit hyperactivity disorder, and stress-induced memory impairment (Aleisa et al., 2006; Weiss et al., 2007; Srivareerat et al., 2009; Rushforth et al., 2011) as well as animals without pathological condition (Levin and Torry, 1996). The mEPM indicated an improvement in long-term memory in both CR and NC groups, but this result was not firmly detected again using MWM.

Long-term nicotine did not change SIRT1, Ku70 and Nampt mRNA levels as was observed with short-term nicotine exposure and with CR. The anorectic effect of short-term chronic nicotine could cause the mice to undergo short term CR and result in up regulated gene expression and potentially provides a neuroprotective effect. Increased SIRT1, Ku70, and Nampt gene expressions were seen in the cortico-hippocampal regions in CR mice in this study. SIRT1 attenuates apoptosis by deacetylating the DNA repair factor Ku70, which sequesters proapoptotic factor Bax away from mitochondria (Cohen et al., 2004b). Nampt is an upstream regulator of SIRT1. Nampt is induced by stress or nutrient deprivation and increases cellular resistance to damage (Yang et al.,

2006b). This indicated that long-term CNE does not work as CR mimicry like resveratrol, and the up-regulation of SIRT and its related genes by CR is perhaps due to a decrease in food consumption, but not in body weight. This supports the idea that these genes are up-regulated to protect against cellular stress such as food deprivation, and imply that long-term CNE does not produce significant cellular stress.

Experiments have only been conducted to restrict caloric consumption for more than six months to observe an up regulation in brain SIRT1 expression. Six months of 70% CR increases brain SIRT1 and non-amyloidogenic processing of amyloid precursor protein (Qin et al., 2006b). Rats with 60 % CR from weaning to 12 months old showed increased SIRT1 levels in the brain (Cohen et al., 2004b). However, CR has been proved to provide neuroprotection with a much shorter period of time. Nine months and even only 3 months of 70 % to 60 % CR provides neuroprotection to AD and PD mouse models (Duan and Mattson, 1999; Wang et al., 2005), and just 2 weeks of 60% CR in early adulthood can attenuate Aβ-plaque deposition in mouse models of AD (Patel et al., 2005). Our study provides the first evidence showing that 4 months of CR (70%) can increase brain SIRT1 mRNA levels.

Nicotine by interacting with nAChRs could activate these cell defense factors through a yet unknown pathway. Nicotine decreases the levels of pro-apoptotic factors including caspase 3 and cytochrome c while SIRT1 deacetylates Ku70 and subsequently blocks activation of caspase 3 and cytochrome c (Garrido et al., 2001; Sawada et al., 2003; Cohen et al., 2004a; Liu and Zhao, 2004), and down regulation of Nampt has been shown to increase caspase 3 cleavage and cytochrome c release (Hsu et al., 2009). In

addition, nicotine administration up regulates nerve growth factor (NGF) and its receptor TrkB in the hippocampus while SIRT1 activation promotes NGF-induced neurite outgrowth in the cells (French et al., 1999; Sugino et al., 2010). Now we know that there is not a direct molecular link between activation of nAChRs and SIRT1-related longevity genes. The neuroprotection provided by nAChRs and SIRT1 activation was through different mechanism.

CHAPTER VI

CONCLUSIONS

Nicotine and nAChR agonists share many similar effects with caloric restriction (CR) and SIRT1 activation. First, they both regulate metabolism by decreasing caloric consumption and body weight. Nicotine decreases appetite and increases energy expenditure, which correlate with the fact that cigarette smokers tend to have lower body weights than non-smokers. Second, they both show well-demonstrated neuroprotective effects *in vitro* and *in vivo*. The goal of this study was to find the possible correlation between nicotine's effects and activation of SIRT1 and its related genes. Using mice that lacked high affinity nicotinic receptors, namely β2-/- mice, we first demonstrated that β2* nAChRs do not directly regulate expression of survival genes. However, we found that loss of β2* nAChRs could result in augmented cellular stress, which indirectly increases expression of SIRT1, Nampt, and Ku70 as an adaptive response to provide protection against neurodegeneration (Chapter II). We also found that loss of endogenous activation of β2* nAChRs has less of an effect on synaptic connections but strongly impairs survival of hippocampal GABAergic neurons (Chapter III). To activate β2* nAChRs, we administered nicotine through drinking water, first in a short-term study and then in a long-term study. In our short-term study, we determined the dose of nicotine to be used in mice, and found that short-term chronic nicotine treatment was anxiolytic, decreases caloric consumption, increases nAChR binding sites, and most importantly increases expression of SIRT1 and its related genes (Chapter IV). Next, we

compared long-term nicotine treatment with CR, which is a known regimen to up-regulate SIRT1 and its related genes, in middle-aged mice to examine the effects of each of these treatments (CR and nicotine treatment) on various aspects of brain aging. Our results indicated that in mice long term CR and nicotine treatment both have a tendency to improve memory in aging mice, but appear to act through different mechanisms. CR treatment up-regulated SIRT1 expression but long-term nicotine did not (Chapter V).

Cognitive improvement is one of the best established therapeutic effects of nicotine (Heishman et al., 2010). In human studies, memory improvement is seen in AD and mild cognitive impairment (MCI) subjects given nicotine (Newhouse et al., 1988; Jones et al., 1992; White and Levin, 1999; Newhouse et al., 2012). Because nicotine can be neurotoxic under certain situations, it is important to elucidate the mechanisms underlying nicotine's neuroprotective effects for better potential therapies against neurodegenerative diseases. One proposed mechanism for nicotine to produce neuroprotective effects is via regulation of nAChR-containing circuits (Nashmi et al., 2007; Xiao et al., 2009). In this case, chronic nicotine could regulate the firing rates of neurons through nAChRs upregulation and prevent neurons from experiencing bursts of firing that could lead to excitotoxic Ca^{2+} influx. At the very least, we demonstrated that long-term nicotine treatment does not cause cellular stress nor does it up regulate SIRT1.

It is known that the effects of acute and chronic nicotine are not the same, and this is largely due to the unique phenomenon that the number of nicotine's receptors (nAChRs) can be up-regulated after chronic nicotine treatment. This selective upregulation directly results in modified neuronal excitability and neuronal interactions.

Here we found that short-term and long-term nicotine treatment also can yield different effects in terms of anxiety levels, food consumption, and SIRT1 and its related gene's expression. It would also be interesting to investigate how and why short- and long-term nicotine exposure cause different effects when both short- and long-term treatment cause an upregulation of nAChRs.

Nicotinic systems can be manipulated to provide help for neural illnesses such as Parkinson's disease, cognitive decline, epilepsy, and schizophrenia. As research in this area progresses, we will elucidate the mechanisms of nicotine's complex effects, understanding what pathway is being triggered and how this is accomplished.

REFERENCES

Abbott LC, Jacobowitz DM (1999) Developmental expression of calretinin-immunoreactivity in the thalamic eminence of the fetal mouse. Int J Dev Neurosci 17:331-345.

Accili D, Arden KC (2004) FoxOs at the crossroads of cellular metabolism, differentiation, and transformation. Cell 117:421-426.

Adler LE, Hoffer LD, Wiser A, Freedman R (1993) Normalization of auditory physiology by cigarette smoking in schizophrenic patients. Am J Psychiatry 150:1856-1861.

Agarwal B, Baur JA (2011) Resveratrol and life extension. Ann N Y Acad Sci 1215:138-143.

Aleisa AM, Alzoubi KH, Gerges NZ, Alkadhi KA (2006) Nicotine blocks stress-induced impairment of spatial memory and long-term potentiation of the hippocampal CA1 region. Int J Neuropsychopharmacol 9:417-426.

Allen SS, Hatsukami D, Brintnell DM, Bade T (2005) Effect of nicotine replacement therapy on post-cessation weight gain and nutrient intake: a randomized controlled trial of postmenopausal female smokers. Addict Behav 30:1273-1280.

Andreasen JT, Nielsen EO, Redrobe JP (2009) Chronic oral nicotine increases brain [3H]epibatidine binding and responsiveness to antidepressant drugs, but not nicotine, in the mouse forced swim test. Psychopharmacology (Berl) 205:517-528.

Andrews ZB, Diano S, Horvath TL (2005) Mitochondrial uncoupling proteins in the CNS: in support of function and survival. Nat Rev Neurosci 6:829-840.

Armstrong JF, Kaufman MH, Harrison DJ, Clarke AR (1995) High-frequency developmental abnormalities in p53-deficient mice. Curr Biol 5:931-936.

Asada H, Kawamura Y, Maruyama K, Kume H, Ding R, Ji FY, Kanbara N, Kuzume H, Sanbo M, Yagi T, Obata K (1996) Mice lacking the 65 kDa isoform of glutamic acid decarboxylase (GAD65) maintain normal levels of GAD67 and GABA in their brains but are susceptible to seizures. Biochem Biophys Res Commun 229:891-895.

Asada H, Kawamura Y, Maruyama K, Kume H, Ding RG, Kanbara N, Kuzume H, Sanbo M, Yagi T, Obata K (1997) Cleft palate and decreased brain gamma-aminobutyric acid in mice lacking the 67-kDa isoform of glutamic acid decarboxylase. Proc Natl Acad Sci U S A 94:6496-6499.

Ascoli GA, Alonso-Nanclares L, Anderson SA, Barrionuevo G, Benavides-Piccione R, Burkhalter A, Buzsaki G, Cauli B, Defelipe J, Fairen A, Feldmeyer D, Fishell G, Fregnac Y, Freund TF, Gardner D, Gardner EP, Goldberg JH, Helmstaedter M, Hestrin S, Karube F, Kisvarday ZF, Lambolez B, Lewis DA, Marin O, Markram H, Munoz A, Packer A, Petersen CC, Rockland KS, Rossier J, Rudy B, Somogyi P, Staiger JF, Tamas G, Thomson AM, Toledo-Rodriguez M, Wang Y, West DC, Yuste R (2008) Petilla terminology: nomenclature of features of GABAergic interneurons of the cerebral cortex. Nat Rev Neurosci 9:557-568.

Bach ME, Barad M, Son H, Zhuo M, Lu YF, Shih R, Mansuy I, Hawkins RD, Kandel ER (1999) Age-related defects in spatial memory are correlated with defects in the late phase of hippocampal long-term potentiation in vitro and are attenuated by drugs that enhance the cAMP signaling pathway. Proc Natl Acad Sci U S A 96:5280-5285.

Backman L, Ginovart N, Dixon RA, Wahlin TB, Wahlin A, Halldin C, Farde L (2000) Age-related cognitive deficits mediated by changes in the striatal dopamine system. Am J Psychiatry 157:635-637.

Backman L, Nyberg L, Lindenberger U, Li SC, Farde L (2006) The correlative triad among aging, dopamine, and cognition: current status and future prospects. Neurosci Biobehav Rev 30:791-807.

Balfour DJ (2002) The neurobiology of tobacco dependence: a commentary. Respiration 69:7-11.

Ballesteros-Yanez I, Benavides-Piccione R, Bourgeois JP, Changeux JP, DeFelipe J (2010) Alterations of cortical pyramidal neurons in mice lacking high-affinity nicotinic receptors. Proc Natl Acad Sci U S A 107:11567-11572.

Bao J, Lei D, Du Y, Ohlemiller KK, Beaudet AL, Role LW (2005) Requirement of nicotinic acetylcholine receptor subunit beta2 in the maintenance of spiral ganglion neurons during aging. J Neurosci 25:3041-3045.

Barnes CA (1979) Memory deficits associated with senescence: a neurophysiological and behavioral study in the rat. J Comp Physiol Psychol 93:74-104.

Barnes CA (1987) Neurological and behavioral investigations of memory failure in aging animals. Int J Neurol 21-22:130-136.

Bartzokis G (2004) Age-related myelin breakdown: a developmental model of cognitive decline and Alzheimer's disease. Neurobiol Aging 25:5-18; author reply 49-62.

Baur JA, Sinclair DA (2006) Therapeutic potential of resveratrol: the in vivo evidence. Nat Rev Drug Discov 5:493-506.

Beker F, Weber M, Fink RH, Adams DJ (2003) Muscarinic and nicotinic ACh receptor activation differentially mobilize Ca2+ in rat intracardiac ganglion neurons. J Neurophysiol 90:1956-1964.

Bellinger L, Cepeda-Benito A, Wellman PJ (2003) Meal patterns in male rats during and after intermittent nicotine administration. Pharmacology, Biochemistry and Behavior 74:495-504.

Bendlin BB, Canu E, Willette A, Kastman EK, McLaren DG, Kosmatka KJ, Xu G, Field AS, Colman RJ, Coe CL, Weindruch RH, Alexander AL, Johnson SC (2011) Effects of aging and calorie restriction on white matter in rhesus macaques. Neurobiol Aging 32:2319 e2311-2311.

Benowitz NL (1996) Cotinine as a biomarker of environmental tobacco smoke exposure. Epidemiol Rev 18:188-204.

Benowitz NL (1999) Nicotine addiction. Prim Care 26:611-631.

Benowitz NL, Jacob P, 3rd (1984) Daily intake of nicotine during cigarette smoking. Clin Pharmacol Ther 35:499-504.

Benowitz NL, Jacob P, 3rd (1994) Metabolism of nicotine to cotinine studied by a dual stable isotope method. Clin Pharmacol Ther 56:483-493.

Benowitz NL, Jacob P, 3rd, Denaro C, Jenkins R (1991) Stable isotope studies of nicotine kinetics and bioavailability. Clin Pharmacol Ther 49:270-277.

Benowitz NL, Kuyt F, Jacob P, 3rd, Jones RT, Osman AL (1983) Cotinine disposition and effects. Clinical Pharmacology and Therapeutics 34:604-611.

Benwell ME, Balfour DJ, Anderson JM (1988) Evidence that tobacco smoking increases the density of (-)-[3H]nicotine binding sites in human brain. J Neurochem 50:1243-1247.

Berchtold NC, Oliff HS, Isackson P, Cotman CW (1999) Hippocampal BDNF mRNA shows a diurnal regulation, primarily in the exon III transcript. Brain Research Molecular Brain Research 71:11-22.

Bevins RA, Besheer J (2006) Object recognition in rats and mice: a one-trial non-matching-to-sample learning task to study 'recognition memory'. Nat Protoc 1:1306-1311.

Biala G, Kruk M (2009) Influence of bupropion and calcium channel antagonists on the nicotine-induced memory-related response of mice in the elevated plus maze. Pharmacol Rep 61:236-244.

Bitterman KJ, Anderson RM, Cohen HY, Latorre-Esteves M, Sinclair DA (2002) Inhibition of silencing and accelerated aging by nicotinamide, a putative negative regulator of yeast sir2 and human SIRT1. J Biol Chem 277:45099-45107.

Blatter DD, Bigler ED, Gale SD, Johnson SC, Anderson CV, Burnett BM, Parker N, Kurth S, Horn SD (1995) Quantitative volumetric analysis of brain MR: normative database spanning 5 decades of life. AJNR Am J Neuroradiol 16:241-251.

Borradaile NM, Pickering JG (2009) NAD(+), sirtuins, and cardiovascular disease. Curr Pharm Des 15:110-117.

Brain KL, Trout SJ, Jackson VM, Dass N, Cunnane TC (2001) Nicotine induces calcium spikes in single nerve terminal varicosities: a role for intracellular calcium stores. Neuroscience 106:395-403.

Breese CR, Marks MJ, Logel J, Adams CE, Sullivan B, Collins AC, Leonard S (1997) Effect of smoking history on [3H]nicotine binding in human postmortem brain. J Pharmacol Exp Ther 282:7-13.

Brioni JD, O'Neill AB, Kim DJ, Buckley MJ, Decker MW, Arneric SP (1994) Anxiolytic-like effects of the novel cholinergic channel activator ABT-418. J Pharmacol Exp Ther 271:353-361.

Brown RW, Kolb B (2001) Nicotine sensitization increases dendritic length and spine density in the nucleus accumbens and cingulate cortex. Brain Res 899:94-100.

Brunet A, Sweeney LB, Sturgill JF, Chua KF, Greer PL, Lin Y, Tran H, Ross SE, Mostoslavsky R, Cohen HY, Hu LS, Cheng HL, Jedrychowski MP, Gygi SP, Sinclair DA, Alt FW, Greenberg ME (2004) Stress-dependent regulation of FOXO transcription factors by the SIRT1 deacetylase. Science 303:2011-2015.

Brunzell DH, Russell DS, Picciotto MR (2003) In vivo nicotine treatment regulates mesocorticolimbic CREB and ERK signaling in C57Bl/6J mice. Journal of Neurochemistry 84:1431-1441.

Buccafusco JJ, Letchworth SR, Bencherif M, Lippiello PM (2005) Long-lasting cognitive improvement with nicotinic receptor agonists: mechanisms of pharmacokinetic-pharmacodynamic discordance. Trends Pharmacol Sci 26:352-360.

Burgess N, Maguire EA, O'Keefe J (2002) The human hippocampus and spatial and episodic memory. Neuron 35:625-641.

Buss RR, Sun W, Oppenheim RW (2006) Adaptive roles of programmed cell death during nervous system development. Annu Rev Neurosci 29:1-35.

Caldarone BJ, Duman CH, Picciotto MR (2000) Fear conditioning and latent inhibition in mice lacking the high affinity subclass of nicotinic acetylcholine receptors in the brain. Neuropharmacology 39:2779-2784.

Caldarone BJ, King SL, Picciotto MR (2008) Sex differences in anxiety-like behavior and locomotor activity following chronic nicotine exposure in mice. Neurosci Lett 439:187-191.

Calhoun ME, Kurth D, Phinney AL, Long JM, Hengemihle J, Mouton PR, Ingram DK, Jucker M (1998) Hippocampal neuron and synaptophysin-positive bouton number in aging C57BL/6 mice. Neurobiol Aging 19:599-606.

Cameron HA, Woolley CS, McEwen BS, Gould E (1993) Differentiation of newly born neurons and glia in the dentate gyrus of the adult rat. Neuroscience 56:337-344.

Changeux JP, Bertrand D, Corringer PJ, Dehaene S, Edelstein S, Lena C, Le Novere N, Marubio L, Picciotto M, Zoli M (1998) Brain nicotinic receptors: structure and regulation, role in learning and reinforcement. Brain Res Brain Res Rev 26:198-216.

Chattopadhyaya B, Di Cristo G, Wu CZ, Knott G, Kuhlman S, Fu Y, Palmiter RD, Huang ZJ (2007) GAD67-mediated GABA synthesis and signaling regulate inhibitory synaptic innervation in the visual cortex. Neuron 54:889-903.

Chen D, Guarente L (2007) SIR2: a potential target for calorie restriction mimetics. Trends Mol Med 13:64-71.

Chen J, Zhou Y, Mueller-Steiner S, Chen LF, Kwon H, Yi S, Mucke L, Gan L (2005a) SIRT1 protects against microglia-dependent amyloid-beta toxicity through inhibiting NF-kappaB signaling. J Biol Chem 280:40364-40374.

Chen J, Zhou Y, Mueller-Steiner S, Chen LF, Kwon H, Yi S, Mucke L, Gan L (2005b) SIRT1 protects against microglia-dependent amyloid-beta toxicity through inhibiting NF-kappaB signaling. Journal of Biological Chemistry 280:40364-40374.

Cheng HL, Mostoslavsky R, Saito S, Manis JP, Gu Y, Patel P, Bronson R, Appella E, Alt FW, Chua KF (2003) Developmental defects and p53 hyperacetylation in Sir2 homolog (SIRT1)-deficient mice. Proc Natl Acad Sci U S A 100:10794-10799.

Civitarese AE, Carling S, Heilbronn LK, Hulver MH, Ukropcova B, Deutsch WA, Smith SR, Ravussin E (2007) Calorie restriction increases muscle mitochondrial biogenesis in healthy humans. PLoS Med 4:e76.

Cobos I, Calcagnotto ME, Vilaythong AJ, Thwin MT, Noebels JL, Baraban SC, Rubenstein JL (2005) Mice lacking Dlx1 show subtype-specific loss of interneurons, reduced inhibition and epilepsy. Nat Neurosci 8:1059-1068.

Cohen HY, Lavu S, Bitterman KJ, Hekking B, Imahiyerobo TA, Miller C, Frye R, Ploegh H, Kessler BM, Sinclair DA (2004a) Acetylation of the C terminus of Ku70 by CBP and PCAF controls Bax-mediated apoptosis. Mol Cell 13:627-638.

Cohen HY, Miller C, Bitterman KJ, Wall NR, Hekking B, Kessler B, Howitz KT, Gorospe M, de Cabo R, Sinclair DA (2004b) Calorie restriction promotes mammalian cell survival by inducing the SIRT1 deacetylase. Science 305:390-392.

Colman RJ, Anderson RM, Johnson SC, Kastman EK, Kosmatka KJ, Beasley TM, Allison DB, Cruzen C, Simmons HA, Kemnitz JW, Weindruch R (2009) Caloric restriction delays disease onset and mortality in rhesus monkeys. Science 325:201-204.

Compton RF, Sandborn WJ, Lawson GM, Sheets AJ, Mays DC, Zins BJ, Tremaine WJ, Lipsky JJ, Mahoney DW, Zinsmeister AR, Offord KP, Hurt RD, Evans BK, Green J (1997) A dose-ranging pharmacokinetic study of nicotine tartrate following single-dose delayed-release oral and intravenous administration. Aliment Pharmacol Ther 11:865-874.

Cooper E, Couturier S, Ballivet M (1991) Pentameric structure and subunit stoichiometry of a neuronal nicotinic acetylcholine receptor. Nature 350:235-238.

Corkin S (2002) What's new with the amnesic patient H.M.? Nat Rev Neurosci 3:153-160.

Corringer PJ, Sallette J, Changeux JP (2006) Nicotine enhances intracellular nicotinic receptor maturation: a novel mechanism of neural plasticity? Journal of Physiology, Paris 99:162-171.

Cossart R, Dinocourt C, Hirsch JC, Merchan-Perez A, De Felipe J, Ben-Ari Y, Esclapez M, Bernard C (2001) Dendritic but not somatic GABAergic inhibition is decreased in experimental epilepsy. Nat Neurosci 4:52-62.

Couturier S, Bertrand D, Matter JM, Hernandez MC, Bertrand S, Millar N, Valera S, Barkas T, Ballivet M (1990) A neuronal nicotinic acetylcholine receptor subunit (alpha 7) is developmentally regulated and forms a homo-oligomeric channel blocked by alpha-BTX. Neuron 5:847-856.

Cropley VL, Fujita M, Innis RB, Nathan PJ (2006) Molecular imaging of the dopaminergic system and its association with human cognitive function. Biol Psychiatry 59:898-907.

Dajas-Bailador FA, Mogg AJ, Wonnacott S (2002) Intracellular Ca2+ signals evoked by stimulation of nicotinic acetylcholine receptors in SH-SY5Y cells: contribution of voltage-operated Ca2+ channels and Ca2+ stores. J Neurochem 81:606-614.

De Biasi M (2002) Nicotinic receptor mutant mice in the study of autonomic function. Curr Drug Targets CNS Neurol Disord 1:331-336.

de Leon J, Dadvand M, Canuso C, White AO, Stanilla JK, Simpson GM (1995) Schizophrenia and smoking: an epidemiological survey in a state hospital. Am J Psychiatry 152:453-455.

Dempsey D, Jacob P, 3rd, Benowitz NL (2000) Nicotine metabolism and elimination kinetics in newborns. Clin Pharmacol Ther 67:458-465.

Deupree DL, Bradley J, Turner DA (1993) Age-related alterations in potentiation in the CA1 region in F344 rats. Neurobiol Aging 14:249-258.

Di Liberto V, Bonomo A, Frinchi M, Belluardo N, Mudo G (2010) Group II metabotropic glutamate receptor activation by agonist LY379268 treatment increases the expression of brain derived neurotrophic factor in the mouse brain. Neuroscience 165:863-873.

Dirks AJ, Leeuwenburgh C (2006) Caloric restriction in humans: potential pitfalls and health concerns. Mech Ageing Dev 127:1-7.

Drag LL, Bieliauskas LA (2010) Contemporary review 2009: cognitive aging. J Geriatr Psychiatry Neurol 23:75-93.

Duan W, Lee J, Guo Z, Mattson MP (2001) Dietary restriction stimulates BDNF production in the brain and thereby protects neurons against excitotoxic injury. Journal of Molecular Neuroscience 16:1-12.

Duan W, Mattson MP (1999) Dietary restriction and 2-deoxyglucose administration improve behavioral outcome and reduce degeneration of dopaminergic neurons in models of Parkinson's disease. Journal of Neuroscience Research 57:195-206.

Eldridge LL, Knowlton BJ, Furmanski CS, Bookheimer SY, Engel SA (2000) Remembering episodes: a selective role for the hippocampus during retrieval. Nat Neurosci 3:1149-1152.

Elgoyhen AB, Johnson DS, Boulter J, Vetter DE, Heinemann S (1994) Alpha 9: an acetylcholine receptor with novel pharmacological properties expressed in rat cochlear hair cells. Cell 79:705-715.

Elgoyhen AB, Vetter DE, Katz E, Rothlin CV, Heinemann SF, Boulter J (2001) alpha10: a determinant of nicotinic cholinergic receptor function in mammalian vestibular and cochlear mechanosensory hair cells. Proc Natl Acad Sci U S A 98:3501-3506.

Erixon-Lindroth N, Farde L, Wahlin TB, Sovago J, Halldin C, Backman L (2005) The role of the striatal dopamine transporter in cognitive aging. Psychiatry Res 138:1-12.

Ferezou I, Cauli B, Hill EL, Rossier J, Hamel E, Lambolez B (2002) 5-HT3 receptors mediate serotonergic fast synaptic excitation of neocortical vasoactive intestinal peptide/cholecystokinin interneurons. J Neurosci 22:7389-7397.

Ferguson SG, Shiffman S, Rohay JM, Gitchell JG, Garvey AJ (2011) Effect of compliance with nicotine gum dosing on weight gained during a quit attempt. Addiction 106:651-656.

Fish KN, Sweet RA, Lewis DA (2011) Differential distribution of proteins regulating GABA synthesis and reuptake in axon boutons of subpopulations of cortical interneurons. Cereb Cortex 21:2450-2460.

Fratiglioni L, Wang HX (2000) Smoking and Parkinson's and Alzheimer's disease: review of the epidemiological studies. Behavioural Brain Research 113:117-120.

Freedman R, Hall M, Adler LE, Leonard S (1995) Evidence in postmortem brain tissue for decreased numbers of hippocampal nicotinic receptors in schizophrenia. Biol Psychiatry 38:22-33.

French SJ, Humby T, Horner CH, Sofroniew MV, Rattray M (1999) Hippocampal neurotrophin and trk receptor mRNA levels are altered by local administration of nicotine, carbachol and pilocarpine. Brain Res Mol Brain Res 67:124-136.

Fukuda S, Kaga S, Zhan L, Bagchi D, Das DK, Bertelli A, Maulik N (2006) Resveratrol ameliorates myocardial damage by inducing vascular endothelial growth factor-angiogenesis and tyrosine kinase receptor Flk-1. Cell Biochem Biophys 44:43-49.

Gao J, Wang WY, Mao YW, Graff J, Guan JS, Pan L, Mak G, Kim D, Su SC, Tsai LH (2010) A novel pathway regulates memory and plasticity via SIRT1 and miR-134. Nature 466:1105-1109.

Garrido R, Malecki A, Hennig B, Toborek M (2000) Nicotine attenuates arachidonic acid-induced neurotoxicity in cultured spinal cord neurons. Brain Res 861:59-68.

Garrido R, Mattson MP, Hennig B, Toborek M (2001) Nicotine protects against arachidonic-acid-induced caspase activation, cytochrome c release and apoptosis of cultured spinal cord neurons. J Neurochem 76:1395-1403.

Garten A, Petzold S, Korner A, Imai S, Kiess W (2009) Nampt: linking NAD biology, metabolism and cancer. Trends Endocrinol Metab 20:130-138.

Gazzaley A, D'Esposito M (2005) Bold functional MRI and cognitive aging. In: Cognitive neuroscience of aging(Cabeza, R. et al., eds), pp 107-131 Oxford: Oxford University Press.

Geinisman Y, deToledo-Morrell L, Morrell F, Persina IS, Rossi M (1992) Age-related loss of axospinous synapses formed by two afferent systems in the rat dentate gyrus as revealed by the unbiased stereological dissector technique. Hippocampus 2:437-444.

Giannakou ME, Partridge L (2004) The interaction between FOXO and SIRT1: tipping the balance towards survival. Trends Cell Biol 14:408-412.

Gilbert DG, Robinson JH, Chamberlin CL, Spielberger CD (1989) Effects of smoking/nicotine on anxiety, heart rate, and lateralization of EEG during a stressful movie. Psychophysiology 26:311-320.

Gioanni Y, Rougeot C, Clarke PB, Lepouse C, Thierry AM, Vidal C (1999) Nicotinic receptors in the rat prefrontal cortex: increase in glutamate release and facilitation of mediodorsal thalamo-cortical transmission. Eur J Neurosci 11:18-30.

Gonchar Y, Burkhalter A (1997) Three distinct families of GABAergic neurons in rat visual cortex. Cereb Cortex 7:347-358.

Gonzalez-Burgos G, Fish KN, Lewis DA (2011) GABA neuron alterations, cortical circuit dysfunction and cognitive deficits in schizophrenia. Neural Plast 2011:723184.

Gonzalez-Burgos G, Lewis DA (2008) GABA neurons and the mechanisms of network oscillations: implications for understanding cortical dysfunction in schizophrenia. Schizophr Bull 34:944-961.

Gonzalez CL, Gharbawie OA, Whishaw IQ, Kolb B (2005) Nicotine stimulates dendritic arborization in motor cortex and improves concurrent motor skill but impairs subsequent motor learning. Synapse 55:183-191.

Gould TJ, Higgins JS (2003) Nicotine enhances contextual fear conditioning in C57BL/6J mice at 1 and 7 days post-training. Neurobiol Learn Mem 80:147-157.

Grady SR, Moretti M, Zoli M, Marks MJ, Zanardi A, Pucci L, Clementi F, Gotti C (2009) Rodent habenulo-interpeduncular pathway expresses a large variety of uncommon nAChR subtypes, but only the alpha3beta4* and alpha3beta3beta4* subtypes mediate acetylcholine release. J Neurosci 29:2272-2282.

Gray R, Rajan AS, Radcliffe KA, Yakehiro M, Dani JA (1996) Hippocampal synaptic transmission enhanced by low concentrations of nicotine. Nature 383:713-716.

Guarente L (2007) Sirtuins in aging and disease. Cold Spring Harb Symp Quant Biol 72:483-488.

Guttmann CR, Jolesz FA, Kikinis R, Killiany RJ, Moss MB, Sandor T, Albert MS (1998) White matter changes with normal aging. Neurology 50:972-978.

Haider B, McCormick DA (2009) Rapid neocortical dynamics: cellular and network mechanisms. Neuron 62:171-189.

Haigis MC, Sinclair DA (2010) Mammalian sirtuins: biological insights and disease relevance. Annu Rev Pathol 5:253-295.

Hajek P, Jackson P, Belcher M (1988) Long-term use of nicotine chewing gum. Occurrence, determinants, and effect on weight gain. JAMA 260:1593-1596.

Halagappa VK, Guo Z, Pearson M, Matsuoka Y, Cutler RG, Laferla FM, Mattson MP (2007) Intermittent fasting and caloric restriction ameliorate age-related behavioral deficits in the triple-transgenic mouse model of Alzheimer's disease. Neurobiol Dis 26:212-220.

Harrist A, Beech RD, King SL, Zanardi A, Cleary MA, Caldarone BJ, Eisch A, Zoli M, Picciotto MR (2004) Alteration of hippocampal cell proliferation in mice lacking the beta 2 subunit of the neuronal nicotinic acetylcholine receptor. Synapse 54:200-206.

Hasher L, Zachs R (1988) Working memory, comprehension, and aging: a review and a new view. In: The psychology of learning and motivation(Bower, H., ed), pp 193-225 San Diego, CA: Academic Press.

Hastings NB, Gould E (1999) Rapid extension of axons into the CA3 region by adult-generated granule cells. J Comp Neurol 413:146-154.

Haug H (1983) Anatomical changes in the aging brain: morphometric analysis of the human prosencephalon In: Brain aging neuropathology and neuropharmacology(Cervos-Nacarro, J. and Sarkander, H., eds), pp 1-12 New York, NY: Raven Press.

Haug H, Eggers R (1991) Morphometry of the human cortex cerebri and corpus striatum during aging. Neurobiol Aging 12:336-338; discussion 352-335.

Head D, Buckner RL, Shimony JS, Williams LE, Akbudak E, Conturo TE, McAvoy M, Morris JC, Snyder AZ (2004) Differential vulnerability of anterior white matter in nondemented aging with minimal acceleration in dementia of the Alzheimer type: evidence from diffusion tensor imaging. Cereb Cortex 14:410-423.

Head D, Rodrigue KM, Kennedy KM, Raz N (2008) Neuroanatomical and cognitive mediators of age-related differences in episodic memory. Neuropsychology 22:491-507.

Heishman SJ, Kleykamp BA, Singleton EG (2010) Meta-analysis of the acute effects of nicotine and smoking on human performance. Psychopharmacology (Berl) 210:453-469.

Hellstrom-Lindahl E, Court JA (2000) Nicotinic acetylcholine receptors during prenatal development and brain pathology in human aging. Behav Brain Res 113:159-168.

Henningfield JE, Keenan RM (1993) Nicotine delivery kinetics and abuse liability. J Consult Clin Psychol 61:743-750.

Hoekman MF, Jacobs FM, Smidt MP, Burbach JP (2006) Spatial and temporal expression of FoxO transcription factors in the developing and adult murine brain. Gene Expr Patterns 6:134-140.

Hof PR, Morrison JH (2004) The aging brain: morphomolecular senescence of cortical circuits. Trends Neurosci 27:607-613.

Howitz KT, Bitterman KJ, Cohen HY, Lamming DW, Lavu S, Wood JG, Zipkin RE, Chung P, Kisielewski A, Zhang LL, Scherer B, Sinclair DA (2003) Small molecule activators of sirtuins extend Saccharomyces cerevisiae lifespan. Nature 425:191-196.

Hsu CP, Oka S, Shao D, Hariharan N, Sadoshima J (2009) Nicotinamide phosphoribosyltransferase regulates cell survival through NAD+ synthesis in cardiac myocytes. Circ Res 105:481-491.

Huang LZ, Hsiao SH, Trzeciakowski J, Frye GD, Winzer-Serhan UH (2006) Chronic nicotine induces growth retardation in neonatal rat pups. Life Sci 78:1483-1493.

Huang LZ, Winzer-Serhan UH (2006a) Chronic neonatal nicotine upregulates heteromeric nicotinic acetylcholine receptor binding without change in subunit mRNA expression. Brain Research 1113:94-109.

Huang LZ, Winzer-Serhan UH (2006b) Effects of paraformaldehyde fixation on nicotinic acetylcholine receptor binding in adult and developing rat brain sections. Journal of Neuroscience Methods 153:312-317.

Huang LZ, Winzer-Serhan UH (2007) Nicotine regulates mRNA expression of feeding peptides in the arcuate nucleus in neonatal rat pups. Dev Neurobiol 67:363-377.

Huang PS, Son JH, Abbott LC, Winzer-Serhan UH (2011) Regulated expression of neuronal SIRT1 and related genes by aging and neuronal beta2-containing nicotinic cholinergic receptors. Neuroscience 196:189-202.

Hukkanen J, Jacob P, 3rd, Benowitz NL (2005) Metabolism and disposition kinetics of nicotine. Pharmacol Rev 57:79-115.

Hursting SD, Lavigne JA, Berrigan D, Perkins SN, Barrett JC (2003) Calorie restriction, aging, and cancer prevention: mechanisms of action and applicability to humans. Annu Rev Med 54:131-152.

Imai S (2009) Nicotinamide phosphoribosyltransferase (Nampt): a link between NAD biology, metabolism, and diseases. Curr Pharm Des 15:20-28.

Imai S (2010) "Clocks" in the NAD World: NAD as a metabolic oscillator for the regulation of metabolism and aging. Biochim Biophys Acta 1804:1584-1590.

Imai S, Armstrong CM, Kaeberlein M, Guarente L (2000) Transcriptional silencing and longevity protein Sir2 is an NAD-dependent histone deacetylase. Nature 403:795-800.

Imai S, Guarente L (2010) Ten years of NAD-dependent SIR2 family deacetylases: implications for metabolic diseases. Trends Pharmacol Sci 31:212-220.

Ingram DK, Anson RM, de Cabo R, Mamczarz J, Zhu M, Mattison J, Lane MA, Roth GS (2004) Development of calorie restriction mimetics as a prolongevity strategy. Ann N Y Acad Sci 1019:412-423.

Jackson KJ, Walters CL, Damaj MI (2009) Beta 2 subunit-containing nicotinic receptors mediate acute nicotine-induced activation of calcium/calmodulin-dependent protein kinase II-dependent pathways in vivo. J Pharmacol Exp Ther 330:541-549.

Jackson SP (2002) Sensing and repairing DNA double-strand breaks. Carcinogenesis 23:687-696.

Janson AM, Fuxe K, Sundstrom E, Agnati LF, Goldstein M (1988) Chronic nicotine treatment partly protects against the 1-methyl-4-phenyl-2,3,6-tetrahydropyridine-induced degeneration of nigrostriatal dopamine neurons in the black mouse. Acta Physiol Scand 132:589-591.

Jeong J, Juhn K, Lee H, Kim SH, Min BH, Lee KM, Cho MH, Park GH, Lee KH (2007) SIRT1 promotes DNA repair activity and deacetylation of Ku70. Exp Mol Med 39:8-13.

Jernigan TL, Archibald SL, Fennema-Notestine C, Gamst AC, Stout JC, Bonner J, Hesselink JR (2001) Effects of age on tissues and regions of the cerebrum and cerebellum. Neurobiol Aging 22:581-594.

Ji D, Dani JA (2000) Inhibition and disinhibition of pyramidal neurons by activation of nicotinic receptors on hippocampal interneurons. J Neurophysiol 83:2682-2690.

Ji F, Obata K (1999) Development of the GABA system in organotypic culture of hippocampal and cerebellar slices from a 67-kDa isoform of glutamic acid decarboxylase (GAD67)-deficient mice. Neurosci Res 33:233-237.

Jindahra P, Petrie A, Plant GT (2012) The time course of retrograde trans-synaptic degeneration following occipital lobe damage in humans. Brain 135:534-541.

Jones GM, Sahakian BJ, Levy R, Warburton DM, Gray JA (1992) Effects of acute subcutaneous nicotine on attention, information processing and short-term memory in Alzheimer's disease. Psychopharmacology (Berl) 108:485-494.

Jonnala RR, Terry AV, Jr., Buccafusco JJ (2002) Nicotine increases the expression of high affinity nerve growth factor receptors in both in vitro and in vivo. Life Sci 70:1543-1554.

Ju YJ, Lee KH, Park JE, Yi YS, Yun MY, Ham YH, Kim TJ, Choi HM, Han GJ, Lee JH, Lee J, Han JS, Lee KM, Park GH (2006) Decreased expression of DNA repair proteins Ku70 and Mre11 is associated with aging and may contribute to the cellular senescence. Exp Mol Med 38:686-693.

Kaeberlein M, McVey M, Guarente L (1999) The SIR2/3/4 complex and SIR2 alone promote longevity in Saccharomyces cerevisiae by two different mechanisms. Genes Dev 13:2570-2580.

Kalamida D, Poulas K, Avramopoulou V, Fostieri E, Lagoumintzis G, Lazaridis K, Sideri A, Zouridakis M, Tzartos SJ (2007) Muscle and neuronal nicotinic acetylcholine receptors. Structure, function and pathogenicity. FEBS J 274:3799-3845.

Kaneko S, Maeda T, Kume T, Kochiyama H, Akaike A, Shimohama S, Kimura J (1997) Nicotine protects cultured cortical neurons against glutamate-induced cytotoxicity via alpha7-neuronal receptors and neuronal CNS receptors. Brain Res 765:135-140.

Kanfi Y, Peshti V, Gozlan YM, Rathaus M, Gil R, Cohen HY (2008) Regulation of SIRT1 protein levels by nutrient availability. FEBS Lett 582:2417-2423.

Karlin A (2002) Emerging structure of the nicotinic acetylcholine receptors. Nat Rev Neurosci 3:102-114.

Kash SF, Johnson RS, Tecott LH, Noebels JL, Mayfield RD, Hanahan D, Baekkeskov S (1997) Epilepsy in mice deficient in the 65-kDa isoform of glutamic acid decarboxylase. Proc Natl Acad Sci U S A 94:14060-14065.

Kash SF, Tecott LH, Hodge C, Baekkeskov S (1999) Increased anxiety and altered responses to anxiolytics in mice deficient in the 65-kDa isoform of glutamic acid decarboxylase. Proc Natl Acad Sci U S A 96:1698-1703.

Kastman EK, Willette AA, Coe CL, Bendlin BB, Kosmatka KJ, McLaren DG, Xu G, Canu E, Field AS, Alexander AL, Voytko ML, Beasley TM, Colman RJ, Weindruch RH, Johnson SC (2010) A calorie-restricted diet decreases brain iron accumulation and preserves motor performance in old rhesus monkeys. J Neurosci 30:7940-7947.

Kawaguchi Y, Kubota Y (1997) GABAergic cell subtypes and their synaptic connections in rat frontal cortex. Cereb Cortex 7:476-486.

Kawamata J, Shimohama S (2011) Stimulating nicotinic receptors trigger multiple pathways attenuating cytotoxicity in models of Alzheimer's and Parkinson's diseases. J Alzheimers Dis 24 Suppl 2:95-109.

Kenny PJ, File SE, Rattray M (2000) Acute nicotine decreases, and chronic nicotine increases the expression of brain-derived neurotrophic factor mRNA in rat hippocampus. Brain Res Mol Brain Res 85:234-238.

Kihara T, Shimohama S, Sawada H, Honda K, Nakamizo T, Shibasaki H, Kume T, Akaike A (2001) alpha 7 nicotinic receptor transduces signals to phosphatidylinositol 3-kinase to block A beta-amyloid-induced neurotoxicity. J Biol Chem 276:13541-13546.

Kim-Han JS, Reichert SA, Quick KL, Dugan LL (2001) BMCP1: a mitochondrial uncoupling protein in neurons which regulates mitochondrial function and oxidant production. J Neurochem 79:658-668.

Kim D, Nguyen MD, Dobbin MM, Fischer A, Sananbenesi F, Rodgers JT, Delalle I, Baur JA, Sui G, Armour SM, Puigserver P, Sinclair DA, Tsai LH (2007a) SIRT1 deacetylase protects against neurodegeneration in models for Alzheimer's disease and amyotrophic lateral sclerosis. EMBO Journal 26:3169-3179.

Kim D, Nguyen MD, Dobbin MM, Fischer A, Sananbenesi F, Rodgers JT, Delalle I, Baur JA, Sui G, Armour SM, Puigserver P, Sinclair DA, Tsai LH (2007b) SIRT1 deacetylase protects against neurodegeneration in models for Alzheimer's disease and amyotrophic lateral sclerosis. Embo J 26:3169-3179.

Kivinummi T, Kaste K, Rantamaki T, Castren E, Ahtee L (2011) Alterations in BDNF and phospho-CREB levels following chronic oral nicotine treatment and its withdrawal in dopaminergic brain areas of mice. Neurosci Lett 491:108-112.

Klausberger T, Somogyi P (2008) Neuronal diversity and temporal dynamics: the unity of hippocampal circuit operations. Science 321:53-57.

Kleijn J, Folgering JH, van der Hart MC, Rollema H, Cremers TI, Westerink BH (2011) Direct effect of nicotine on mesolimbic dopamine release in rat nucleus accumbens shell. Neurosci Lett 493:55-58.

Kumar S, Parkash J, Kataria H, Kaur G (2009) Interactive effect of excitotoxic injury and dietary restriction on neurogenesis and neurotrophic factors in adult male rat brain. Neuroscience Research 65:367-374.

Langston RF, Stevenson CH, Wilson CL, Saunders I, Wood ER (2010) The role of hippocampal subregions in memory for stimulus associations. Behav Brain Res 215:275-291.

Lavu S, Boss O, Elliott PJ, Lambert PD (2008) Sirtuins--novel therapeutic targets to treat age-associated diseases. Nat Rev Drug Discov 7:841-853.

Le Houezec J, Martin C, Cohen C, Molimard R (1989) Failure of behavioral dependence induction and oral nicotine bioavailability in rats. Physiology and Behavior 45:103-108.

Le Novere N, Changeux JP (1995) Molecular evolution of the nicotinic acetylcholine receptor: an example of multigene family in excitable cells. J Mol Evol 40:155-172.

Lee M, Martin-Ruiz C, Graham A, Court J, Jaros E, Perry R, Iversen P, Bauman M, Perry E (2002) Nicotinic receptor abnormalities in the cerebellar cortex in autism. Brain 125:1483-1495.

Lee PN (1994) Smoking and Alzheimer's disease: a review of the epidemiological evidence. Neuroepidemiology 13:131-144.

Lee S, Hjerling-Leffler J, Zagha E, Fishell G, Rudy B (2010) The largest group of superficial neocortical GABAergic interneurons expresses ionotropic serotonin receptors. J Neurosci 30:16796-16808.

Lena C, Changeux JP (1998) Allosteric nicotinic receptors, human pathologies. J Physiol Paris 92:63-74.

Lena C, Changeux JP (1999) The role of beta 2-subunit-containing nicotinic acetylcholine receptors in the brain explored with a mutant mouse. Ann N Y Acad Sci 868:611-616.

Lena C, Changeux JP, Mulle C (1993) Evidence for "preterminal" nicotinic receptors on GABAergic axons in the rat interpeduncular nucleus. J Neurosci 13:2680-2688.

Leonard S, Gault J, Hopkins J, Logel J, Vianzon R, Short M, Drebing C, Berger R, Venn D, Sirota P, Zerbe G, Olincy A, Ross RG, Adler LE, Freedman R (2002) Association of promoter variants in the alpha7 nicotinic acetylcholine receptor subunit gene with an inhibitory deficit found in schizophrenia. Arch Gen Psychiatry 59:1085-1096.

Levin ED, Bencan Z, Cerutti DT (2007) Anxiolytic effects of nicotine in zebrafish. Physiology and Behavior 90:54-58.

Levin ED, Bradley A, Addy N, Sigurani N (2002) Hippocampal alpha 7 and alpha 4 beta 2 nicotinic receptors and working memory. Neuroscience 109:757-765.

Levin ED, Rezvani AH (2000) Development of nicotinic drug therapy for cognitive disorders. Eur J Pharmacol 393:141-146.

Levin ED, Rezvani AH (2002) Nicotinic treatment for cognitive dysfunction. Curr Drug Targets CNS Neurol Disord 1:423-431.

Levin ED, Simon BB (1998) Nicotinic acetylcholine involvement in cognitive function in animals. Psychopharmacology (Berl) 138:217-230.

Levin ED, Torry D (1996) Acute and chronic nicotine effects on working memory in aged rats. Psychopharmacology (Berl) 123:88-97.

Levitt P, Eagleson KL, Powell EM (2004) Regulation of neocortical interneuron development and the implications for neurodevelopmental disorders. Trends Neurosci 27:400-406.

Lin SJ, Defossez PA, Guarente L (2000) Requirement of NAD and SIR2 for life-span extension by calorie restriction in Saccharomyces cerevisiae. Science 289:2126-2128.

Lindstrom JM (2000) Acetylcholine receptors and myasthenia. Muscle Nerve 23:453-477.

Lister JP, Barnes CA (2009) Neurobiological changes in the hippocampus during normative aging. Arch Neurol 66:829-833.

Liu D, Chan SL, de Souza-Pinto NC, Slevin JR, Wersto RP, Zhan M, Mustafa K, de Cabo R, Mattson MP (2006) Mitochondrial UCP4 mediates an adaptive shift in

energy metabolism and increases the resistance of neurons to metabolic and oxidative stress. Neuromolecular Med 8:389-414.

Liu Q, Zhao B (2004) Nicotine attenuates beta-amyloid peptide-induced neurotoxicity, free radical and calcium accumulation in hippocampal neuronal cultures. Br J Pharmacol 141:746-754.

Lovell MA, Markesbery WR (2007) Oxidative damage in mild cognitive impairment and early Alzheimer's disease. J Neurosci Res 85:3036-3040.

Lu KT, Ko MC, Chen BY, Huang JC, Hsieh CW, Lee MC, Chiou RY, Wung BS, Peng CH, Yang YL (2008) Neuroprotective effects of resveratrol on MPTP-induced neuron loss mediated by free radical scavenging. J Agric Food Chem 56:6910-6913.

Luchsinger JA, Tang MX, Shea S, Mayeux R (2002) Caloric intake and the risk of Alzheimer disease. Arch Neurol 59:1258-1263.

Luciana M, Collins PF, Depue RA (1998) Opposing roles for dopamine and serotonin in the modulation of human spatial working memory functions. Cereb Cortex 8:218-226.

Luo J, Nikolaev AY, Imai S, Chen D, Su F, Shiloh A, Guarente L, Gu W (2001) Negative control of p53 by Sir2alpha promotes cell survival under stress. Cell 107:137-148.

Maggio R, Riva M, Vaglini F, Fornai F, Molteni R, Armogida M, Racagni G, Corsini GU (1998) Nicotine prevents experimental parkinsonism in rodents and induces striatal increase of neurotrophic factors. J Neurochem 71:2439-2446.

Marcello E, Epis R, Saraceno C, Di Luca M (2012) Synaptic dysfunction in Alzheimer's disease. Adv Exp Med Biol 970:573-601.

Markram H, Toledo-Rodriguez M, Wang Y, Gupta A, Silberberg G, Wu C (2004) Interneurons of the neocortical inhibitory system. Nat Rev Neurosci 5:793-807.

Marks MJ, Burch JB, Collins AC (1983) Effects of chronic nicotine infusion on tolerance development and nicotinic receptors. J Pharmacol Exp Ther 226:817-825.

Martin-Ruiz CM, Lee M, Perry RH, Baumann M, Court JA, Perry EK (2004) Molecular analysis of nicotinic receptor expression in autism. Brain Res Mol Brain Res 123:81-90.

Martin LF, Kem WR, Freedman R (2004) Alpha-7 nicotinic receptor agonists: potential new candidates for the treatment of schizophrenia. Psychopharmacology (Berl) 174:54-64.

Masoro EJ (2005) Overview of caloric restriction and ageing. Mech Ageing Dev 126:913-922.

Mattison JA, Roth GS, Lane MA, Ingram DK (2007) Dietary restriction in aging nonhuman primates. Interdiscip Top Gerontol 35:137-158.

Mattson MP (2003) Will caloric restriction and folate protect against AD and PD? Neurology 60:690-695.

Mattson MP, Chan SL, Duan W (2002) Modification of brain aging and neurodegenerative disorders by genes, diet, and behavior. Physiol Rev 82:637-672.

McBain CJ, Fisahn A (2001) Interneurons unbound. Nat Rev Neurosci 2:11-23.

McBurney MW, Yang X, Jardine K, Hixon M, Boekelheide K, Webb JR, Lansdorp PM, Lemieux M (2003) The mammalian SIR2alpha protein has a role in embryogenesis and gametogenesis. Mol Cell Biol 23:38-54.

McCaffree J (2004) What you should know about calorie restriction. J Am Diet Assoc 104:1524, 1526.

McCallum SE, Collins AC, Paylor R, Marks MJ (2006) Deletion of the beta 2 nicotinic acetylcholine receptor subunit alters development of tolerance to nicotine and eliminates receptor upregulation. Psychopharmacology (Berl) 184:314-327.

Mechawar N, Saghatelyan A, Grailhe R, Scoriels L, Gheusi G, Gabellec MM, Lledo PM, Changeux JP (2004) Nicotinic receptors regulate the survival of newborn neurons in the adult olfactory bulb. Proc Natl Acad Sci U S A 101:9822-9826.

Michan S, Sinclair D (2007) Sirtuins in mammals: insights into their biological function. Biochem J 404:1-13.

Miller RP, Rotenberg KS, Adir J (1977) Effect of dose on the pharmacokinetics of intravenous nicotine in the rat. Drug Metab lism and Disposition: The Biological Fate of Chemicals 5:436-443.

Mineur YS, Abizaid A, Rao Y, Salas R, DiLeone RJ, Gundisch D, Diano S, De Biasi M, Horvath TL, Gao XB, Picciotto MR (2011) Nicotine decreases food intake through activation of POMC neurons. Science 332:1330-1332.

Miyoshi G, Hjerling-Leffler J, Karayannis T, Sousa VH, Butt SJ, Battiste J, Johnson JE, Machold RP, Fishell G (2010) Genetic fate mapping reveals that the caudal ganglionic eminence produces a large and diverse population of superficial cortical interneurons. J Neurosci 30:1582-1594.

Molander L, Hansson A, Lunell E (2001) Pharmacokinetics of nicotine in healthy elderly people. Clin Pharmacol Ther 69:57-65.

Morales M, Bloom FE (1997) The 5-HT3 receptor is present in different subpopulations of GABAergic neurons in the rat telencephalon. J Neurosci 17:3157-3167.

Morrison JH, Hof PR (1997) Life and death of neurons in the aging brain. Science 278:412-419.

Mozley LH, Gur RC, Mozley PD, Gur RE (2001) Striatal dopamine transporters and cognitive functioning in healthy men and women. Am J Psychiatry 158:1492-1499.

Mukhin AG, Kimes AS, Chefer SI, Matochik JA, Contoreggi CS, Horti AG, Vaupel DB, Pavlova O, Stein EA (2008) Greater nicotinic acetylcholine receptor density in smokers than in nonsmokers: a PET study with 2-18F-FA-85380. J Nucl Med 49:1628-1635.

Nanri M, Yamamoto J, Miyake H, Watanabe H (1998) Protective effect of GTS-21, a novel nicotinic receptor agonist, on delayed neuronal death induced by ischemia in gerbils. Jpn J Pharmacol 76:23-29.

Narasimhaiah R, Tuchman A, Lin SL, Naegele JR (2005) Oxidative damage and defective DNA repair is linked to apoptosis of migrating neurons and progenitors during cerebral cortex development in Ku70-deficient mice. Cereb Cortex 15:696-707.

Nashmi R, Xiao C, Deshpande P, McKinney S, Grady SR, Whiteaker P, Huang Q, McClure-Begley T, Lindstrom JM, Labarca C, Collins AC, Marks MJ, Lester HA (2007) Chronic nicotine cell specifically upregulates functional alpha 4* nicotinic receptors: basis for both tolerance in midbrain and enhanced long-term potentiation in perforant path. J Neurosci 27:8202-8218.

Nemoto S, Fergusson MM, Finkel T (2004) Nutrient availability regulates SIRT1 through a forkhead-dependent pathway. Science 306:2105-2108.

Newhouse P, Kellar K, Aisen P, White H, Wesnes K, Coderre E, Pfaff A, Wilkins H, Howard D, Levin ED (2012) Nicotine treatment of mild cognitive impairment: a 6-month double-blind pilot clinical trial. Neurology 78:91-101.

Newhouse PA, Potter A, Kelton M, Corwin J (2001) Nicotinic treatment of Alzheimer's disease. Biol Psychiatry 49:268-278.

Newhouse PA, Potter A, Singh A (2004) Effects of nicotinic stimulation on cognitive performance. Curr Opin Pharmacol 4:36-46.

Newhouse PA, Sunderland T, Tariot PN, Blumhardt CL, Weingartner H, Mellow A, Murphy DL (1988) Intravenous nicotine in Alzheimer's disease: a pilot study. Psychopharmacology (Berl) 95:171-175.

Noebels JL (2003) The biology of epilepsy genes. Annu Rev Neurosci 26:599-625.

Nolte J (2002) The Human Brain: An Introduction to Its Functional Anatomy. St. Louis, Missouri, USA: Mosby.

Nordberg A, Hellstrom-Lindahl E, Lee M, Johnson M, Mousavi M, Hall R, Perry E, Bednar I, Court J (2002) Chronic nicotine treatment reduces beta-amyloidosis in the brain of a mouse model of Alzheimer's disease (APPsw). J Neurochem 81:655-658.

Nuutinen S, Ahtee L, Tuominen RK (2005) Time and brain region specific up-regulation of low affinity neuronal nicotinic receptors during chronic nicotine administration in mice. Eur J Pharmacol 515:83-89.

O'Neill AB, Morgan SJ, Brioni JD (1998) Histological and behavioral protection by (-)-nicotine against quinolinic acid-induced neurodegeneration in the hippocampus. Neurobiology of Learning and Memory 69:46-64.

Onoda N, Nehmi A, Weiner D, Mujumdar S, Christen R, Los G (2001) Nicotine affects the signaling of the death pathway, reducing the response of head and neck cancer cell lines to DNA damaging agents. Head Neck 23:860-870.

Orr-Urtreger A, Goldner FM, Saeki M, Lorenzo I, Goldberg L, De Biasi M, Dani JA, Patrick JW, Beaudet AL (1997) Mice deficient in the alpha7 neuronal nicotinic acetylcholine receptor lack alpha-bungarotoxin binding sites and hippocampal fast nicotinic currents. J Neurosci 17:9165-9171.

Owman C, Fuxe K, Janson AM, Kahrstrom J (1989) Chronic nicotine treatment eliminates asymmetry in striatal glucose utilization following unilateral

transection of the mesostriatal dopamine pathway in rats. Neuroscience Letters 102:279-283.

Parker JA, Arango M, Abderrahmane S, Lambert E, Tourette C, Catoire H, Neri C (2005) Resveratrol rescues mutant polyglutamine cytotoxicity in nematode and mammalian neurons. Nat Genet 37:349-350.

Patel NV, Gordon MN, Connor KE, Good RA, Engelman RW, Mason J, Morgan DG, Morgan TE, Finch CE (2005) Caloric restriction attenuates Abeta-deposition in Alzheimer transgenic models. Neurobiology of Aging 26:995-1000.

Pearson KJ, Baur JA, Lewis KN, Peshkin L, Price NL, Labinskyy N, Swindell WR, Kamara D, Minor RK, Perez E, Jamieson HA, Zhang Y, Dunn SR, Sharma K, Pleshko N, Woollett LA, Csiszar A, Ikeno Y, Le Couteur D, Elliott PJ, Becker KG, Navas P, Ingram DK, Wolf NS, Ungvari Z, Sinclair DA, de Cabo R (2008) Resveratrol delays age-related deterioration and mimics transcriptional aspects of dietary restriction without extending life span. Cell Metab 8:157-168.

Pekonen K, Karlsson, C., Laakso, I., Ahtee, L. (1993) Plasma nicotine and cotinine concentrations in mice after chronic oral nicotine administration and challenge doses. European Journal of Pharmaceutical Sciences 1:13-18.

Perkins KA, Grobe JE (1992) Increased desire to smoke during acute stress. British Journal of Addiction 87:1037-1040.

Perry DC, Davila-Garcia MI, Stockmeier CA, Kellar KJ (1999) Increased nicotinic receptors in brains from smokers: membrane binding and autoradiography studies. J Pharmacol Exp Ther 289:1545-1552.

Perry DC, Kellar KJ (1995) [3H]epibatidine labels nicotinic receptors in rat brain: an autoradiographic study. Journal of Pharmacology and Experimental Therapeutics 275:1030-1034.

Persson J, Nyberg L, Lind J, Larsson A, Nilsson LG, Ingvar M, Buckner RL (2006) Structure-function correlates of cognitive decline in aging. Cereb Cortex 16:907-915.

Petersen DR, Norris KJ, Thompson JA (1984) A comparative study of the disposition of nicotine and its metabolites in three inbred strains of mice. Drug Metab lism and Disposition: The Biological Fate of Chemicals 12:725-731.

Pfefferbaum A, Mathalon DH, Sullivan EV, Rawles JM, Zipursky RB, Lim KO (1994) A quantitative magnetic resonance imaging study of changes in brain morphology from infancy to late adulthood. Arch Neurol 51:874-887.

Picard F, Guarente L (2005) Molecular links between aging and adipose tissue. Int J Obes (Lond) 29 Suppl 1:S36-39.

Picciotto MR, Addy NA, Mineur YS, Brunzell DH (2008) It is not "either/or": activation and desensitization of nicotinic acetylcholine receptors both contribute to behaviors related to nicotine addiction and mood. Prog Neurobiol 84:329-342.

Picciotto MR, Brunzell DH, Caldarone BJ (2002) Effect of nicotine and nicotinic receptors on anxiety and depression. Neuroreport 13:1097-1106.

Picciotto MR, Caldarone BJ, Brunzell DH, Zachariou V, Stevens TR, King SL (2001) Neuronal nicotinic acetylcholine receptor subunit knockout mice: physiological and behavioral phenotypes and possible clinical implications. Pharmacol Ther 92:89-108.

Picciotto MR, Zoli M (2008a) Neuroprotection via nAChRs: the role of nAChRs in neurodegenerative disorders such as Alzheimer's and Parkinson's disease. Frontiers in Bioscience 13:492-504.

Picciotto MR, Zoli M (2008b) Neuroprotection via nAChRs: the role of nAChRs in neurodegenerative disorders such as Alzheimer's and Parkinson's disease. Front Biosci 13:492-504.

Picciotto MR, Zoli M, Lena C, Bessis A, Lallemand Y, Le Novere N, Vincent P, Pich EM, Brulet P, Changeux JP (1995) Abnormal avoidance learning in mice lacking functional high-affinity nicotine receptor in the brain. Nature 374:65-67.

Picciotto MR, Zoli M, Rimondini R, Lena C, Marubio LM, Pich EM, Fuxe K, Changeux JP (1998) Acetylcholine receptors containing the beta2 subunit are involved in the reinforcing properties of nicotine. Nature 391:173-177.

Pienaar IS, Burn D, Morris C, Dexter D (2012) Synaptic protein alterations in Parkinson's disease. Mol Neurobiol 45:126-143.

Pietila K, Ahtee L (2000) Chronic nicotine administration in the drinking water affects the striatal dopamine in mice. Pharmacol Biochem Behav 66:95-103.

Pietila K, Lahde T, Attila M, Ahtee L, Nordberg A (1998) Regulation of nicotinic receptors in the brain of mice withdrawn from chronic oral nicotine treatment. Naunyn Schmiedebergs Arch Pharmacol 357:176-182.

Piper MD, Bartke A (2008) Diet and aging. Cell Metab 8:99-104.

Plazas PV, Katz E, Gomez-Casati ME, Bouzat C, Elgoyhen AB (2005) Stoichiometry of the alpha9alpha10 nicotinic cholinergic receptor. J Neurosci 25:10905-10912.

Pomerleau OF, Downey KK, Stelson FW, Pomerleau CS (1995) Cigarette smoking in adult patients diagnosed with attention deficit hyperactivity disorder. J Subst Abuse 7:373-378.

Pouille F, Scanziani M (2001) Enforcement of temporal fidelity in pyramidal cells by somatic feed-forward inhibition. Science 293:1159-1163.

Prall WC, Czibere A, Jager M, Spentzos D, Libermann TA, Gattermann N, Haas R, Aivado M (2007) Age-related transcription levels of KU70, MGST1 and BIK in CD34+ hematopoietic stem and progenitor cells. Mech Ageing Dev 128:503-510.

Puig MV, Santana N, Celada P, Mengod G, Artigas F (2004) In vivo excitation of GABA interneurons in the medial prefrontal cortex through 5-HT3 receptors. Cereb Cortex 14:1365-1375.

Qin W, Chachich M, Lane M, Roth G, Bryant M, de Cabo R, Ottinger MA, Mattison J, Ingram D, Gandy S, Pasinetti GM (2006a) Calorie restriction attenuates Alzheimer's disease type brain amyloidosis in Squirrel monkeys (Saimiri sciureus). J Alzheimers Dis 10:417-422.

Qin W, Yang T, Ho L, Zhao Z, Wang J, Chen L, Zhao W, Thiyagarajan M, MacGrogan D, Rodgers JT, Puigserver P, Sadoshima J, Deng H, Pedrini S, Gandy S, Sauve AA, Pasinetti GM (2006b) Neuronal SIRT1 activation as a novel mechanism underlying the prevention of Alzheimer disease amyloid neuropathology by calorie restriction. Journal of Biological Chemistry 281:21745-21754.

Quick MW, Ceballos RM, Kasten M, McIntosh JM, Lester RA (1999) Alpha3beta4 subunit-containing nicotinic receptors dominate function in rat medial habenula neurons. Neuropharmacology 38:769-783.

Ramadori G, Lee CE, Bookout AL, Lee S, Williams KW, Anderson J, Elmquist JK, Coppari R (2008) Brain SIRT1: anatomical distribution and regulation by energy availability. J Neurosci 28:9989-9996.

Raman A, Ramsey JJ, Kemnitz JW, Baum ST, Newton W, Colman RJ, Weindruch R, Beasley MT, Schoeller DA (2007) Influences of calorie restriction and age on energy expenditure in the rhesus monkey. Am J Physiol Endocrinol Metab 292:E101-106.

Ramsey JJ, Colman RJ, Binkley NC, Christensen JD, Gresl TA, Kemnitz JW, Weindruch R (2000) Dietary restriction and aging in rhesus monkeys: the University of Wisconsin study. Exp Gerontol 35:1131-1149.

Rapp PR, Rosenberg RA, Gallagher M (1987) An evaluation of spatial information processing in aged rats. Behav Neurosci 101:3-12.

Rasband WS (1997-2011) ImageJ. Bethesda, Maryland, USA: U. S. National Institutes of Health. http://imagej.nih.gov/ij/.

Rasmussen T, Schliemann T, Sorensen JC, Zimmer J, West MJ (1996) Memory impaired aged rats: no loss of principal hippocampal and subicular neurons. Neurobiol Aging 17:143-147.

Rathouz MM, Berg DK (1994) Synaptic-type acetylcholine receptors raise intracellular calcium levels in neurons by two mechanisms. J Neurosci 14:6935-6945.

Raz N (2005) The aging brain observed in vivo: differential changes and their modifiers. In: Cognitive neuroscience of aging: linking cognitive and cerebral aging(Cabeza, R. et al., eds), pp 19-57 New York, NY: Oxford University Press.

Raz N, Gunning-Dixon FM, Head D, Dupuis JH, Acker JD (1998) Neuroanatomical correlates of cognitive aging: evidence from structural magnetic resonance imaging. Neuropsychology 12:95-114.

Raz N, Gunning FM, Head D, Dupuis JH, McQuain J, Briggs SD, Loken WJ, Thornton AE, Acker JD (1997) Selective aging of the human cerebral cortex observed in vivo: differential vulnerability of the prefrontal gray matter. Cereb Cortex 7:268-282.

Raz N, Lindenberger U, Rodrigue KM, Kennedy KM, Head D, Williamson A, Dahle C, Gerstorf D, Acker JD (2005) Regional brain changes in aging healthy adults: general trends, individual differences and modifiers. Cereb Cortex 15:1676-1689.

Reeves S, Bench C, Howard R (2002) Ageing and the nigrostriatal dopaminergic system. Int J Geriatr Psychiatry 17:359-370.

Revollo JR, Grimm AA, Imai S (2004) The NAD biosynthesis pathway mediated by nicotinamide phosphoribosyltransferase regulates Sir2 activity in mammalian cells. J Biol Chem 279:50754-50763.

Rezvani AH, Levin ED (2001) Cognitive effects of nicotine. Biological Psychiatry 49:258-267.

Ribeiro-Carvalho A, Lima CS, Medeiros AH, Siqueira NR, Filgueiras CC, Manhaes AC, Abreu-Villaca Y (2009) Combined exposure to nicotine and ethanol in adolescent mice: effects on the central cholinergic systems during short and long term withdrawal. Neuroscience 162:1174-1186.

Rogina B, Helfand SL (2004) Sir2 mediates longevity in the fly through a pathway related to calorie restriction. Proc Natl Acad Sci U S A 101:15998-16003.

Romanelli MN, Gratteri P, Guandalini L, Martini E, Bonaccini C, Gualtieri F (2007) Central nicotinic receptors: structure, function, ligands, and therapeutic potential. ChemMedChem 2:746-767.

Rosen G, Williams A, Capra J, Connolly M, Cruz B, Lu L, Airey D, Kulkarni K, Williams R (2000) The Mouse Brain Library @ www.mbl.org. Int Mouse Genome Conference 14: 166. www.mbl.org.

Roth GS, Mattison JA, Ottinger MA, Chachich ME, Lane MA, Ingram DK (2004) Aging in rhesus monkeys: relevance to human health interventions. Science 305:1423-1426.

Rudy B, Fishell G, Lee S, Hjerling-Leffler J (2011) Three groups of interneurons account for nearly 100% of neocortical GABAergic neurons. Dev Neurobiol 71:45-61.

Rushforth SL, Steckler T, Shoaib M (2011) Nicotine improves working memory span capacity in rats following sub-chronic ketamine exposure. Neuropsychopharmacology 36:2774-2781.

Ryan RE, Ross SA, Drago J, Loiacono RE (2001) Dose-related neuroprotective effects of chronic nicotine in 6-hydroxydopamine treated rats, and loss of neuroprotection in alpha4 nicotinic receptor subunit knockout mice. Br J Pharmacol 132:1650-1656.

Sakamoto J, Miura T, Shimamoto K, Horio Y (2004) Predominant expression of Sir2alpha, an NAD-dependent histone deacetylase, in the embryonic mouse heart and brain. FEBS Lett 556:281-286.

Salminen A, Kaarniranta K (2009) NF-kappaB signaling in the aging process. J Clin Immunol 29:397-405.

Salomon AR, Marcinowski KJ, Friedland RP, Zagorski MG (1996) Nicotine inhibits amyloid formation by the beta-peptide. Biochemistry 35:13568-13578.

Salthouse TA (1996) The processing-speed theory of adult age differences in cognition. Psychol Rev 103:403-428.

Sanchis D, Fleury C, Chomiki N, Goubern M, Huang Q, Neverova M, Gregoire F, Easlick J, Raimbault S, Levi-Meyrueis C, Miroux B, Collins S, Seldin M, Richard D, Warden C, Bouillaud F, Ricquier D (1998) BMCP1, a novel mitochondrial carrier with high expression in the central nervous system of humans and rodents, and respiration uncoupling activity in recombinant yeast. J Biol Chem 273:34611-34615.

Sangha S, Narayanan RT, Bergado-Acosta JR, Stork O, Seidenbecher T, Pape HC (2009) Deficiency of the 65 kDa isoform of glutamic acid decarboxylase impairs extinction of cued but not contextual fear memory. J Neurosci 29:15713-15720.

Sargent PB (1993a) The diversity of neuronal nicotinic acetylcholine receptors. Annu Rev Neurosci 16:403-443.

Sargent PB (1993b) The diversity of neuronal nicotinic acetylcholine receptors. Annual Review of Neuroscience 16:403-443.

Sawada M, Sun W, Hayes P, Leskov K, Boothman DA, Matsuyama S (2003) Ku70 suppresses the apoptotic translocation of Bax to mitochondria. Nat Cell Biol 5:320-329.

Schneider JS, Van Velson M, Menzaghi F, Lloyd GK (1998) Effects of the nicotinic acetylcholine receptor agonist SIB-1508Y on object retrieval performance in MPTP-treated monkeys: comparison with levodopa treatment. Ann Neurol 43:311-317.

Schwartz RD, Kellar KJ (1985) In vivo regulation of [3H]acetylcholine recognition sites in brain by nicotinic cholinergic drugs. J Neurochem 45:427-433.

Seguela P, Wadiche J, Dineley-Miller K, Dani JA, Patrick JW (1993) Molecular cloning, functional properties, and distribution of rat brain alpha 7: a nicotinic cation channel highly permeable to calcium. J Neurosci 13:596-604.

Semba J, Miyoshi R, Kito S (1996) Nicotine protects against the dexamethasone potentiation of kainic acid-induced neurotoxicity in cultured hippocampal neurons. Brain Res 735:335-338.

Shankar SK (2010) Biology of aging brain. Indian J Pathol Microbiol 53:595-604.

Sharma G, Vijayaraghavan S (2001) Nicotinic cholinergic signaling in hippocampal astrocytes involves calcium-induced calcium release from intracellular stores. Proc Natl Acad Sci U S A 98:4148-4153.

Sheikh SN, Martin SB, Martin DL (1999) Regional distribution and relative amounts of glutamate decarboxylase isoforms in rat and mouse brain. Neurochem Int 35:73-80.

Shimohama S, Kihara T (2001) Nicotinic receptor-mediated protection against beta-amyloid neurotoxicity. Biol Psychiatry 49:233-239.

Shoop RD, Chang KT, Ellisman MH, Berg DK (2001) Synaptically driven calcium transients via nicotinic receptors on somatic spines. J Neurosci 21:771-781.

Sibille E, Su J, Leman S, Le Guisquet AM, Ibarguen-Vargas Y, Joeyen-Waldorf J, Glorioso C, Tseng GC, Pezzone M, Hen R, Belzung C (2007) Lack of serotonin1B receptor expression leads to age-related motor dysfunction, early onset of brain molecular aging and reduced longevity. Mol Psychiatry 12:1042-1056, 1975.

Simon P, Dupuis R, Costentin J (1994) Thigmotaxis as an index of anxiety in mice. Influence of dopaminergic transmissions. Behavioural Brain Research 61:59-64.

Small SA, Chawla MK, Buonocore M, Rapp PR, Barnes CA (2004) Imaging correlates of brain function in monkeys and rats isolates a hippocampal subregion differentially vulnerable to aging. Proc Natl Acad Sci U S A 101:7181-7186.

Smith GC, Jackson SP (1999) The DNA-dependent protein kinase. Genes Dev 13:916-934.

Socci DJ, Arendash GW (1996) Chronic nicotine treatment prevents neuronal loss in neocortex resulting from nucleus basalis lesions in young adult and aged rats. Molecular and Chemical Neuropathology 27:285-305.

Socci DJ, Sanberg PR, Arendash GW (1995) Nicotine enhances Morris water maze performance of young and aged rats. Neurobiol Aging 16:857-860.

Soghomonian JJ, Martin DL (1998) Two isoforms of glutamate decarboxylase: why? Trends Pharmacol Sci 19:500-505.

Soloway SB (1976) Naturally occurring insecticides. Environ Health Perspect 14:109-117.

Son JH, Winzer-Serhan UH (2009) Chronic neonatal nicotine exposure increases mRNA expression of neurotrophic factors in the postnatal rat hippocampus. Brain Research 1278:1-14.

Sparks JA, Pauly JR (1999) Effects of continuous oral nicotine administration on brain nicotinic receptors and responsiveness to nicotine in C57Bl/6 mice. Psychopharmacology (Berl) 141:145-153.

Srivareerat M, Tran TT, Salim S, Aleisa AM, Alkadhi KA (2009) Chronic nicotine restores normal Abeta levels and prevents short-term memory and E-LTP impairment in Abeta rat model of Alzheimer's disease. Neurobiol Aging.

Staley JK, Krishnan-Sarin S, Cosgrove KP, Krantzler E, Frohlich E, Perry E, Dubin JA, Estok K, Brenner E, Baldwin RM, Tamagnan GD, Seibyl JP, Jatlow P, Picciotto MR, London ED, O'Malley S, van Dyck CH (2006) Human tobacco smokers in early abstinence have higher levels of beta2* nicotinic acetylcholine receptors than nonsmokers. J Neurosci 26:8707-8714.

Stanfield BB, Trice JE (1988) Evidence that granule cells generated in the dentate gyrus of adult rats extend axonal projections. Exp Brain Res 72:399-406.

Stark AK, Pakkenberg B (2004) Histological changes of the dopaminergic nigrostriatal system in aging. Cell Tissue Res 318:81-92.

Steinlein OK, Mulley JC, Propping P, Wallace RH, Phillips HA, Sutherland GR, Scheffer IE, Berkovic SF (1995) A missense mutation in the neuronal nicotinic acetylcholine receptor alpha 4 subunit is associated with autosomal dominant nocturnal frontal lobe epilepsy. Nat Genet 11:201-203.

Sugano T, Yanagita T, Yokoo H, Satoh S, Kobayashi H, Wada A (2006) Enhancement of insulin-induced PI3K/Akt/GSK-3beta and ERK signaling by neuronal nicotinic receptor/PKC-alpha/ERK pathway: up-regulation of IRS-1/-2 mRNA and protein in adrenal chromaffin cells. J Neurochem 98:20-33.

Sugino T, Maruyama M, Tanno M, Kuno A, Houkin K, Horio Y (2010) Protein deacetylase SIRT1 in the cytoplasm promotes nerve growth factor-induced neurite outgrowth in PC12 cells. FEBS Lett 584:2821-2826.

Suhara T, Fukuda H, Inoue O, Itoh T, Suzuki K, Yamasaki T, Tateno Y (1991) Age-related changes in human D1 dopamine receptors measured by positron emission tomography. Psychopharmacology (Berl) 103:41-45.

Sullivan EV, Rosenbloom M, Serventi KL, Pfefferbaum A (2004) Effects of age and sex on volumes of the thalamus, pons, and cortex. Neurobiol Aging 25:185-192.

Summers KL, Giacobini E (1995) Effects of local and repeated systemic administration of (-)nicotine on extracellular levels of acetylcholine, norepinephrine, dopamine, and serotonin in rat cortex. Neurochem Res 20:753-759.

Tang BL, Chua CE (2008) SIRT1 and neuronal diseases. Molecular Aspects of Medicine 29:187-200.

Tani Y, Saito K, Imoto M, Ohno T (1998) Pharmacological characterization of nicotinic receptor-mediated acetylcholine release in rat brain--an in vivo microdialysis study. Eur J Pharmacol 351:181-188.

Tanner CM, Goldman SM, Aston DA, Ottman R, Ellenberg J, Mayeux R, Langston JW (2002) Smoking and Parkinson's disease in twins. Neurology 58:581-588.

Tate JC, Pomerleau OF, Pomerleau CS (1993) Temporal stability and within-subject consistency of nicotine withdrawal symptoms. Journal of Substance Abuse 5:355-363.

Terry AV, Jr., Buccafusco JJ (2003) The cholinergic hypothesis of age and Alzheimer's disease-related cognitive deficits: recent challenges and their implications for novel drug development. J Pharmacol Exp Ther 306:821-827.

Thompson PM, Hayashi KM, de Zubicaray G, Janke AL, Rose SE, Semple J, Herman D, Hong MS, Dittmer SS, Doddrell DM, Toga AW (2003) Dynamics of gray matter loss in Alzheimer's disease. J Neurosci 23:994-1005.

Tissenbaum HA, Guarente L (2001) Increased dosage of a sir-2 gene extends lifespan in Caenorhabditis elegans. Nature 410:227-230.

Toborek M, Garrido R, Malecki A, Kaiser S, Mattson MP, Hennig B, Young B (2000) Nicotine attenuates arachidonic acid-induced overexpression of nitric oxide synthase in cultured spinal cord neurons. Exp Neurol 161:609-620.

Tomizawa M, Casida JE (2003) Selective toxicity of neonicotinoids attributable to specificity of insect and mammalian nicotinic receptors. Annu Rev Entomol 48:339-364.

Torocsik A, Oberfrank F, Sershen H, Lajtha A, Nemesy K, Vizi ES (1991) Characterization of somatodendritic neuronal nicotinic receptors located on the myenteric plexus. Eur J Pharmacol 202:297-302.

Trevelyan AJ, Sussillo D, Watson BO, Yuste R (2006) Modular propagation of epileptiform activity: evidence for an inhibitory veto in neocortex. J Neurosci 26:12447-12455.

Tsuneki H, Klink R, Lena C, Korn H, Changeux JP (2000) Calcium mobilization elicited by two types of nicotinic acetylcholine receptors in mouse substantia nigra pars compacta. Eur J Neurosci 12:2475-2485.

Tulving E, Markowitsch HJ (1998) Episodic and declarative memory: role of the hippocampus. Hippocampus 8:198-204.

Ueno K, Togashi H, Matsumoto M, Ohashi S, Saito H, Yoshioka M (2002) Alpha4beta2 nicotinic acetylcholine receptor activation ameliorates impairment of spontaneous alternation behavior in stroke-prone spontaneously hypertensive rats, an animal model of attention deficit hyperactivity disorder. J Pharmacol Exp Ther 302:95-100.

Urakawa N, Nagata T, Kudo K, Kimura K, Imamura T (1994) Simultaneous determination of nicotine and cotinine in various human tissues using capillary gas chromatography/mass spectrometry. Int J Legal Med 106:232-236.

van der Veer E, Ho C, O'Neil C, Barbosa N, Scott R, Cregan SP, Pickering JG (2007) Extension of human cell lifespan by nicotinamide phosphoribosyltransferase. J Biol Chem 282:10841-10845.

van Dyck CH, Seibyl JP, Malison RT, Laruelle M, Zoghbi SS, Baldwin RM, Innis RB (2002) Age-related decline in dopamine transporters: analysis of striatal subregions, nonlinear effects, and hemispheric asymmetries. Am J Geriatr Psychiatry 10:36-43.

van Lookeren Campagne M, Gill R (1998) Tumor-suppressor p53 is expressed in proliferating and newly formed neurons of the embryonic and postnatal rat brain: comparison with expression of the cell cycle regulators p21Waf1/Cip1, p27Kip1, p57Kip2, p16Ink4a, cyclin G1, and the proto-oncogene Bax. J Comp Neurol 397:181-198.

Vargha-Khadem F, Gadian DG, Watkins KE, Connelly A, Van Paesschen W, Mishkin M (1997) Differential effects of early hippocampal pathology on episodic and semantic memory. Science 277:376-380.

Vaziri H, Dessain SK, Ng Eaton E, Imai SI, Frye RA, Pandita TK, Guarente L, Weinberg RA (2001) hSIR2(SIRT1) functions as an NAD-dependent p53 deacetylase. Cell 107:149-159.

Vernier JM, El-Abdellaoui H, Holsenback H, Cosford ND, Bleicher L, Barker G, Bontempi B, Chavez-Noriega L, Menzaghi F, Rao TS, Reid R, Sacaan AI, Suto C, Washburn M, Lloyd GK, McDonald IA (1999) 4-[[2-(1-Methyl-2-pyrrolidinyl)ethyl]thio]phenol hydrochloride (SIB-1553A): a novel cognitive enhancer with selectivity for neuronal nicotinic acetylcholine receptors. J Med Chem 42:1684-1686.

Volkow ND, Gur RC, Wang GJ, Fowler JS, Moberg PJ, Ding YS, Hitzemann R, Smith G, Logan J (1998) Association between decline in brain dopamine activity with age and cognitive and motor impairment in healthy individuals. Am J Psychiatry 155:344-349.

von Bohlen und Halbach O, Unsicker K (2002) Morphological alterations in the amygdala and hippocampus of mice during ageing. Eur J Neurosci 16:2434-2440.

Vorhees CV, Williams MT (2006) Morris water maze: procedures for assessing spatial and related forms of learning and memory. Nat Protoc 1:848-858.

Wada E, Wada K, Boulter J, Deneris E, Heinemann S, Patrick J, Swanson LW (1989) Distribution of alpha 2, alpha 3, alpha 4, and beta 2 neuronal nicotinic receptor subunit mRNAs in the central nervous system: a hybridization histochemical study in the rat. J Comp Neurol 284:314-335.

Wada E, Way J, Lebacq-Verheyden AM, Battey JF (1990) Neuromedin B and gastrin-releasing peptide mRNAs are differentially distributed in the rat nervous system. J Neurosci 10:2917-2930.

Wager-Srdar SA, Levine AS, Morley JE, Hoidal JR, Niewoehner DE (1984) Effects of cigarette smoke and nicotine on feeding and energy. Physiology and Behavior 32:389-395.

Walf AA, Frye CA (2007) The use of the elevated plus maze as an assay of anxiety-related behavior in rodents. Nat Protoc 2:322-328.

Wang H, Davila-Garcia MI, Yarl W, Gondre-Lewis MC (2011) Gestational nicotine exposure regulates expression of AMPA and NMDA receptors and their signaling apparatus in developing and adult rat hippocampus. Neuroscience 188:168-181.

Wang HY, Lee DH, Davis CB, Shank RP (2000) Amyloid peptide Abeta(1-42) binds selectively and with picomolar affinity to alpha7 nicotinic acetylcholine receptors. J Neurochem 75:1155-1161.

Wang J, Ho L, Qin W, Rocher AB, Seror I, Humala N, Maniar K, Dolios G, Wang R, Hof PR, Pasinetti GM (2005) Caloric restriction attenuates beta-amyloid neuropathology in a mouse model of Alzheimer's disease. FASEB Journal 19:659-661.

Wang J, Kim JM, Donovan DM, Becker KG, Li MD (2009) Significant modulation of mitochondrial electron transport system by nicotine in various rat brain regions. Mitochondrion 9:186-195.

Warburton DM, Wesnes K, Shergold K, James M (1986) Facilitation of learning and state dependency with nicotine. Psychopharmacology (Berl) 89:55-59.

Wehr M, Zador AM (2003) Balanced inhibition underlies tuning and sharpens spike timing in auditory cortex. Nature 426:442-446.

Weindruch R, Sohal RS (1997) Seminars in medicine of the Beth Israel Deaconess Medical Center. Caloric intake and aging. N Engl J Med 337:986-994.

Weiss S, Nosten-Bertrand M, McIntosh JM, Giros B, Martres MP (2007) Nicotine improves cognitive deficits of dopamine transporter knockout mice without long-term tolerance. Neuropsychopharmacology 32:2465-2478.

Wessler I, Apel C, Garmsen M, Klein A (1992) Effects of nicotine receptor agonists on acetylcholine release from the isolated motor nerve, small intestine and trachea of rats and guinea-pigs. Clin Investig 70:182-189.

West RL (1996) An application of prefrontal cortex function theory to cognitive aging. Psychol Bull 120:272-292.

White HK, Levin ED (1999) Four-week nicotine skin patch treatment effects on cognitive performance in Alzheimer's disease. Psychopharmacology (Berl) 143:158-165.

White HK, Levin ED (2004) Chronic transdermal nicotine patch treatment effects on cognitive performance in age-associated memory impairment. Psychopharmacology 171:465-471.

Whitehouse PJ, Martino AM, Antuono PG, Lowenstein PR, Coyle JT, Price DL, Kellar KJ (1986) Nicotinic acetylcholine binding sites in Alzheimer's disease. Brain Res 371:146-151.

Whitehouse PJ, Martino AM, Wagster MV, Price DL, Mayeux R, Atack JR, Kellar KJ (1988) Reductions in [3H]nicotinic acetylcholine binding in Alzheimer's disease and Parkinson's disease: an autoradiographic study. Neurology 38:720-723.

Wilens TE, Biederman J, Spencer TJ, Bostic J, Prince J, Monuteaux MC, Soriano J, Fine C, Abrams A, Rater M, Polisner D (1999) A pilot controlled clinical trial of ABT-418, a cholinergic agonist, in the treatment of adults with attention deficit hyperactivity disorder. Am J Psychiatry 156:1931-1937.

Wilson AL, Langley LK, Monley J, Bauer T, Rottunda S, McFalls E, Kovera C, McCarten JR (1995) Nicotine patches in Alzheimer's disease: pilot study on learning, memory, and safety. Pharmacology, Biochemistry and Behavior 51:509-514.

Winzer-Serhan UH, Broide RS, Chen Y, Leslie FM (1999) Highly sensitive radioactive in situ hybridization using full length hydrolyzed riboprobes to detect alpha 2 adrenoceptor subtype mRNAs in adult and developing rat brain. Brain Research Brain Research Protocols 3:229-241.

Witter MP, Groenewegen HJ, Lopes da Silva FH, Lohman AH (1989) Functional organization of the extrinsic and intrinsic circuitry of the parahippocampal region. Prog Neurobiol 33:161-253.

Wolf G (2006) Calorie restriction increases life span: a molecular mechanism. Nutrition Reviews 64:89-92.

Wonnacott S (1997) Presynaptic nicotinic ACh receptors. Trends Neurosci 20:92-98.

Xiao C, Nashmi R, McKinney S, Cai H, McIntosh JM, Lester HA (2009) Chronic nicotine selectively enhances alpha4beta2* nicotinic acetylcholine receptors in the nigrostriatal dopamine pathway. J Neurosci 29:12428-12439.

Xu W, Orr-Urtreger A, Nigro F, Gelber S, Sutcliffe CB, Armstrong D, Patrick JW, Role LW, Beaudet AL, De Biasi M (1999) Multiorgan autonomic dysfunction in mice lacking the beta2 and the beta4 subunits of neuronal nicotinic acetylcholine receptors. J Neurosci 19:9298-9305.

Xu X, Roby KD, Callaway EM (2010) Immunochemical characterization of inhibitory mouse cortical neurons: three chemically distinct classes of inhibitory cells. J Comp Neurol 518:389-404.

Yang H, Lavu S, Sinclair DA (2006a) Nampt/PBEF/Visfatin: a regulator of mammalian health and longevity? Exp Gerontol 41:718-726.

Yang H, Lavu S, Sinclair DA (2006b) Nampt/PBEF/Visfatin: a regulator of mammalian health and longevity? Experimental Gerontology 41:718-726.

Zamani MR, Allen YS (2001) Nicotine and its interaction with beta-amyloid protein: a short review. Biol Psychiatry 49:221-232.

Zanardi A, Ferrari R, Leo G, Maskos U, Changeux JP, Zoli M (2007) Loss of high-affinity nicotinic receptors increases the vulnerability to excitotoxic lesion and decreases the positive effects of an enriched environment. FASEB J 21:4028-4037.

Zanardi A, Leo G, Biagini G, Zoli M (2002) Nicotine and neurodegeneration in ageing. Toxicol Lett 127:207-215.

Zarrindast MR, Sadegh M, Shafaghi B (1996) Effects of nicotine on memory retrieval in mice. Eur J Pharmacol 295:1-6.

Zhang L, Dong Y, Doyon WM, Dani JA (2012) Withdrawal from chronic nicotine exposure alters dopamine signaling dynamics in the nucleus accumbens. Biol Psychiatry 71:184-191.

Zins BJ, Sandborn WJ, Mays DC, Lawson GM, McKinney JA, Tremaine WJ, Mahoney DW, Zinsmeister AR, Hurt RD, Offord KP, Lipsky JJ (1997) Pharmacokinetics of nicotine tartrate after single-dose liquid enema, oral, and intravenous administration. J Clin Pharmacol 37:426-436.

Zoli M, Le Novere N, Hill JA, Jr., Changeux JP (1995) Developmental regulation of nicotinic ACh receptor subunit mRNAs in the rat central and peripheral nervous systems. J Neurosci 15:1912-1939.

Zoli M, Picciotto MR, Ferrari R, Cocchi D, Changeux JP (1999) Increased neurodegeneration during ageing in mice lacking high-affinity nicotine receptors. Embo J 18:1235-1244.

VITA

Name: Pei-San Huang

Address: Department of Veterinary Integrative Biosciences
MS 4458
Texas A&M University
College Station, TX

Email Address: phuang@cvm.tamu.edu

Education: B.V.M., National Taiwan University, Taiwan, 2006

Professional experience: Veterinary practice, Taiwan, 2005-2006

Publications:

- Huang PS, Son JH, Abbott LC, Winzer-Serhan UH (2011) Regulated expression of neuronal SIRT1 and related genes by aging and neuronal β2-containing nicotinic cholinergic receptors. Neuroscience 196:189-202.
- Huang PS, Abbott LC, Winzer-Serhan UH. Effects of chronic oral nicotine on food consumption, anxiety and expression of SIRT1 and related genes in young adult mouse brain. In preparation.
- Huang PS, Abbott LC, Winzer-Serhan UH. Long-term nicotine and caloric restriction treatment improve memory in middle-aged mice and differentially regulate SIRT1, Nampt and Ku70 gene expression in cortical areas. In preparation.
- Huang PS, Abbott LC, Winzer-Serhan UH. Lack of high affinity nicotinic acetylcholine receptors decreases the number of GABAergic interneurons but not synaptic density in the hippocampal region of aged mice. In preparation.